



Electricity and The Duplicit Electron

Table of Contents

Introduction

Electron Models

The Backstory about Positrons

Pair Production

Positron Creation from Electrons

Pre-Existing Positrons within Matter

The Nature of Electric Currents

Electric and Magnetic Fields

Chemical Battery Power Sources

Bitron Bond Primer

Electromagnetic Induction

Electromagnetic (Motor) Force

Eddy Currents and the Hall Effect

Static Electricity (Electrostatic Charge)

Capacitors and Inductors

Micro and Radio Waves

Semiconductors and the P-N Junction

Photovoltaic Cells, Photodiodes and LEDs

NPN and PNP Transistors

Concluding Remarks

References

Appendix A. STEM Electron Rationale

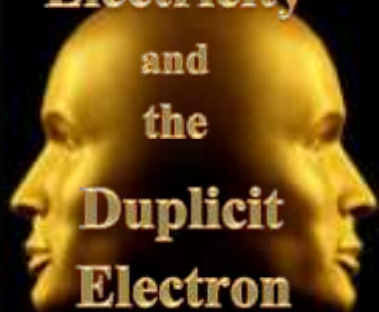
Appendix B. Electron Size and g -Factor

**The STEM
Approach
Volume 1**

by

David L Johnson

**Electricity
and
the
Duplicit
Electron**



December 2024

Introduction

The electron represents one of the most exciting and important particles in atomic science. Electrons are very small and mobile fundamental (or elementary) particles that engage in orbitals around atomic nuclei, or can move as an electric current through a conductor, or can spectacularly jump en-masse through dielectric material in the form of lightning or an electric arc. They are also important in atomic bonding and chemical reactions.

The electron is one of the most studied of the fundamental particles, and its negative charge defines the **unit charge** which forms the base-line measurement of electric charge (in **coulombs**) and electric current (in **amperes**). However, despite all that is known about the electron, its size remains in dispute and, although there are several electron models, its structure remains a mystery and open to conjecture.

In 1759, working in conjunction with Benjamin Franklin, Robert Symmer suggested that two component forms (or **two-fluids**) constituted electricity, but this model never gained prominence. With the development of nuclear atomic model, protons within the nucleus of atoms within matter were considered to provide positive charge and orbital electrons the negative charge. Because atoms within metallic conductors such as copper wire are stationary, it was logical to simply describe and attribute electricity to the **one-way movement of electrons** from a negative terminal to a positive terminal. One unfortunate legacy of Franklin (and indirectly to Symmer) is that his **one-fluid** explanation for electric current resulted in electrons being considered to move from positive to negative, and this interpretation has been adopted as the convention for the design and implementation of electrical devices.

Nowadays, electric current is understood to be caused by the movement of electrons, but electric charge carriers aren't always electrons, and they aren't always negative. In animals (including humans), electric charge carriers are primarily sodium, potassium, calcium, and magnesium ions, which are all positively charged: when a nerve passes an electric signal, it consists of positive charge movement. In the ionosphere, there are positive charge carriers such as oxygen, hydrogen, and helium ions, in combination with electrons. For gas discharge, the electrical current is also due to ion and electron movement. Lightning can also be in terms of either negative or positive charge discharge. Solar wind, which is electrical current derived from the sun, comprises of positive (protons) and negative charge (electrons). In the ocean, it is the movement of salt ions, and not just electrons, that sustain an electrical current. And, interestingly, for semiconductors, electric current cannot be fully explained simply in terms of the movement of electrons (the negative charge carrier), and a positive charge carrier is required.

With like charges repelling and opposite charges attracting, we treat negative electric charge as being distinctly different to positive electric charge, or at least that the electric fields associated with each type of charge to be different. This paper considers what **electric charge** and its associated **electric field** might consist of, and attempts to explain the reasons why the positive and negative fields of charges interact with each other as they do: are the charge differences due to composition or structure, or both?

In terms of like-pole repulsion and opposite pole attraction, **magnetic fields** are quite similar to electric fields, and are inter-related as implicit in the term '**electromagnetic**'. This paper looks at several models for the electron and its role in electric currents, and explores the nature of and differences between electric and magnetic fields with reference to the STEM electron model.

This paper is the first of a three volume series about the STEM approach. The Volume 2 paper addresses [Atomic Structure](#) and Volume 3 [the Nature of Light](#).

Electron Models

In textbooks, electrons are usually portrayed as small monopole spherical particles. However, when fed into the **Dirac** and **Schrödinger** wave equations, spherical particles generate unwanted and unmanageable singularities. Consequently, the spherical electron model was reduced to a dimensionless dot, referred to as a **point-form definition**. A consequence of this mathematical expediency is that all the electron's energy and mass is concentrated at a dimensionless dot, which has no radial width, which means that the point-form defined electron cannot have conventional angular momentum due to a physical spin. Because of this problem, the electron's observable angular momentum is considered to be **intrinsic spin** (i.e. an inherent property that defies explanation), with a **spin-up electron** having a quantum number $m_s = +1/2$, and a **spin-down electron** a spin quantum number $m_s = -1/2$. Despite having a point-form definition, electrons and their intrinsic spin are typically represented as shown in figure 1.

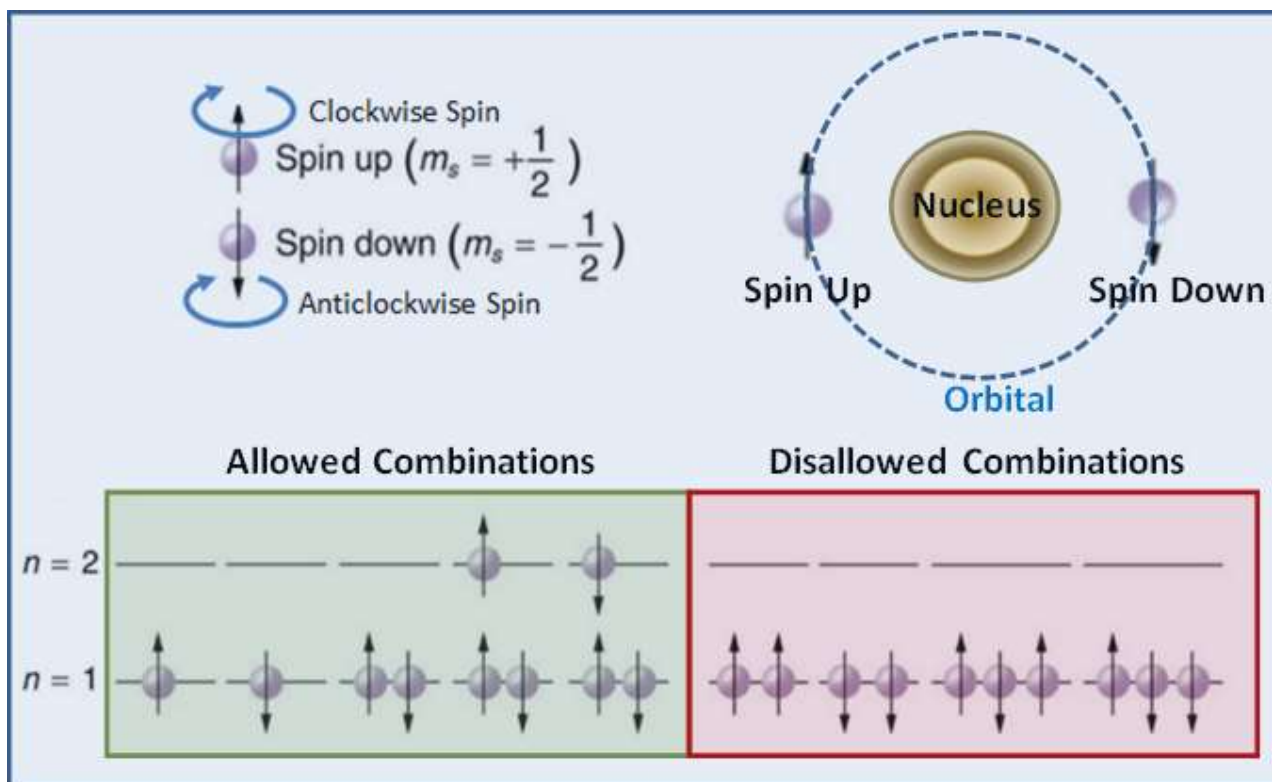


Figure 1: Electron Spin and Atomic Orbitals

According to the QM-based **Standard Model**, a **fermion** is a fundamental (or elementary) type of particle that has **half spin**. An electron is a **lepton**, which is a sub-class the fermion category, that is used to define the base electric charge $-1e$, and a **positron** is an **anti-particle** of an electron with a charge of $+1e$. The [Pauli Exclusion Principle \(PEP\)](#) was first identified by the Austrian physicist Wolfgang Pauli in 1925, and by 1940 PEP had been generalised and extended to include all fermions. Couched in QM terminology, the generalised form of PEP states that two or more **identical fermions** cannot occupy the same quantum state within a quantum system simultaneously. Thus, for electrons, PEP means that two electrons with the same '**up**' or '**down**' spin cannot occupy the same atomic orbital.

From a purely theoretical point of view, QM electrons and positrons are both structureless point-form particles. The QM model is thus essentially a mathematical model of the electron and positron designed to work well with the theoretical mathematical models that piggy-back onto the wave equations, but it is far removed from being a **physical model** for the electron. However, logically, something cannot come from nothing, and thus electrons and positrons must, at very least, consist of an infinitesimally small jot of **fundamental electromagnetic material** that has inherent charge characteristics (negative for electrons and positive for positrons), spin ('intrinsic' or physical) and mass.

Although the point-form definition of the electron and positron might have proven useful for the development of QM concepts, it unfortunately stifles incentive to explore potential structures for fundamental particles such as the electron and positron, and the potential development of a realistic physical model that might better explain their properties and behaviour. And certainly there is no funding available to encourage and support any such research.

A well-documented alternative model to QM-based point-form model is the **Toroidal Solenoidal Electron (TSE)** model, which considers an electron to consist of a spinning electric charge that moves at high speeds in a **solenoidal** pattern around a torus-shaped pathway: based upon references [1] to [6], figure 2 shows examples of variations of the TSE model.

An advantage of a toroidal model over a spherical model is that it can validly be represented by the point at the centre of mass of the torus because no electromagnetic material physically exists at that point. The main electromagnetic properties (mass, charge and spin) are associated with, and can be thus considered to be concentrated at, the centre of mass without having to shrink the physical size of the particle as for the QM model. TSE models are physical models that, mathematically, can be validly treated as a point-form particle to satisfy the QM wave equations. Several authors (references [7] to [10]) claim that TSE models are more realistic and potentially provide an equal, if not better, fit to the observed properties and electromagnetic characteristics of electrons than the QM-based monopole point-charge model does.

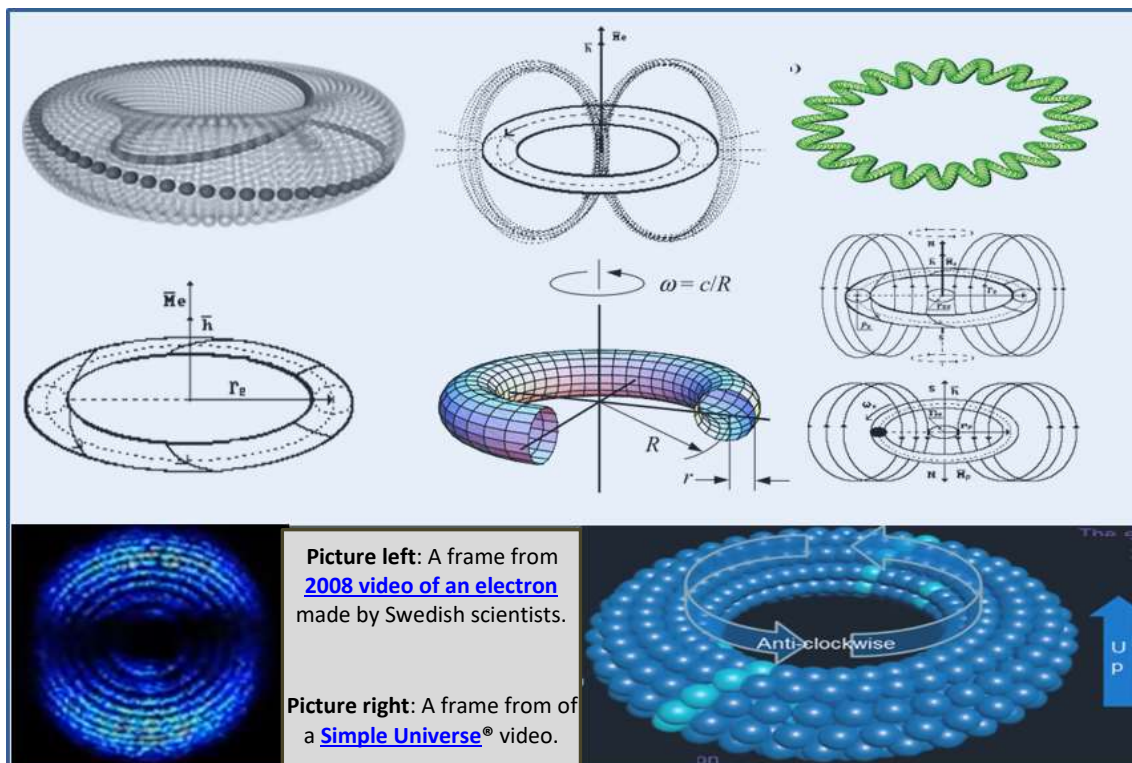


Figure 2: Examples of Torus-Based Electron/Positron Models

More recently, in 2015/2016, D Bowen and R Mulkern (references [12] and [13]) developed the toroidal-based **Charged-Electromagnetic-Wave-Loop (CEWL)** model that, unlike the TSE model, does not have a solenoidal spin of charge around the torus. CEWL considers that an **electron** consists of a negative sinusoidal **electromagnetic wave** moving at the speed of light around a toroidal path so as to generate the electron's charge and magnetic field. For a **positron**, a positive electromagnetic wave is considered to move around the toroid in the opposite direction to that of the electron: figure 3 shows how the magnetic field (green) generated by the CEWL positron (the red wave-form) and the CEWL electron (blue wave-form) has the same circular direction around and through the torus.

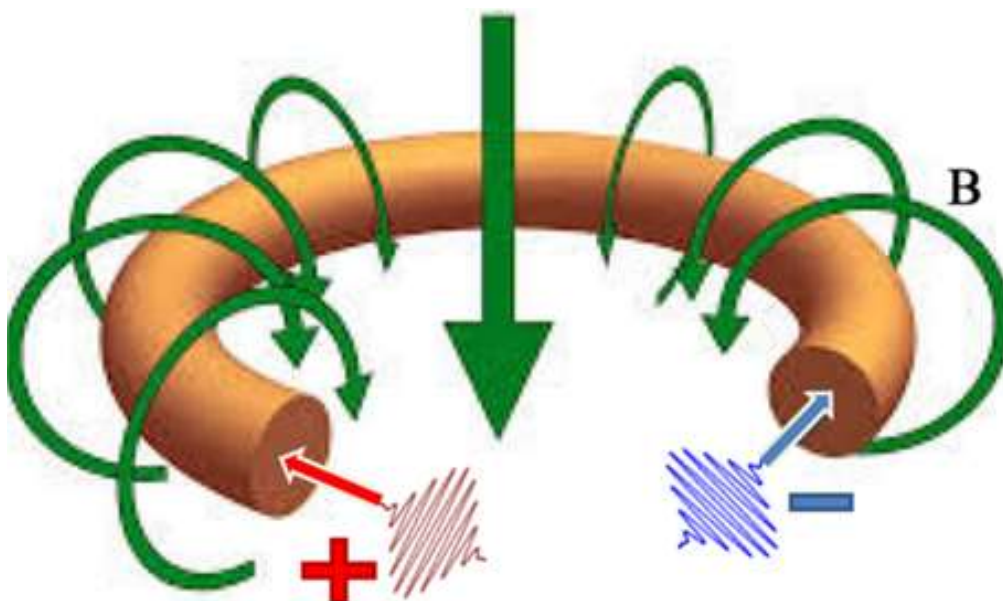
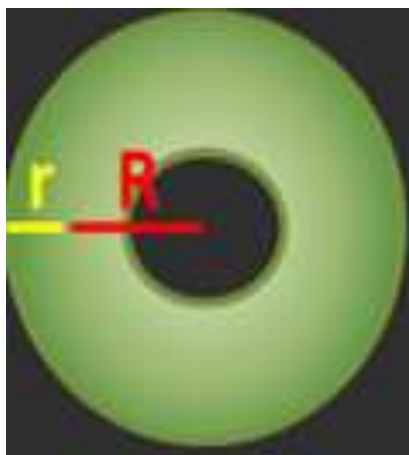


Figure 3: The CEWL Electron/Positron Model

The CODATA radius of the electron, which represents “classical electron radius”, is 2.82×10^{-15} m. Earlier estimates by M MacGregor (reference [16]) placed the radius of an electron in the range 4×10^{-13} to 7×10^{-13} m, which is compatible with the 2015 Bowen and Mulkern (reference [13], with a copy of the calculation shown as figure 4 estimate the radius to be 3.86×10^{-13} m. These two estimates are about 100 times larger than the classical CODATA estimate for an electron radius, and thus it is reasonable to assume that the actual size of an electron remains unknown.



Energy-Core of STEM Electron

Note. A discussion about **electron size** and the derivation of the **electron g-factor** is provided in [Appendix B](#) of this paper.

Known values and definitions:

Q_e (charge of electron) = $1.602176565(35) \times 10^{-19}$ Coulombs [4];

μ_e (bare magnetic moment electron) = $9.27400968(20) \times 10^{-24}$ Amp·m² [5];

g (g factor correction) = 1.00115965218073 [6];

Note: see Postulate 4) below for when and why to apply g factor correction.

C (speed of light) = 2.99792458×10^8 m/s;

T (transit time at speed C around loop of diameter d) = $\pi d/C$;

μ_i (magnetic moment of current around any circle) = Amperes $\times \pi d^2/4$.

For a charge of a single electron going in a circular loop at the speed of light:

$$Amp_e \text{ (Ampere around loop)} = \text{Coulomb/s} = (Q_e/T) = Q_e / \left(\frac{\pi d}{C} \right)$$

$$\mu_i = Amp_e \times \left(\frac{\pi d^2}{4} \right) = Q_e d C / 4$$

Solving for the “ d ” that satisfies the known bare magnetic moment μ_e :

$$d_e \text{ (diameter of electron loop)} = 4\mu_e / (Q_e C) = 7.72318492 \times 10^{-13} \text{ m}$$

$$\text{Length around loop} = \pi \times 7.72318536 \times 10^{-13} \text{ m} = 2.426310 \times 10^{-12} \text{ m}$$

Figure 4: CEWL Calculation of Electron Diameter and Circumference

The energy-centric [Spin Torus Energy Model \(STEM\)](#) is another toroidal model quite similar to the CEWL model. Both these models have half-spin and satisfy the QM wave equations. However, the STEM and CEWL models are fundamentally different from the QM-based Science models and the other toroidal models because they both contend that it is the movement of electromagnetic material within a torus structure that generates the negative and positive electromagnetic charge characteristics of electrons and positrons. They both contend that the difference between negative or positive charge is due to the movement pattern of electromagnetic material rather than there being two distinctly different types of electromagnetic material (i.e. one material-type that carries negative charge and the other that carries positive charge).

Despite their similarities, there are distinct differences between the STEM and CEWL models. The CEWL model considers that the electromagnetic material consists of a negative or a positive electromagnetic wave or pulse, with an electron and a positron consisting of a photon of energy 0.511 MeV that is joined head-to-tail to form a torus-shaped particle.

The STEM model, on the other hand, calls the electromagnetic material ‘**energen**’. As for the infinitesimally small jot of fundamental electromagnetic material must be associated with QM’s point-form definition of electrons and positrons, energen has no structure or form. It is postulated low concentrations of energen display [inviscid flow](#) (or frictionless gas-like) characteristics, and readily forms circular swirls when it is made to flow; and when energen becomes more concentrated it thickens and becomes more viscous whilst retaining the properties of an inviscid liquid that flows and, as such, it displays physical characteristics analogous to a solid torus that spins.

The STEM model for all fundamental particles, including electrons and positrons, consists of an inner torus encompassed by an atmosphere-like outer torus. The inner torus, called its **energy-core**, consists of concentrated energen that has the consistency of a thick inviscid fluid that flows at a rate close to the speed of light (and which is analogous to a solid torus that spins). The energy-core is enveloped by a swirling outer torus of less concentrated energen that also exhibits inviscid flow characteristics but is more fluid-like (or gas-like), referred to as its **field-energy**, and which flows around and through the energy-core torus. A fundamental particle’s field energy is responsible for the electromagnetic characteristics (i.e. magnetic moment, chirality and electromagnetic field), which in turn govern the manner in which they interact with other particles and electromagnetic fields, whereas its energy-core provides the bulk of its particle-like characteristics (i.e. mass and angular momentum).

Largely based upon a Bowen and Mulkern type of calculation (figure 4), the large radius (R in figure 4) of the STEM electron's energy core is considered to be 2.4×10^{-13} m (or 0.24 pm) and the small radius (r) to be 1.6×10^{-13} m (or 0.16 pm) to produce an estimate of the large outer radius ($R+r$) of 4×10^{-13} m (or 0.4 pm).

For the STEM model, as it has no poloidal flow component, the energy-core of an electron is not chiral. However, its atmosphere-like swirling outer torus of field-energy is **chiral** (i.e. it has **helicity**), and can present with **left-handed chirality** (as in figure 5) for electrons or with **right-handed chirality** (as in figure 6a) for positrons.

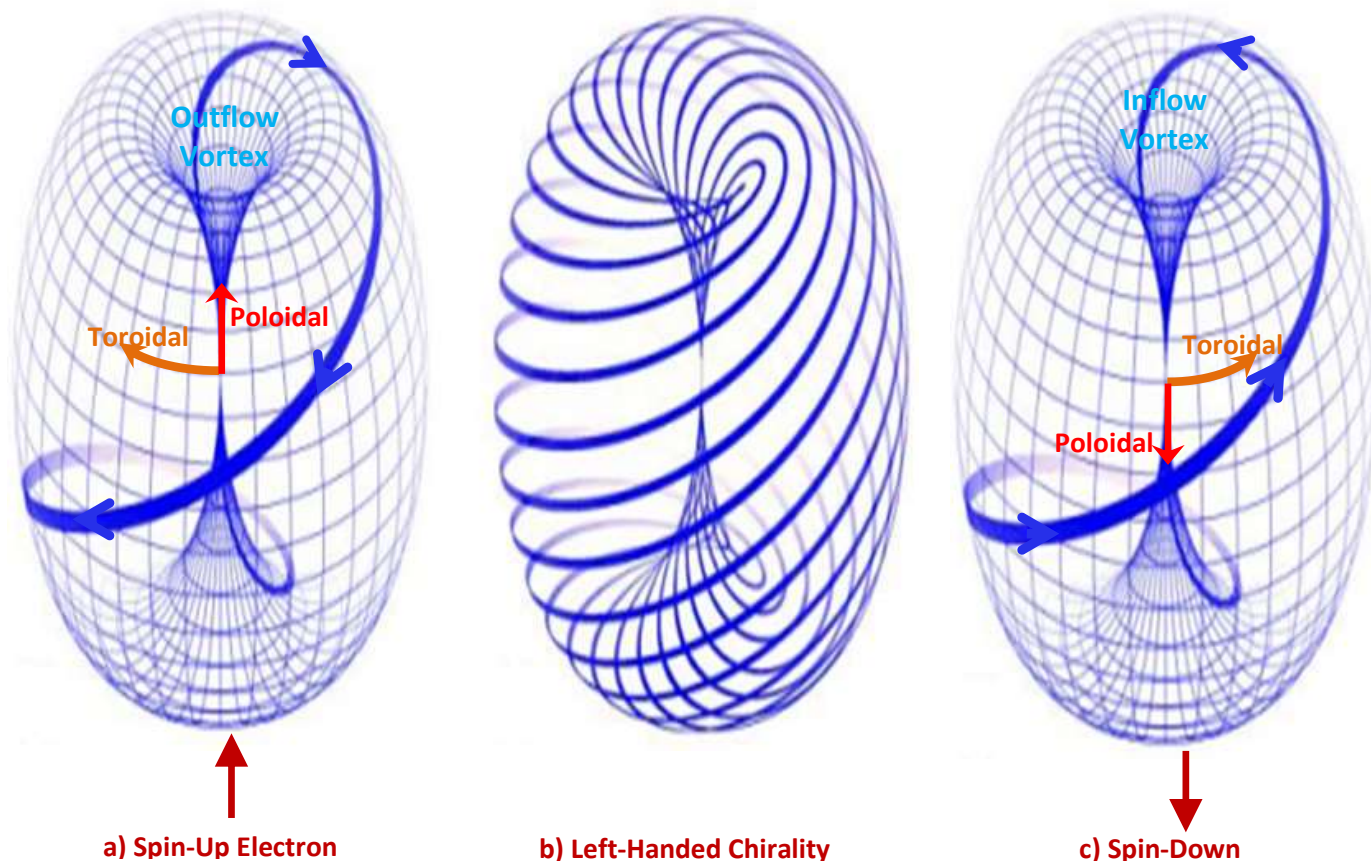


Figure 5: Chirality and Spin-Up/Spin-Down Electrons

The swirling flow pattern of the field-energy forms an **outflow vortex** and an **inflow vortex** at opposite ends of the outer torus as can be seen in figure 5. When the outflow vortex is upmost, as in figure 5a, it is considered to represent **spin-up** electron; and **spin-down** is when the inflow vortex is upmost (i.e. the outflow vortex is at the bottom) as in figure 5c. The **toroidal** and **poloidal** flow components determine whether the flow pattern represents left-handed (for electrons) or right-handed (for positrons = **Maxwell's Right Fist Rule**) chirality. Left-handed chirality can be checked by pointing the thumb of a closed left fist in the poloidal direction at the outflow vortex, with the finger wrap direction indicating the toroidal flow component's direction. Note that this works regardless of whether it is in spin-up or spin-down direction (or in between), and that the right-hand can be used similarly to check for right-handed chirality.

In [this Markoui animation](#), the difference between poloidal (labelled 'revolution') and toroidal (labelled 'rotation') movement components can be appreciated, with the rightmost combined animation having left-handed chirality. This excellent [Markoulakis animation](#), related to a $\frac{1}{2}$ spin fibre model for the electron [19], also shows the net flow of the field energy of an electron and positron (note: **N** is the outflow vortex end and **S** inflow end).

The **core-energy** of the STEM electron accounts for the bulk of an electron's energy, and thus its mass and associated angular momentum. The chiral flow of the external **energy-field** is driven and maintained by the flow/spin of the energy-core, and it is responsible for the electron's **electromagnetic field** characteristics. It is thus a **particle-like** model, with electrons and positrons having distinctly different chiral forms, but with each having the same energy quanta and radial size. When STEM electrons and positrons are represented as point-form particles, the model satisfies the Dirac wave equation and thus, from a mathematical perspective, they can also be considered to be **wave-like**, which helps with a theoretical explanation of the [particle-wave duality](#) often claimed for electrons.

Unique to the STEM model is the concept that, although the field-energy has a chiral twisted flow pattern, due to its viscous nature, the energy-core is considered to either undergo physical spin should it be gel-like, or toroidal flow (i.e. without any poloidal flow component) should it act as an inviscid fluid.

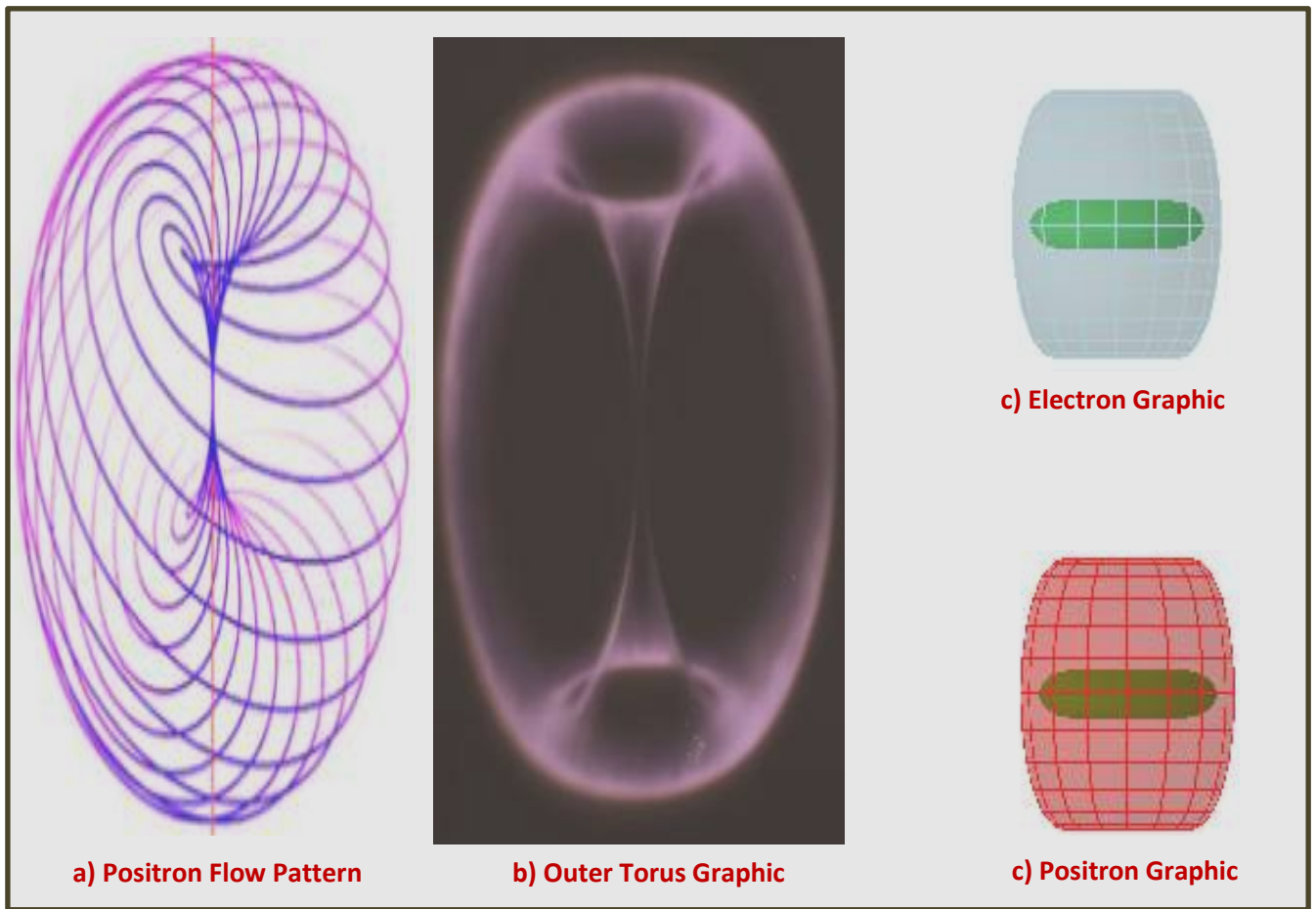


Figure 6: Positron and Electron Graphics

A cross-sectional representation of an electron and a positron is shown in figure 7. The toroidal flow component of the energy-field has the same direction as the core-energy's spin, with the latter being indicated by the red arrow-points and arrow-quills. The arrowed ellipses indicate of figure 7 indicate the poloidal flow direction of the energy-field.

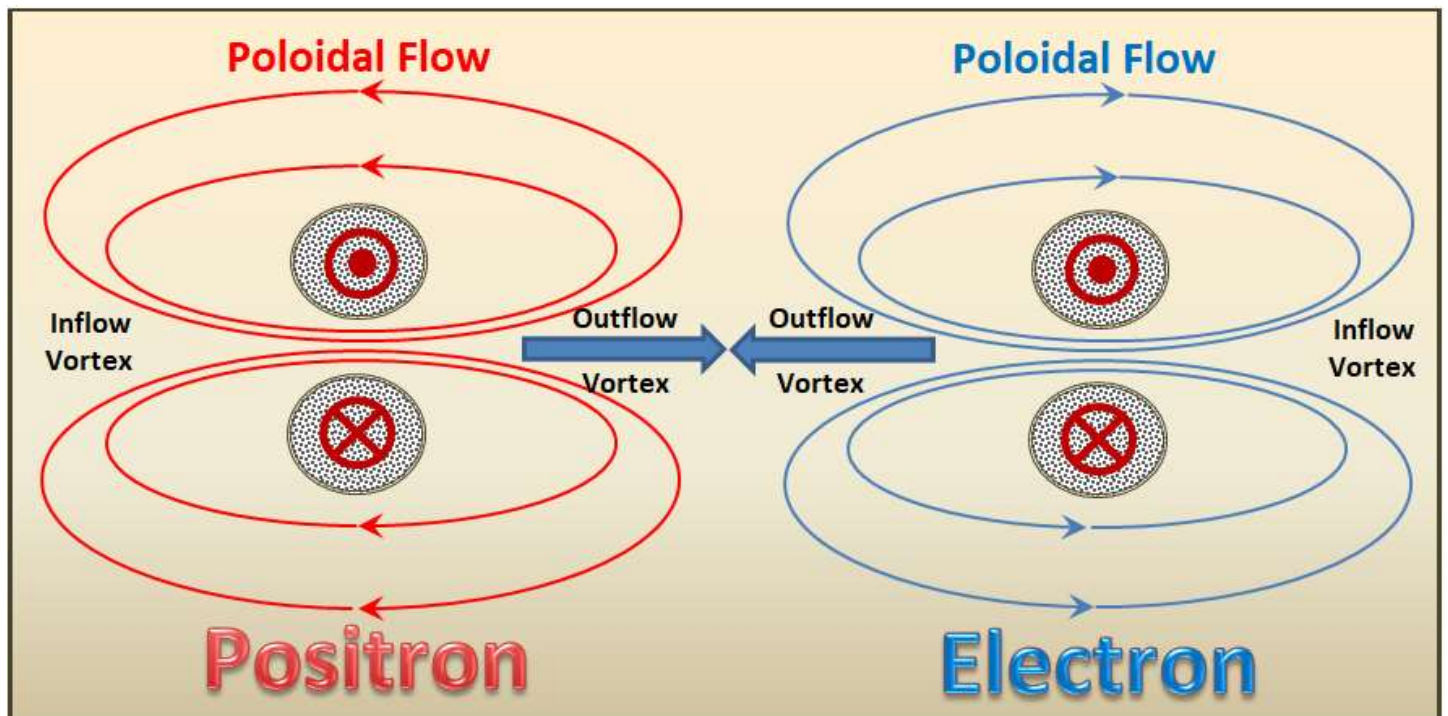


Figure 7: Positron and Electron Cross-Sections

In an energised environment additional energen can build up in the field-energy, so extending the strength and range of the particle's electromagnetic field. In a de-energised environment the field-energy can be reduced so that, at close to absolute zero, it can become ineffective. Although there may be some transfer of energen from energy-core to field-energy and vice versa, despite any such energen interchange, the amount of energen within the energy-core is considered to remain relatively stable, as is the electron's mass.

Chapter Summary

A major problem with the QM-based conventional Science model is that the size of the electron is reduced to a point-form definition to prevent the Dirac and Schrödinger wave equations generating unwanted singularities which, in turn, leads to them being allocated ‘intrinsic’ spin. Toroidal electron models, on the other hand, have nothing (i.e. no electromagnetic material) at their geometric centre of mass, and so can validly be treated mathematically as a dimensionless hypothetical dot with associated physical properties (e.g. width, mass, angular momentum, charge and quantum spin number) that are derived from the surrounding torus structure. A claimed added bonus is that the toroidal electrons, so defined, represent a physical model that satisfies the wave equations.

Apart from the CEWL and STEM models, most electron and positron models, including QM-based models, assume or imply that they are made from fundamentally different kinds of electromagnetic materials: one being responsible for negative charge and the other for positive charge.

The STEM electron and positron are considered to have the same structure as all fundamental particles. These particles consist of an inner torus of concentrated electromagnetic material (which is called **energen**), which forms the **energy-core** and represents the bulk of its robustness, mass and associated angular momentum, and an outer torus of less concentrated **energen** called **field-energy** that envelops the energy-core and is responsible for its electromagnetic characteristics. The field-energy swirls around and through the energy-core torus, driven by the flow/spin of the energy-core. The field-energy has a chiral flow pattern: when it has left-handed chirality, the particle is considered to have negative charge and to be an **electron**; and when it has right-handed chirality it is considered to have positive charge and to be a **positron**.

Note that from this point onwards in this paper, the term ‘**conventional Science**’ relates to the current status quo of Science opinion as it relates to Physics-based models consisting mainly of the **Orbital Nuclear Atomic Model (ONAM)**, the **Standard Model (SM)** and the various forms of **Quantum Mechanics (QM)** specialisations, as well as the theory and practices of the applied disciplines of Chemistry and Electrical Engineering.

The Backstory about Positrons

The mystery about positrons started in 1898 when Ernest Rutherford observed Beta Plus (β^+) decay and discovered mysterious particle emissions that he called **positive beta particles**. They were considered to be a form of weird radiation from the radioactive decay of Uranium, and electrons from Beta Minus (β^-) decay were similarly called **negative beta particles**. It wasn't until 1932 that Carl Anderson officially (re)discovered positrons by accident when conducting experiments related to cosmic radiation. Anderson's discovery was hailed as providing a validation of Paul Dirac's earlier theoretical prediction of the possible existence of the positron, the **anti-particle** of the electron.

Neils Bohr's nuclear model was developed around 1913, and evolved into Erwin Schrodinger's Quantum Mechanics model by 1926. However, positrons did not readily fit into either model because both contend that the only source of positive charge within matter relates to protons within the atomic nucleus. Even after the excitement of Carl Anderson's positron re-discovery in 1932, little has changed, and the mystery surrounding positrons continues.

Electrons are plentiful, and can be readily generated low-energy processes such as **electron guns** and the **Photoelectric Effect**, whereas positrons are relatively rare. Although β^+ decay produces low level concentrations of positrons, and provides a positron source as commonly used for medical probes and scanners, high-energy brute-force techniques (e.g. the 200 MeV high-energy Large-Scale Collider at CERN or Petawatt-plus lasers) are needed to synthetically generate useful quantities of positrons.

However, having a positron source does not provide an insight into their creation. There would seem to be three possible alternative explanations for the means by which positrons are created; namely:

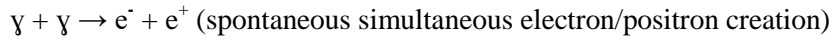
1. Positron creation is an example of the direct dynamic and spontaneous creation of matter from gamma ray radiation via **pair production**.
2. **Positrons are created** by the high-energy impact conversion of electrons into positrons.
3. **Positrons pre-exist within matter** and simply require high-energy impact to release them.

Each alternative explanation will be discussed in turn in its own chapter.

Explanation 1: Pair Production

Electron-positron pair production is the most quoted example of the claimed dynamic creation of matter from photon energy. Pair production requires photon energy in the gamma frequency range, with the minimum net photon energy required being 1.022 MeV, which equates to the combined rest mass equivalence of an electron and a positron. The probability of pair production is claimed to increase with photon energy.

Breit–Wheeler pair production is the process by which a positron–electron pair is created from the collision of two photons in the gamma frequency range, with each gamma ray photon having a minimum energy of 0.511 MeV. It is represented by the following equation:



Despite being lauded within Physics communities and the wider press as an example of matter creation from electromagnetic radiation, the Breit–Wheeler process has never been observed in practice because of the difficulty in preparing colliding gamma ray beams and the very weak probability of such collisions. It is now widely interpreted as the possible splitting of one photon of energy greater than 1.022 MeV. Certainly, the actual pair production mechanism is speculative, and far from being well established, with there being wide variety of diagrams intended to represent and clarify the process. Figure 8 shows just four of these.

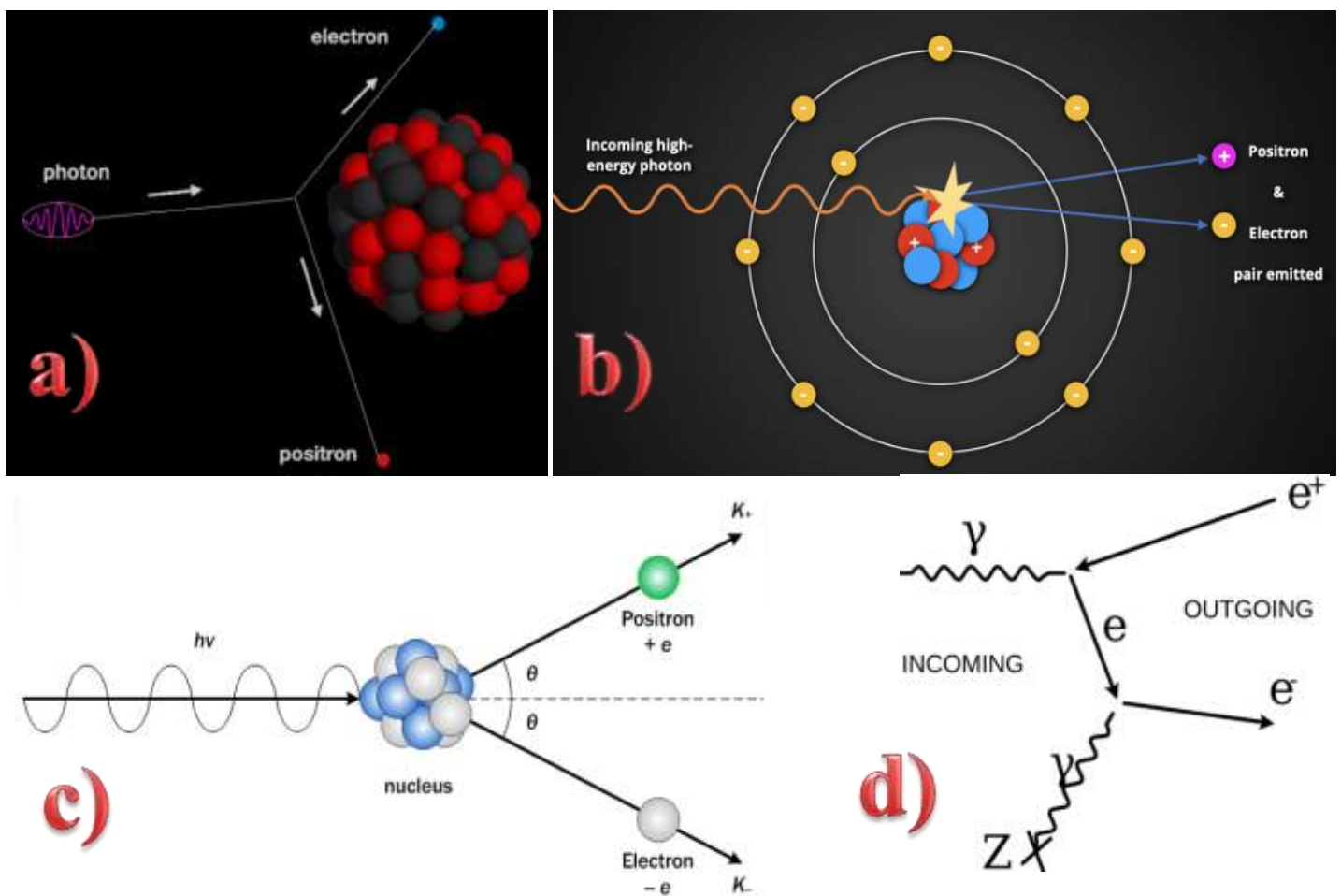


Figure 8: Electron-Positron Pair Production

So, does the claimed Breit–Wheeler pair production occur by the magical splitting of a single photon by an atomic nucleus (as in figure 1a or 1c); the collision of a photon with an atomic nucleus (figure 1b); or the collision of a pair of photons (figure 1d)? It all seems to be very confused and confusing. And note that, only in one diagram (figure 1b), the presence of orbital electrons is acknowledged and represented (albeit simplistically). However, for all such interpretations, the possible and highly likely interference between existing orbital electrons and the newly generated electron and positron particles is totally ignored.

The 2013 article by Sarri (reference [11]) describes one of the first Petawatt (=1015W) laser setups used to generate a positron stream (see figure 9). It provides a detailed discussion of the results and attempts to explain the creation process in terms of pair production.

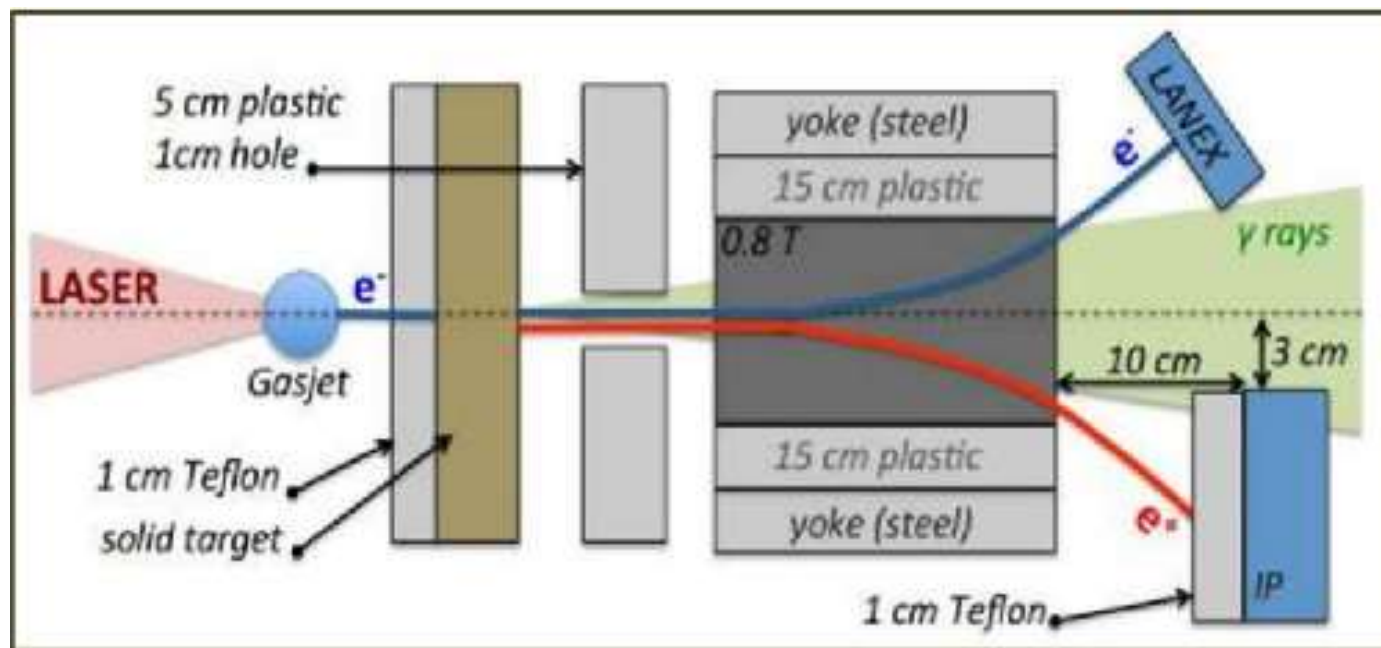


Figure 9: Benchtop Laser Setup for Electron and Positron Generation

The laser approach to positron generation involves bursts of laser light energy that bombard a solid target to produce an energised **electron stream** in the 80-200 MeV range. The Sarri paper suggests that **gamma photons** are then generated by **Bremsstrahlung**, which is caused by the slowing down of the incident energised electrons. Bremsstrahlung is more effective for target atoms with a high Z number (**atomic number**) and a high packing density. The resulting gamma photons are then considered to create an electron-positron pair spontaneously via Breit-Wheeler pair production. These newly-created energised electrons and positrons then escape from the host material and are separated to generate separate electron and positron streams.

This explanation relies upon a quite complex hypothetical process, with electrons being energised by the laser that, via Bremsstrahlung, produce gamma rays that in turn somehow interact or convert into an electron-positron pair. The Sarri paper is technically excellent, and a good read, but its convoluted multi-process interpretation for positron creation is, from the STEM point of view, unduly complicated and far from being convincing or even possible.

Should pair production be the only (or even the main) means of electron and positron creation, it raises the question: *why aren't electrons and positrons present in equal numbers in Nature (i.e. 'normal' matter)?* Pair production creates pairs of electrons and positrons, and conversely **electron-positron annihilation** destroys them in pairs by converting them into gamma radiation. Should these two processes be the only or main ones that create and destroy electrons and positrons, then electrons and positrons should be present in Nature in approximately equal numbers, but they are not. *So why is there a scarcity of positrons in Nature, and where have all the positrons gone?*

Assuming that electrons and positrons are created and destroyed in equal numbers (i.e. in pairs), there are four possible scenarios that might account for why there is such a scarcity of positrons in Nature:

- There is another process, as yet unidentified, that generates the vast quantity of electrons we find within matter without generating an equivalent number of positrons (or conversely, a process that consumes or destroys large numbers of positrons but not electrons),
- Large numbers of positrons exist within **anti-matter** (as opposed to 'normal' matter) atoms, orbiting around negative-charged nuclei, somewhere as yet to be identified in the Universe,
- Positrons are dynamically **created from electrons** by high-energy impact, or
- Positrons **pre-exist within matter**, but to date have remained hidden and undetected.

Options (a) and (b) above would seem to be highly speculative wild-card possibilities that are quite unsupported. No attempt will be made to discuss or expand either of these two options. Options (c) and (d) correspond with earlier mentioned alternative explanations 2 and 3, and are discussed in the next two chapters.

Explanation 2: Positron Creation from Electrons

Should a pair of electrons be traveling with their outflow vortices forward (the ‘normal’ orientation of electrons moving within an electric field according to STEM) and, should they be approaching each other head-on as shown in figure 10, then both their toroidal and poloidal flow components would be in the opposite direction to each other. This means that their energy fields should cushion any imminent collision and cause them to deflect each other or to rebound from each other intact.

However, should these two electrons be moving towards each other at a very high speed (such as a high-speed electron from the Sari setup of figure 9 colliding with an orbital electron), the cushioning effect their opposing energy fields could be rendered ineffective with the field energy of their outflow vortices becoming compressed with direct collision imminent. Such virtually instantaneous compression could be well expected to cause a **reversal of the poloidal flow direction** of the field energy of one or both electrons, which would instantly reverse their chirality. The result would be that one or both electrons would be converted into a positron.

So, instead of deflecting each other or rebounding from each other intact, the result of such high-speed collisions could well be the creation of two positrons recoiling from each other, or an electron and a positron recoiling from each other. Under these circumstances, the mix of particles exiting the target material would be energised electrons that have not collided with other electrons, or have survived a collision intact, combined with newly created positrons converted from electrons by head-on collision.

Sari (reference [11]), on the other hand, interprets the resultant mix of emitted electrons and positrons in terms of pair production. As explained earlier, this requires the generation of gamma rays via Bremsstrahlung of the energised electrons, with pairs of gamma rays would then somehow converting into an electron and a positron via pair production - quite a complex and daunting process compared with the simplicity of STEM’s poloidal flow reversal of electron field energy.

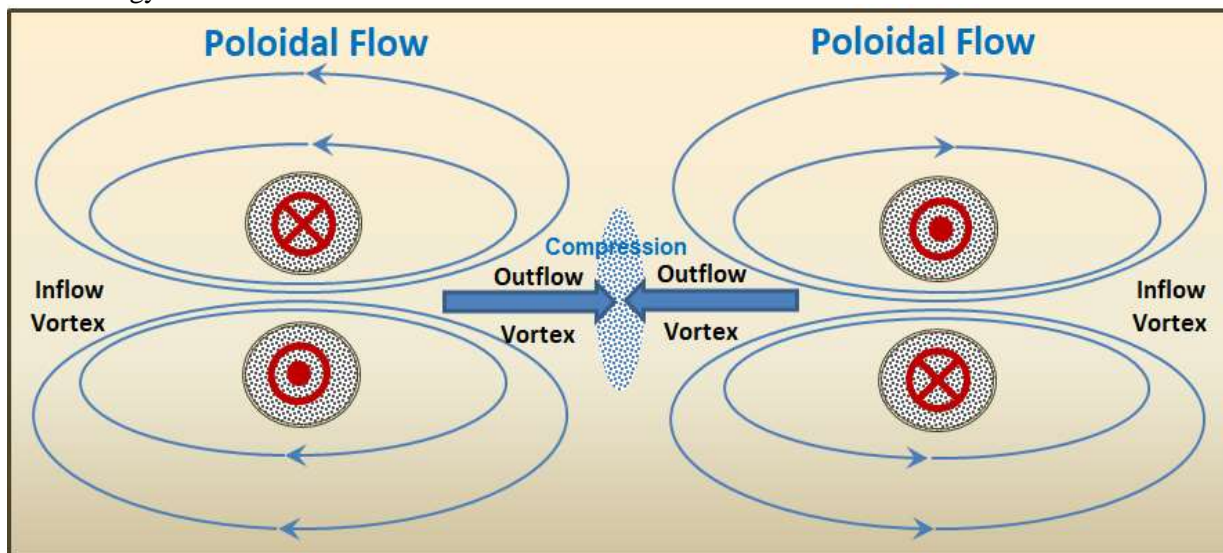


Figure 10: Head-on Collision between Two Electrons

The poloidal flow reversal of electron field energy can be interpreted as a process of **positron creation**, but it is really an electron conversion process. It is worth noting that a similar reversal of poloidal field energy flow direction is used to explain nucleon-type reversal (i.e. changing a neutron into a proton and vice versa) in STEM’s explanation of Beta decay and Electron Capture (see reference [17]).

Explanation 3: Pre-Existing Positrons within Matter

As mentioned earlier, electrons abound within ‘normal’ material, and are readily released by electron guns, or can be ejected from metals by photons within and close to the frequency of visible light in a process called the photoelectric effect. Positrons, on the other hand, can only be produced from ‘normal’ material by high-energy impact of electrons, by gamma radiation, or via radioactive decay. This chapter explores the possibility that, as for electrons, positrons might **pre-exist** within matter but, unlike electrons, can only be released by high energy interactions such as the impact of highly energised electrons and/or by gamma radiation.

For positrons to exist within matter there would need to be a mechanism to keep them well separated from electrons so as to prevent mutual annihilation. One possibility is that they could be embedded into an atomic nucleus, which would keep them well clear of orbital electrons. This could be a possibility should a proton be a composite particle consisting of a neutron with an attached positron. This notion is supported by the generalised Beta+ decay, the equation for which is:



However, there are no known atomic theories or other evidence to support this concept, although there are some atomic theories, such as the [Structured Atomic Model \(SAM\)](#), that promote the concept of a neutron being a proton with an attached or shared electron. The Beta- (Beta Minus) decay process, which is the reverse process of Beta+ decay, converts a neutron into a proton. The generalised Beta- process equation is:



Although Beta- decay supports the SAM approach, it does not support the concept that a proton could be a neutron with an attached positron. To support the concept of a proton being a neutron with an attached positron, a positron would need to be added to the neutron on the left-handed side of the above equation; instead an electron is released by the interaction.

Although having positrons being embedded within the atomic nucleus would keep them well separated from orbital electrons and allow positrons to exist within matter, it is highly unlikely that a positron attaches to a neutron to generate a proton. The only other place that positrons could possibly exist within matter is within orbitals around the atomic nucleus. So let's have a look at the atomic orbital option.

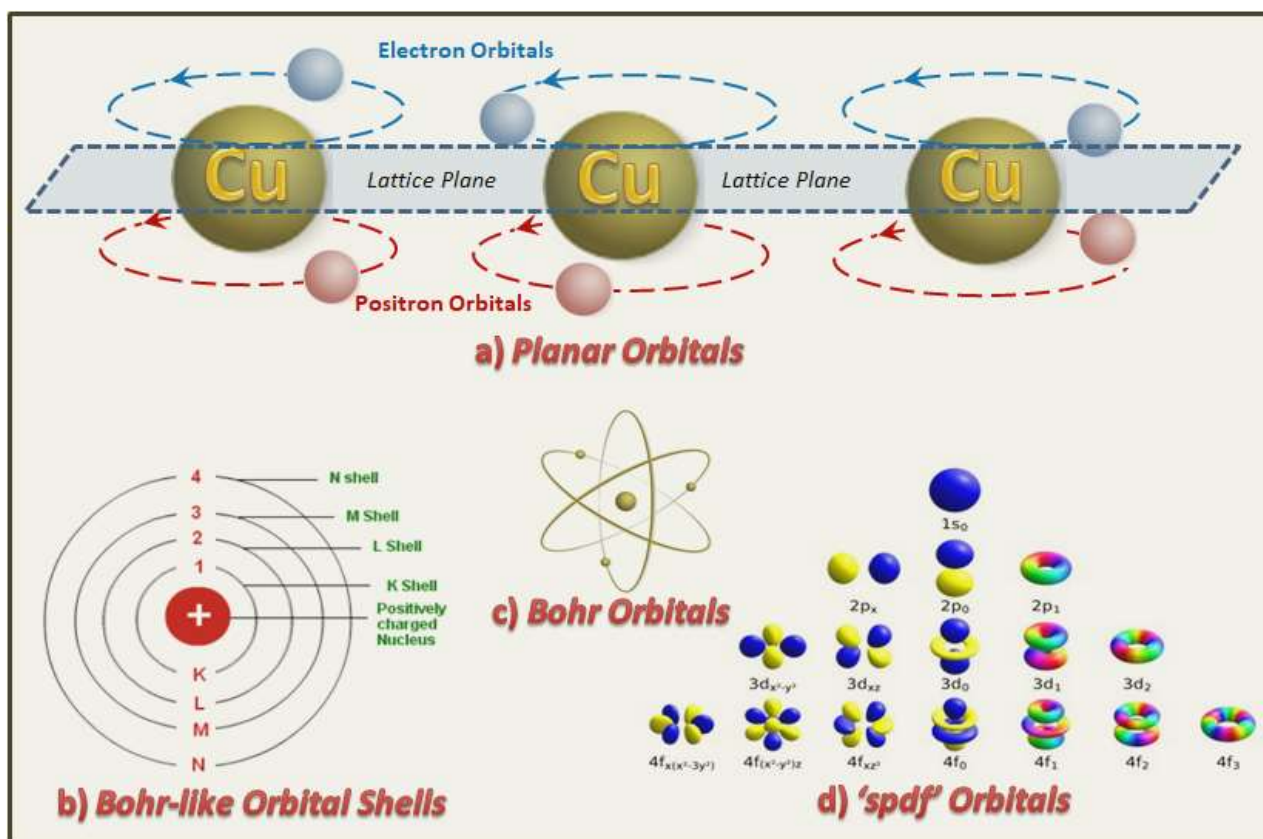


Figure 11: Alternative Atomic Orbital Schemes

For the early Rutherford/Bohr atomic models, electrons assumed shell-like planet-like orbitals (see figures 11b and c) around a nucleus. For planets, gravitational pull keeps them in orbits around the Sun, whereas electric field attraction was considered to keep negatively charged electrons in orbit around a positively charged nucleus. Since the advent of Quantum Mechanics, although 'spdf' orbitals (see figure 11d) that are derived from wave equations are far from planet-like in geometry, the planet-like sentiment remains, particularly in Chemistry texts. However, whereas our Solar has only 8 planets in orbit around the Sun, large atomic nuclei have many, many more electrons buzzing around an atomic nucleus: for example, according to conventional Science, gold, which is an enduring stable atom, has 79 electrons in orbit; uranium 92; and copernicium +112. Considering the speed of the electrons and the confined space around an atomic nucleus, this is a miraculous and mind-boggling proposition that beggars belief.

Although completely different to each other, both SAM and STEM have developed a physical structure for the atomic nucleus. With the STEM approach (see STEM's Atomic Structure paper: reference [17]), there is no need for the number of electrons to equal the number of protons for an element to be considered electrically neutral. The model thus does not support or require atoms to have multiple inner shell electron orbitals such as the inner 'spdf' orbitals or inner Bohr-like shells. Instead, STEM promotes **ionic orbitals** which, although functionally similar to those of conventional Science's conduction band electrons, have **planar orbitals** above and below the atomic nucleus rather than fully encompassing the nucleus. Geometrically, STEM's ionic orbitals are eerily similar to QM's $3d_1$ and $4f_2$ orbitals, and are about as simple a pattern as one can imagine. However, the possibilities unlocked by the adoption of ionic orbitals are amazing, particularly for explaining the cause and nature of electric current, electricity and electromagnetism.

Apart from having a planar geometry, each ionic orbital can support either electrons or positrons (not both). STEM suggests that good conductors, such as the metals, have ionic orbitals above and below their atomic nucleus, with one supporting electrons (e.g. upper as shown in figure 11a) and the other supporting positrons, so keeping electrons and positrons well separated at the atomic scale and preventing ongoing electron-positron annihilation events. This means that positrons may well be present in plain sight, having remained undetected because, apart from electric charge, they are identical. Also, unlike electrons, that are easy to eject from metals, positrons are difficult to remove from their host medium and require high-energy events to forcibly eject them.

As well as supporting the **ionisation** of elements, ionic electrons and positrons can form **covalent bonds** (see figure 12b), but without the electrons having to pass between nuclei of the bonded pair as for the conventional Science approach (see figure 12a), which requires really tricky navigation and timing.

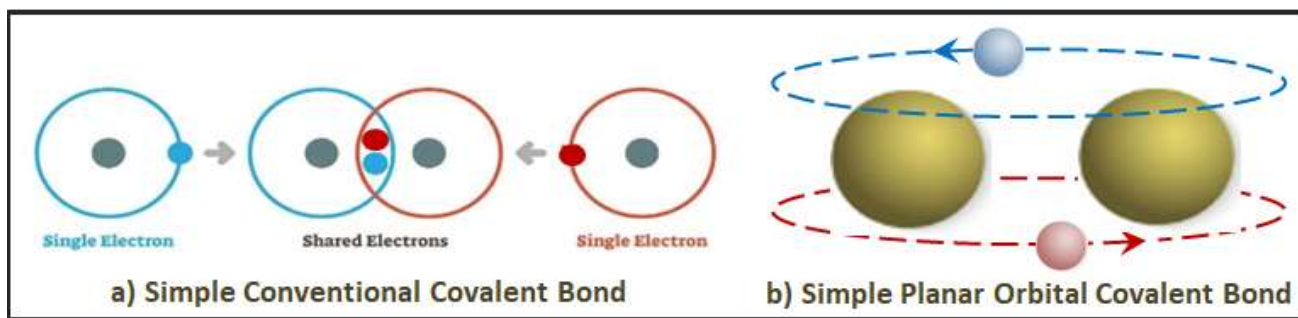


Figure 12: Covalent Bonding Schemes

STEM's proposed structure for the atomic nucleus (see reference [17]) can support ionic orbitals and provides an explanation for why positrons might be so difficult to eject from their host medium. However, even without the support of STEM's nuclear structure, ionic orbitals are just as feasible as the hypothetical QM 'spdf' or Bohr shell orbitals of conventional Science, which are somewhat oddities in themselves and in many ways incomplete.

In way of a summary, should positrons exist within matter, it would thus seem most unlikely that they would exist within the atomic nucleus. However, it is distinctly possible that they could exist within ionic orbitals. With both electrons and positrons having atomic orbitals, the only difference between them is their field energy chirality, which manifests as them carrying different charge: they both have the same mass, size, angular momentum and double-torus structure. They are both very much electrons-like, and hence the term '**duplicit electron**' used in this paper's title.

The proposition that positrons exist within matter and, like electrons, have their own orbitals, does not sit well with the conventional Science view of the atom. As soon as terms such as 'positron orbital' or 'positron charge carrier' are mentioned, the initial reaction of most people varies between confusion through to disbelief because it runs contrary to what they have been led to believe throughout their entire education. To minimise this problem, new terminology has been introduced. STEM uses the term **cetron** to refer to conventional Science's electron: the first two letters of **cetron** stand for 'clockwise electron', indicative of its clockwise toroidal spin (as shown in figure 13a). The term **aptron** is used for a positron, with the first two letters of **aptron** standing for 'anticlockwise positron'.

Furthermore, STEM often uses the term 'electron' generically so as to include positrons. When reference is made specifically to a conventional Science electron, it is variously referred to as a cetron, cetron electron or negative charge carrier (negative CC). A positron is specifically referred to as apron, apron electron or positive CC.

So, *where do positrons come from?* Should they pre-exist and occupy ionic orbitals within matter, it could well be argued that they simply require high-impact collision by energised electrons or gamma rays to dislodge and release them from their parent matter. However, a dynamic creation-and-release process involving high impact electron-to-electron or electron-to-nucleus collisions, as addressed in the previous chapter (i.e. Explanation 2), cannot be dismissed and remains a distinct possibility, particularly for the Beta decay process.

The Nature of Electric Currents

Electrical circuit theory is well established and straight forward, with electric current being defined as the one-way movement of negative **charge carriers (CC)** in the form of electrons. The Science convention, based upon like charge repulsion and opposite charge attraction, is for electrons to move from the **negative-to-positive** terminal of a power source, with Maxwell's left-hand grip rule allowing the determination of the circular magnetic field direction around a wire conductor. If, as for commercial and domestic electrical circuits, Benjamin Franklin's **positive-to-negative** flow convention be used, then Maxwell's right-hand grip rule applies, with CC movement being considered to be that of positive charge. The modified version of Maxwell's Right-Hand Grip Rule (see figure 13a) covers both situations.

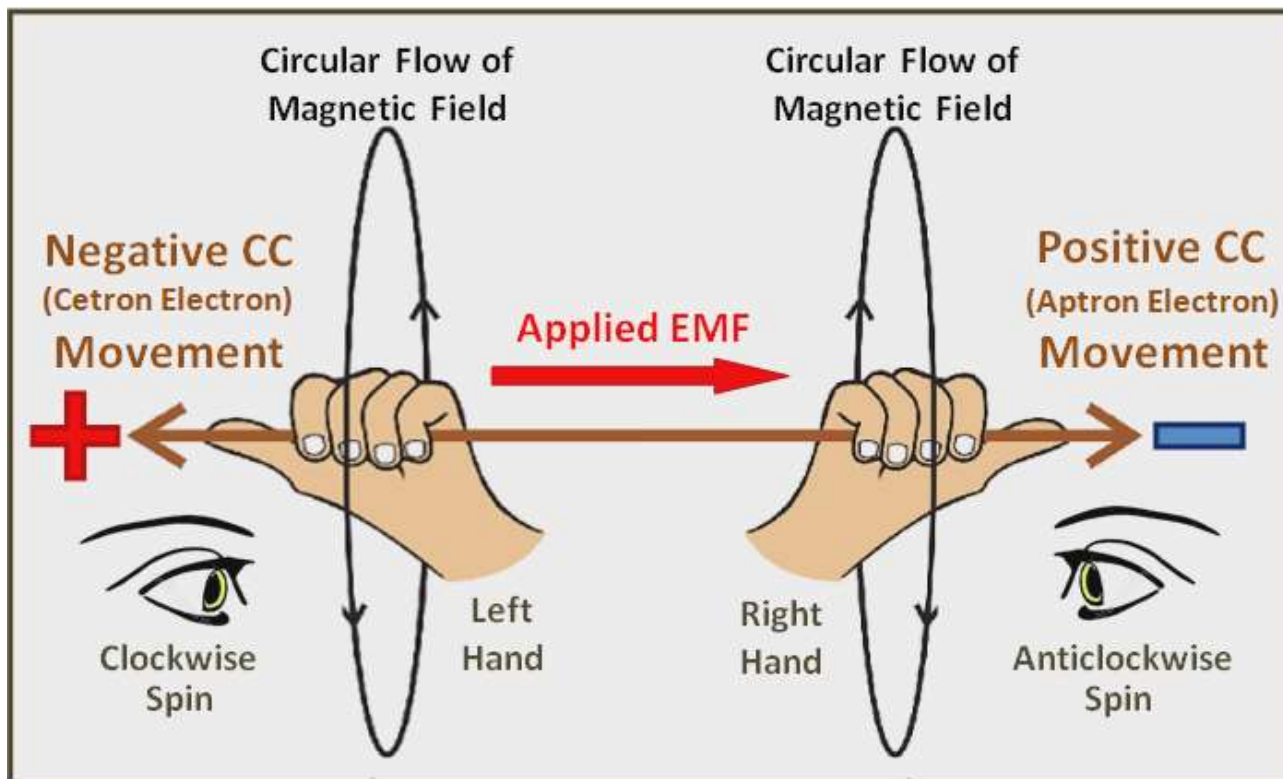


Figure 13a: Modified Maxwell's Right-Hand Grip Rule

With the development of **semiconductor** circuitry in the 1950's, it became apparent that **positive CC** as well as negative CC were required to explain electric current within semiconductor material and phenomena such as the [Hall Effect](#). Initially, panic set in because conventional Science had no positive CC that could do the job. The work-around devised to resolve this dilemma, which has continued to the present day, was the promotion of a quasi-particle, the **positive-hole** (or electron hole).

A positive-hole is a temporal **cation** that is created by the removal of an electron from a neutral atom, typically a silicon atom within the semiconductor substrate. Such cations are considered to be '**temporal**' because, at any stage, the cation (or hole) can acquire another electron to convert back into the neutral atomic state. Thus the holes can be turned ON and OFF, but they definitely cannot move or transfer positive charge because they are **static** atoms that are locked into a rigid crystalline structure.

[Clever animations](#) can create the illusion that holes can move by having the electrons hole-hopping in a coordinated fashion. Also there are convoluted explanations involving [wave-vector dispersion](#) to explain claimed quasiparticle characteristics associated with positive holes. These attempts to validate the concept do not change the fact that positive-holes cannot move as freely as do mobile electrons and, as such, do not and cannot provide the functionality required for a positive charge carrier (i.e. to transfer positive charge).

On the other hand, STEM's apron electron represents an ideal positive CC because it is just as mobile as a cetron electron. A copper atom is considered to have a pair of ionic orbitals; one supporting up to two cetron electrons and the other supporting up to two apron electrons. For **copper wire**, the initial copper rod creation process, and the subsequent multiple passes of stretching, extrusion and annealing, produce a product with outer layers of copper atoms being aligned parallel to the outer surface of wire, but becoming increasingly more randomly aligned near the centre line of the wire. When an externally generated or induced **electromotive force (emf)** is applied across a length of a copper wire, orbiting negative CC respond by skipping between orbitals (not necessarily adjacent) so as to move away from the negative terminal, heading towards the positive terminal. Orbiting positive CC move in the opposite direction away from the positive terminal, heading towards the negative terminal as shown schematically in figure 13b.

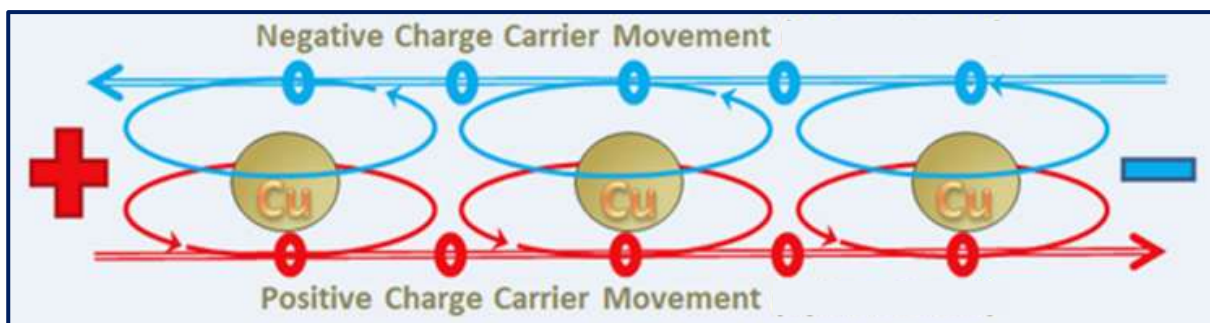


Figure 13b: Positive and Negative Charge Carriers Moving as an Electric Current

The reason why CC move under the influence of an applied emf is that, when the tangential direction of travel of a CC within an ionic orbital aligns with the direction of an applied or induced emf, the nudge received from the emf simply pushes or entices it to keep going in that direction. This results in a large number of CC skipping out of their orbitals and heading towards the appropriate terminal with their **dipolar form** helping to align them and manage their spacing in loosely-formed conga-like lines or, according to Schrödinger, strands are more likely to move as helical spires (or Zitterbewegung: reference [2]). These conga-like lines or helical spires are called **strands**.

Strands form and reform dynamically as dictated by a variety of factors such as obstructions, or flaws, kinks, or changes in carrier metal's structure. When CC meet an unpassable barrier, they either join an available nearby ionic orbital or they accumulate partially aligned, so building charge that represents a local source of emf.

Should the emf direction suddenly change, as for AC electricity, the CC simply start moving in the opposite direction, exiting from the opposite side of their ionic orbitals (i.e. at a point 180° distant), with strands quickly (almost immediately) forming in the opposite direction. A change of applied polarity in an AC circuit is like the music stopping in a game of musical chairs: when the music (emf) stops, there is an almighty scramble of CC seeking available chairs (orbitals), before the music re-starts and CC begin to skip out of their (new) orbitals, but this time moving in the opposite direction, forming new strands in the process.

The manufacturing process for copper wire creates a product whose outer-layer atoms are aligned parallel to the outer surface of wire, but become increasingly more randomly aligned towards the centre-line of the wire resulting in more resistance centrally. For DC circuits and short-distance runs of domestic AC electricity reticulation, the wires used are relatively thin and the **current density** is fairly evenly distributed across the cross-sectional area. However, for **high-voltage AC transmission lines** where the transmission wire used is thicker, the random nature of the central structure becomes more significant and a [skin effect](#) develops.

The **skin effect** is the phenomenon wherein most of the electric current flow takes place within a narrow 'skin-like' outer-zone of the wire. Within thicker long-distance transmission lines, the current density is higher near the wire surface where the copper atom crystal structure is more ordered and regular, which facilitates the ordered migration of CC. With resistance increasing with depth within the wire, with increased frequency and/or voltage, less CC movement and thus current flow occurs centrally, resulting in reduced skin depth. The skin effect thus effectively reduces the functional cross-sectional area of the wire conductor and increases the resistivity of the transmission line: at 60 Hz in a copper cable, an outer skin depth of 8.5 mm carries about 98% of the current load. For high voltage transmission wires the skin effect can be accentuated by CC travelling along the outside surface of the wire so as to cause minor arcing, which makes crackling sounds and ionises molecules in the air: due to the lower work function of cetron electrons compared with aprton electrons, these external runners are invariably cetron electrons.

One practical means of reducing the skin effect is to use transmission lines made from multiple small-diameter wires, such as the woven [Litz wire](#). Also, high-voltage, high-current overhead power lines often use **aluminium cable** strengthened with a **steel core**: the steel core has higher electrical resistance but is central, well beneath the skin depth and where little current flows. For applications involving high current (in the order of thousands of amperes) and short, straight runs, and where high transmission-line strength is not needed, **hollow tube conductors** can be used.

Within a **thin flat copper plate**, due to the pounding, rolling and annealing processes used in its manufacture, the copper atoms are aligned in planar single layer structures that are parallel to the plate faces. Thus the ionic orbital planes are parallel to the plate surfaces, which is most important to the formation of eddy currents (see the [Eddy Currents and the Hall Effect](#) chapter).

According to STEM, an electric current consists of negative and positive CC moving in opposite directions under the influence of an applied emf. So far, this concept is only a **hypothesis**. Let's now look at some **physical evidence** that can support this hypothesis and help to convert it into substantive **theory**.

An overview of the **broad evidentiary support** for there being positive CC involvement in electric current was provided in the introduction to this paper. It included lightning, which can be either negative or positive charge discharge; and solar wind, which is electrical current derived from the sun, comprising of both positive and negative charge. Cations (positive) and anions (negative) are involved in many instances of electric current within gases and liquids, including Redox reactions within chemical batteries. Nerves within animals (including humans) pass an electric signals using CC consisting mainly of positively charged sodium, potassium, calcium, and magnesium ions. The ionosphere where the positive CC are oxygen, hydrogen, and helium ions; electrical gas discharge which is due to cation and electron movement; and electric current within oceans involves salt cations and electrons.

Two forms of **direct evidence** indicating that electric an current involves the movement of both negative and positive CC are **arc welding** and **fractal wood burning**. Also, in the 2019 article '[Electrons and Holes as Catalysts in Organic Electro Synthesis](#)', Franke and Little claim that electrons and holes (i.e. aprton electrons) can act as catalysts to facilitate a number of redox-neutral transformations such as molecular rearrangements, Diels-Alder-type cycloadditions and radical substitution reactions (Note. the [Chemical Battery Power Sources](#) chapter addresses Redox reactions).

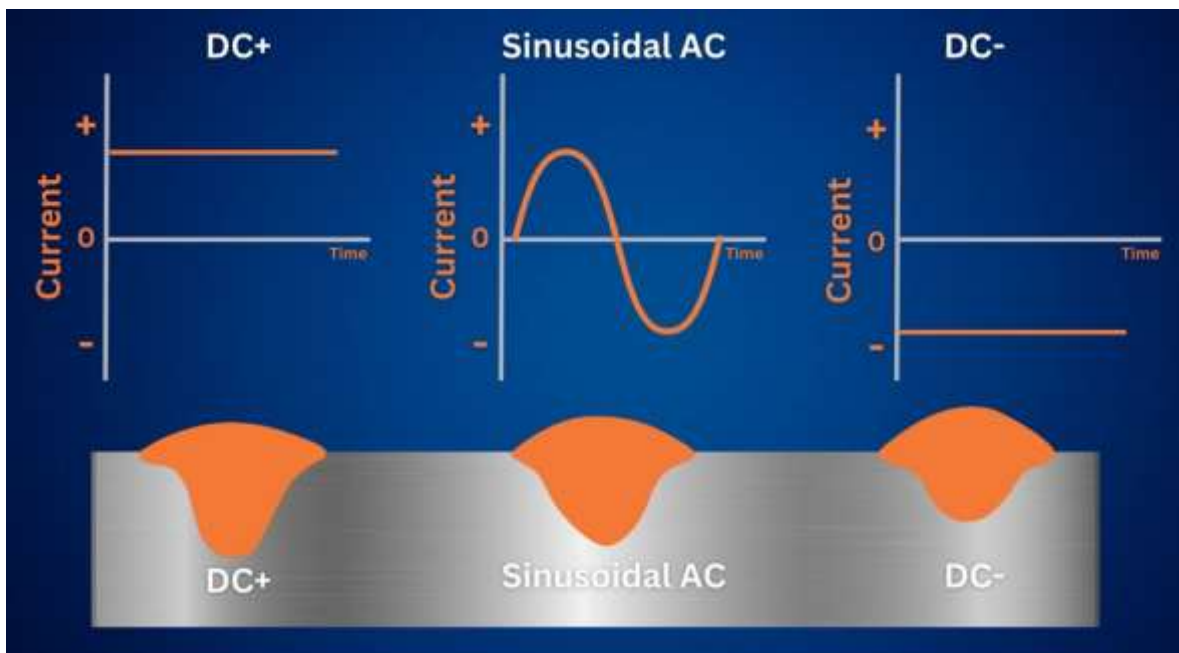


Figure 14a: DC and AC Weld Characteristics




Figure 14b: Fractal Wood Burning Example

For arc welding the welding rod may be attached to the positive or the negative terminal of a DC power supply, or to an AC power source. The arcs are created by CC jumping from the tip of the welding rod across the gap to complete the electric circuit, so generating enough heat (up to 6500^oF) to cause a partial melt of the target and the weld rod. Electrode-negative (**DC-** or straight) polarity involves the attachment of the welding rod to the negative terminal of DC power and, for electrode-positive (**DC+** or reverse or DCEP) polarity, it is attached to positive terminal. Should DC current be due to the one-way movement of cetron electrons then DC- welding is easily explained by cetron electrons from the rod causing the arc, but DC+ welding would not be possible unless cetron electrons jump from the weld-target to the welding rod, or should protons jump from the welding rod to the target, which they don't.

The characteristics of DC+ and DC- are different: DC- polarity has a faster melt-off of the electrode, faster deposition rates, and involves less power usage. Also, due to the higher work function of apron electrons that create the arc, a DC+ welding rod heats up more than a DC- rod, and because the apron electrons have to be more energised (i.e. acquire more kinetic energy) to exit the welding rod, a deeper weld results, as represented in figure 14a. However, the heating aspect of the DC+ rod is useful to melt welding flux and provide a seal to the new weld, which is most useful in many situations (e.g. underwater welding). Because it involves the alternating use of cetron and apron electrons, sinusoidal AC welding characteristics fall somewhere between those of DC- and DC+.

Fractal (or Lichtenberg) wood burning involves the use of high voltage (in the order of 2,000 volts) DC electricity to generate stunning and unique Lichtenberg figures that spread outwards through the wood from each electrode. Figure 14b is an example of the Lichtenberg figures generated by fractal wood burning. It is really worth viewing wood burning in action as demonstrated in these 3 samples: [video 1](#), [video 2](#) and [video 3](#).



Warning Fractal wood burning is an extremely dangerous process and many people die each year by attempting to create their own burnings. It is a far more dangerous process than indicated by the three videos referenced. [This video](#) provides some insight into the potential dangers. Wood burning is not just fascinating: it is deadly. So do not try it yourself unless you study the topic in depth and know what the required safety measures are, and can afford the time and financial cost to install them before proceeding.

As can be seen in all fractal wood burning videos, the Lichtenberg figures develop simultaneously from both the positive and negative electrodes as the electric current follows leader lines within the wood that represent the pathways of least resistance. Due to the high resistance of the wood, it heats up and burns to form carbon, which is a good conductor, and which allows the burning to move outwards from the electrodes. Multiple burn paths quickly develop and simultaneously expand from each electrode to produce quite stunning and unique Lichtenberg figures.

The fact that, for fractal wood burning, Lichtenberg figures develop simultaneously from both electrodes, cannot be explained by just cetron electrons moving away from a negative electrode towards a positive electrode, which is conventional Science's definition of DC electricity. On the other hand, the phenomenon can be easily explained should DC electric current consist of the simultaneous two-way movement of cetron and apron electrons in opposite directions. In fact, with the STEM approach, simultaneous burning would be expected from each electrode, and thus fractal wood burning is compelling evidence that the STEM-supported concept of electric current is valid and correct.

The above two direct forms of evidence elevate STEM's **hypothesis** that an electric current consists of negative and positive CC moving in opposite directions under the influence of an applied emf to the status of a substantive **theory**.

A simple **experiment** that would further **validate the theory** relates to arc welding. It is: *locate a strong magnet so that its magnetic field is 90^o to the arc direction of welder. Using an appropriate weld-rod type, with the welder wired for DC-welding, the weld arc should consist of cetron electrons and be (slightly?) deflected by the magnetic field as shown in the diagram right. With the welder wired for DC+ welding, the weld arc should consist of apron electrons and be deflected in the opposite direction by the magnetic field as shown right.*

The experiment should also be able to quantify the increase of kinetic energy of the apron electrons from the DC+ weld compared to the cetron electrons derived from the DC- weld.

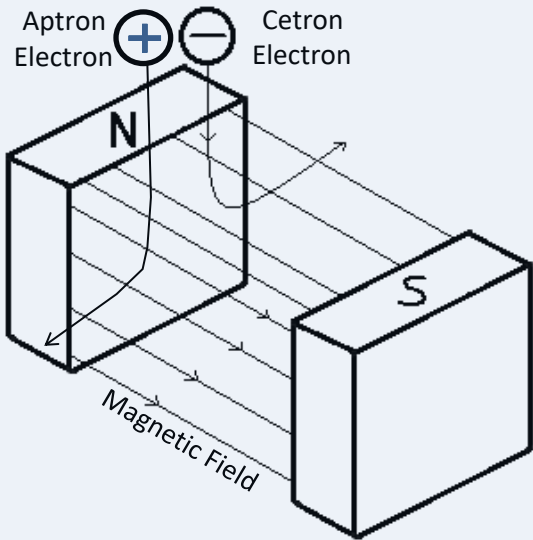


Figure 15a is a 3D X-ray representation of cetron and apron electrons freed from their ionic orbitals and moving through a copper wire under the influence of an applied emf (\mathbf{E}). The CC move as an electric current with their outflow vortices foremost. Each CC is annotated with a curved arrow indicating the direction of its outer energy field flow, with its toroidal and poloidal flow components indicated by \mathbf{T} and \mathbf{P} respectively. Note that the poloidal flow component of the cetrons is in the opposite direction to that of aprons so that they cancel each other out. However, their toroidal flow component is in the same direction and thus combines to produce the **circular magnetic field** that has a direction in agreement with the modified Maxwell's Grip Rule of figure 13a.

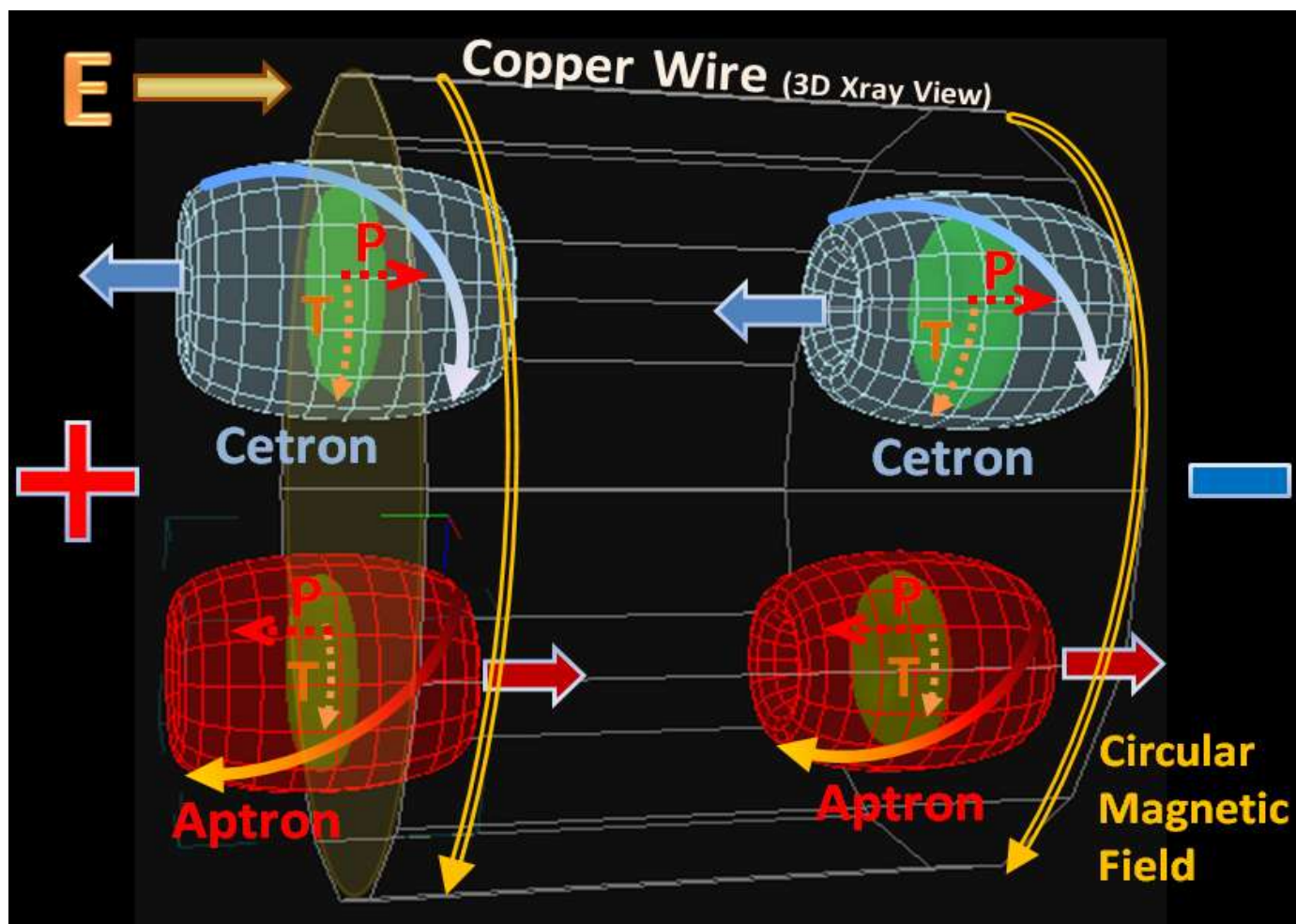


Figure 15a: EMF Induced Cetron and Apron Electron Movement

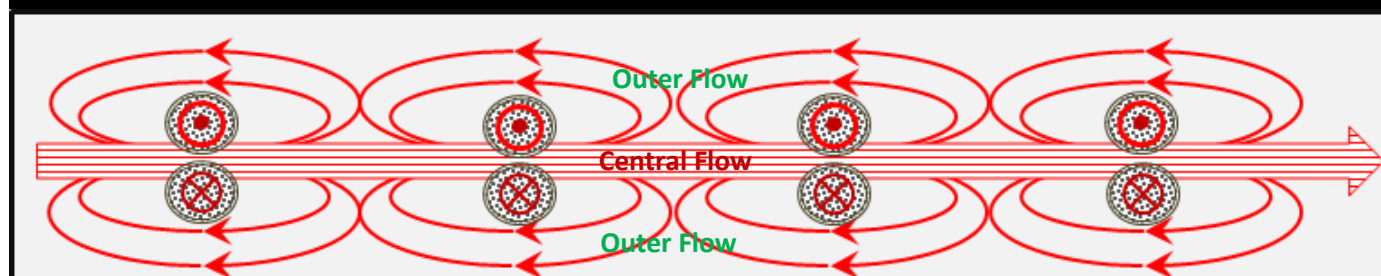


Figure 15b: Apron Electron Strand Formation

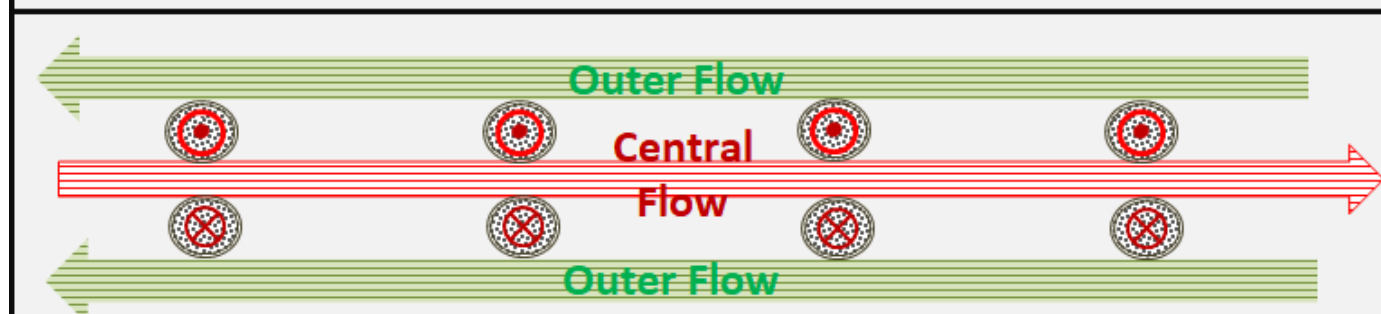


Figure 15c: Central and Outer Flows of an Apron Strand

Figure 15b is an idealised representation of positrons moving as a strand, with the field energy flowing through their energy cores combining to form a central jet of field energy labelled as its **central flow**. Their outer flows also combine to form an outer hollow cylinder of field energy labelled as its **outer flow**. Figure 15c is a generalised representation of the two flows, with the central flow streaming in the direction of CC movement and the outer flow moving in the opposite direction. The same outer/central flow pattern is generated for cetrons moving in strand formations in the opposite direction.

In a normal current-carrying wire (i.e. one not containing a capacitor), when the applied emf stops, the CC relocate to the closest amenable ionic orbital, which causes the circular magnetic field around the wire to dissipate.

The average speed of the CC within strands is in the order of 40 to 80 centimetres per hour, whereas the central flow field energy jets through the wire conductor at close to the speed of light. Thus, although the CC move relatively slowly through an electric circuit and are responsible for the current's amperage, circuits activate (or power up) almost instantly upon being switched on due to the speed of the field energy of the central flows. The outer flows are more subdued and less concentrated, but are sufficient to balance the field energy flows within the circuit.

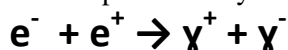
Should a pair of **metal probes** be attached to each terminal of a DC power source then the CC cannot move beyond the break in circuit represented by the probes. Instead, CC accumulate in static strand-like structures at the outer surface of the probe tips, with their central outflows extending beyond the probe tips as an **electric field**: a positive field due to the accumulation of apron electrons on the positive terminal side and a negative field due to the cetron electrons on the negative terminal side. The next chapter discusses the nature of these electric fields in more detail.

Should the probes be replaced by a pair of flat copper plates that are held parallel and close to each other, a **capacitor** is created. The gap between the plates means that no current flows between the plates, and the CC accumulate as strand-like structures at the outer surfaces of the plates, generating an electric field across the gap. Capacitor electric charge and discharge is described in more detail in the [Capacitors and Inductors](#) chapter.

The STEM suggestion that both electrons (cetrons) and positrons (aptrons) exist within matter is **new** and contrary to common belief. Below two of the most frequent questions related to this concept and STEM's response:

1. *Should electrons and positons exist together within matter, wouldn't they mutually self-destruct via the [electron-positron annihilation](#) phenomenon?*

Response: Electron-positron annihilation occurs when a cetron and apron electron collide and annihilate each other, resulting in the creation of a pair of gamma rays, each with opposite chirality, which separate in opposite directions. The energy of each gamma ray is approximately equal to the rest mass of an electron (i.e. 0.511 MeV). The annihilation process is represented by the equation:



Electron-positron annihilation occurs when positrons are allowed to randomly intermingle and interact with electrons. However, when electrons and positrons move together in the same direction, such as with positron generation in a laboratoty (e.g. as described in the 2013 article by Sarri: reference [11]) or travel within **cosmic radiation**, electron-positron annihilation does not take place, with the cetron electrons able to be easily separated from the apron electrons (or positrons) by a magnetic field,

Within a metal conductor, the negative and positive CC are confined to their separate **ionic orbitals**; and when an emf is applied, they start to skip between orbitals, with all such movement being in same-charge strand-like structures. Thus, electron-positron annihilation cannot and does not readily take place within a metal conductor.

The electron-positron annihilation phenomenon is covered in more detail in the STEM's paper on EMR and Light (see reference [18]), but here is a brief overview. Should an electron and positon be involved in a the moderately low-speed head-on collision as represented in figure 7, the poloidal component of their outflow field energy is compressed, causing instantaneous recoil. However, due to having the same toroidal flow direction, they have mutual attraction that is sufficient to prevent total separation upon initial recoil, and a rapid hammering process (hit-recoil-hit-...) ensues that converts the total energen of the particles into a pair of gamma frequency electromagnetic radiation (EMR), with photon emissions in opposite directions (i.e. 180° away from each other).

2. *If great numbers of both positrons and electrons co-exist in approximately equal numbers within metal conductors, why has the presence of positrons in matter remained undetected experimentally?*

Response: The work function for positive CC is considerably higher than that for negative CC. Thus, for low energy interactions such as the photoelectric effect, electron guns and cathode ray tubes, only electrons are emitted. Positrons are only emitted in response to high energy impact involving more than 1 MeV, such as gamma or X-ray bombardment, or by highly energised particles (e.g. electrons).

Although the reason for the much higher work function required to release positive CC is not really known, there are several possibilities. One possibility is that, for metal conductors, electron orbitals mainly face outwards whereas positron orbitals face inwards, which shields them from the relatively low energy level EMR (e.g. light). Another possibility is that motor force, derived from the electromagnetic fields of atoms within a metallic lattice, pushes 'freed' positron electrons inwards and pushes 'freed' electron electrons outwards. Yet another possibility relates to the dipole nature of electron and positron electrons: the electron electron has a pseudo-positive side (its inflow vortex side) that would be facing the nucleus as it exits the electromagnetic field of the atom, which gives it an extra push via like-pole repulsion. The reverse would apply to positron electrons, with their pseudo-negative side holding them back due to opposite-pole attraction. With there being so many possible reasons for the higher work function, there is no obvious winner, and more targeted laboratory-based research is required.

Structurally, the only difference between positive and negative CC is the chiral difference of their field energy. Moving in opposite directions as an electric current, they both contribute to the net electric charge movement and to the circular magnetic field generated around a wire conductor due to current flow. Due to their close similarity, it is most difficult to tell them apart, particularly within a metal conductor, and, with current conventional Science theory, nobody has been predicting their existence within matter, let alone be actively searching for them.

Importantly, both types of CC are needed to adequately explain the fractal wood burning phenomenon, the Hall Effect and [Eddy currents](#). Along similar lines, the arcs generated by DC- and DC+ welding rods are physical manifestations of electron electrons and positron electrons forcedly jumping a gap: a fact easily observed but rarely noted or researched by Scientists. However, in defence of Scientists, most welding technology research is undertaken by industrial OR groups rather than by particle Physicists.

Any movement of electric charge via CC, albeit in terms of just negative or just positive CC or combined, will generate a circular magnetic field around a wire conductor, and thus can be described as being an **electric current**. However, STEM contends that, for all electric circuits powered by an applied emf (albeit produced by a chemical battery, a solar-cell, a piezo-electric device, or a thermocouple device) or by **magnetic induction**, an electric current consists of electron and positron electrons moving simultaneously in opposite directions through the circuit, with each type of CC contributing equally to the circular magnetic field so generated around a current-carrying wire conductor.

The flow pattern of the energy fields of CC is important to an explanation of **motor force** (see the [Electromagnetic/Motor Force](#) chapter); and facilitates **electromagnetic induction** (the ability to induce an electric current by passing a wire through a magnetic field, as explained in the [Electromagnetic Induction](#) chapter).

As a closing note, [this video by Eric Dalgetty](#) provides an example of an electron-only electric current. Dalgetty generates a low-energy electron stream from a tungsten filament, which impacts a metal conductor collector plate. In order to maximise electron production and cause an electric current to flow, the voltage between the collector plate and anode is quite high (about 600 volts), with the copper wire coil and plate acting as a capacitor, albeit a very inefficient capacitor (see the [Capacitors and Inductors](#) chapter). The significant increase of electron concentration within the collector plate causes an electrical imbalance (i.e. an emf), and drift movement of electron electrons from negatively charged collector plate through the wire towards the LED takes place. The emf generated by the added electrons causes positron electrons to move in the opposite direction (STEM refers to this as a **sybiotic response**), with the net current movement lighting up the LED (which is wired to light up in forward bias mode). The current generated by this fairly unique setup would most likely involve more electron than positron electron movement.

It is also worth pointing out that, although conventional Science describes and quantifies the close relationship between magnetic and electric fields, it does not explain the cause of the characteristics of the fields nor provide an explanation for why or how they are related. The STEM approach provides feasible explanations for the phenomena of electromagnetism and electricity without violating any of the empirically derived laws and equations related to these phenomena. And importantly, the specific claim that electron orbitals are planar, and can support both electrons and positrons, has major implications for current atomic theory.

Electric and Magnetic Fields

An **electric field** can be represented as a vector quantity in that it has both magnitude and direction. For visualisation purposes, the abstract concept of **electric lines of force** (or **electric field lines**) was introduced by Michael Faraday in 1837, and nothing much has changed since then. Electric field lines are imaginary lines drawn to show the direction of movement of a hypothetical positive charge (e.g. a proton) within the electric field created by a single electric charge. Electric field lines point radially away from a positive charge and radially inwards for a negative charge as shown in figure 16a. Should the electric field lines be defined as being the movement of a hypothetical negative charge (as opposed to a positive charge) then the misleading arrow direction would be reversed.

As shown in the lower half of figure 16a, the STEM representation of an electric field superficially resembles Faraday's electric field lines, but without the rather meaningless directional arrows. Rather than being abstract lines, the radial spoke-like lines represent field energy emitted by the electric charge that is chiral, and which STEM calls **wisps**. The **red** wisps indicate that the field energy has right-handed chirality as derived from a positive charge, and the **blue** wisps indicate left-handed chirality from a negative charge. The wisps colour reduces outwards reflecting an outwards radial decrease of field energy density, and thus reduced field strength and a reduction of chiral coherence.

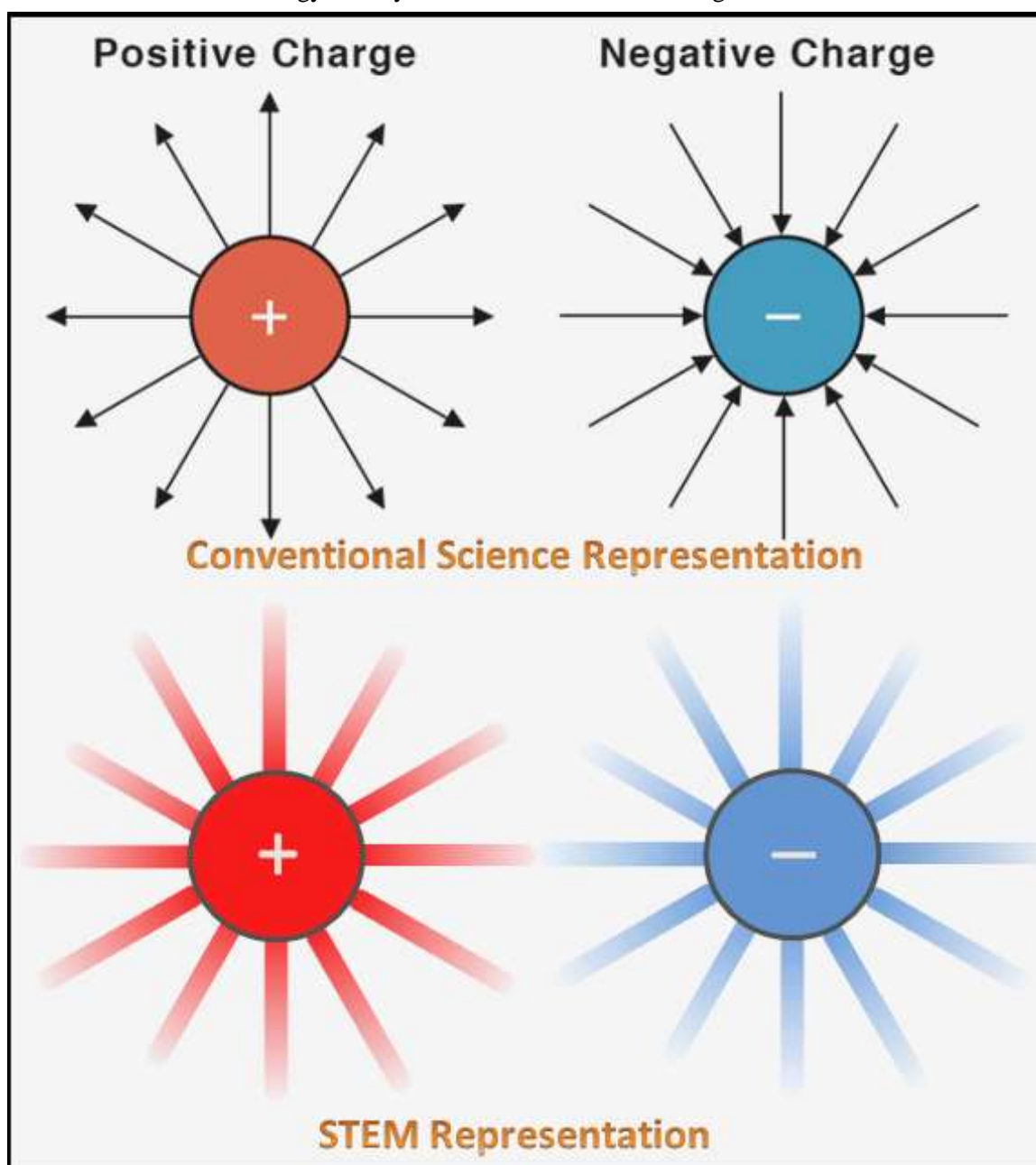


Figure 16a: Positive and Negative Monopole Electric Charge Representation

Often quoted sources of monopole negative and positive electric charge are the electron ($-1e$) and the proton ($+1e$). However, for all intensive purposes, a positive and negative electric charge effect can be created by attaching a pair of **metal probes** to the opposite terminals of a DC power source. As shown as figure 16b using the STEM notation, the electric fields associated with these probes approximate to one half of a monopole electric charge.

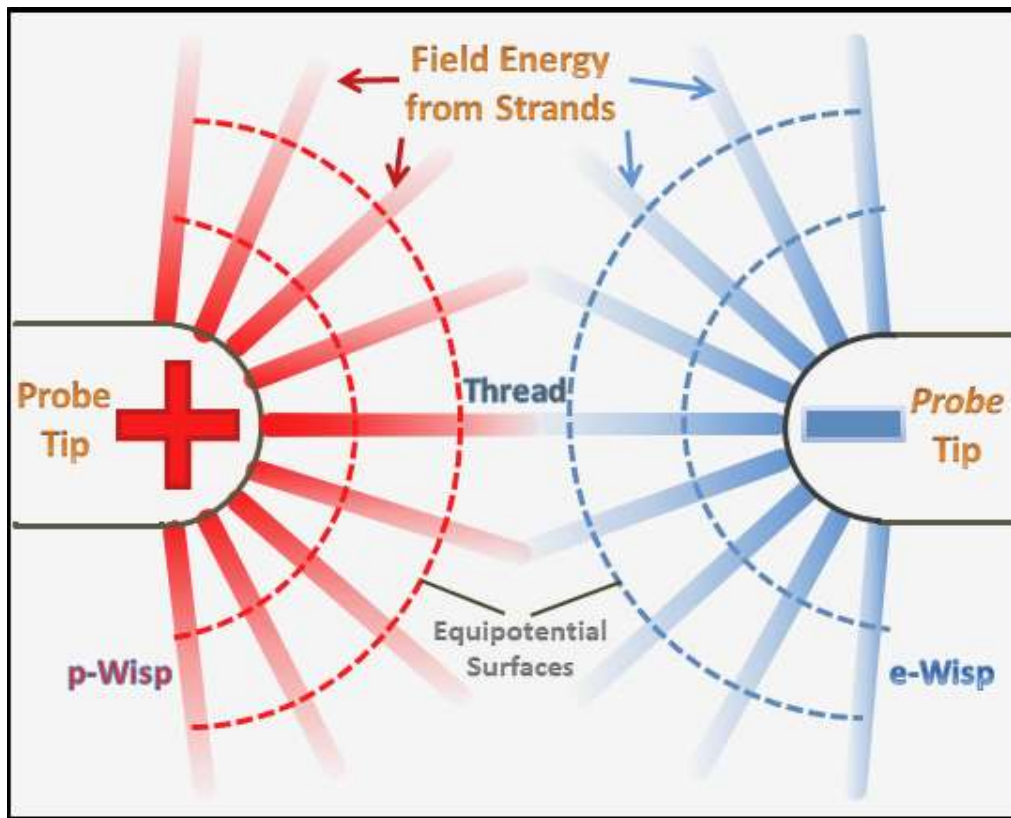


Figure 16b: Wisp Distribution around Powered-up Probe Tips

In a powered-up probe setup, the applied **emf** pushes CC towards the probe tips but, because they cannot move beyond the probe tips, they concentrate at the surface of the probe tips, forming static outwards-facing strand-like structures, with their combined inner flow field-energy extending outward beyond the probe tips as **wisps**. Upon initial power-up, a concentration (or compaction) process takes place involving minor movement of free CC as they align and shuffle closer together as wisps form and strengthen, which registers as a **transient micro-current**, after which there is no further forward movement of CC.

P-wisp emanate from the positive charge side and have right-handed chirality, and **n-wisp** from the negative side have left-handed chirality. In air, the distance that a wisp extends radially beyond its probe tip is dependent upon the strength of the emf being applied by the power source, and shape of the probe tip. The circular red and blue dashed lines of figure 16b represent **isoclines** of equal wisp-related density (or intensity).

Figure 17 is a typical representation of conventional Science’s electric lines of force between a pair of fictional monopole positive and negative charges. An electric line of force is a smooth curve drawn in an electric field for which the tangent at any point on the curve indicates the direction of the electric field at that point. To represent the lines of force that would be associated with a corresponding pair of positive and negative probes, the appropriate regions have been greyed-out in figure 17.

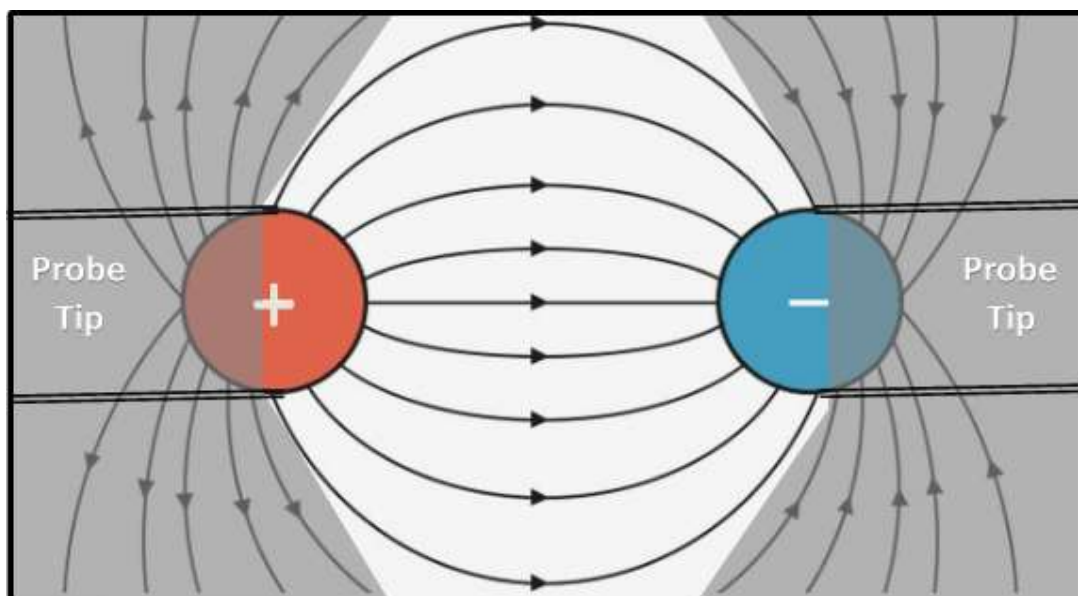


Figure 17: Lines of Force for Opposite Polarity Monopole Charges (or Probe Tips)

As for any monopole electric charge, the wisps emanating from the probe tips consist of a jet of field energy moving in a straight line, as represented in figure 16b and the top part of figure 18. Wisps are chiral, with their flow pattern reflecting the toroidal and poloidal flow components of the CC from which they are derived. Whenever n-wisps and p-wisps intersect (and there are billions of intersections in 3D), their flow components are additive (or subtractive). Looking at just the toroidal component at selected intersection points, a tangent to the **net toroidal flow** can be determined: they are the thin dark lines annotated as ‘Tangents to Net Circular Flow’ in figure 18.

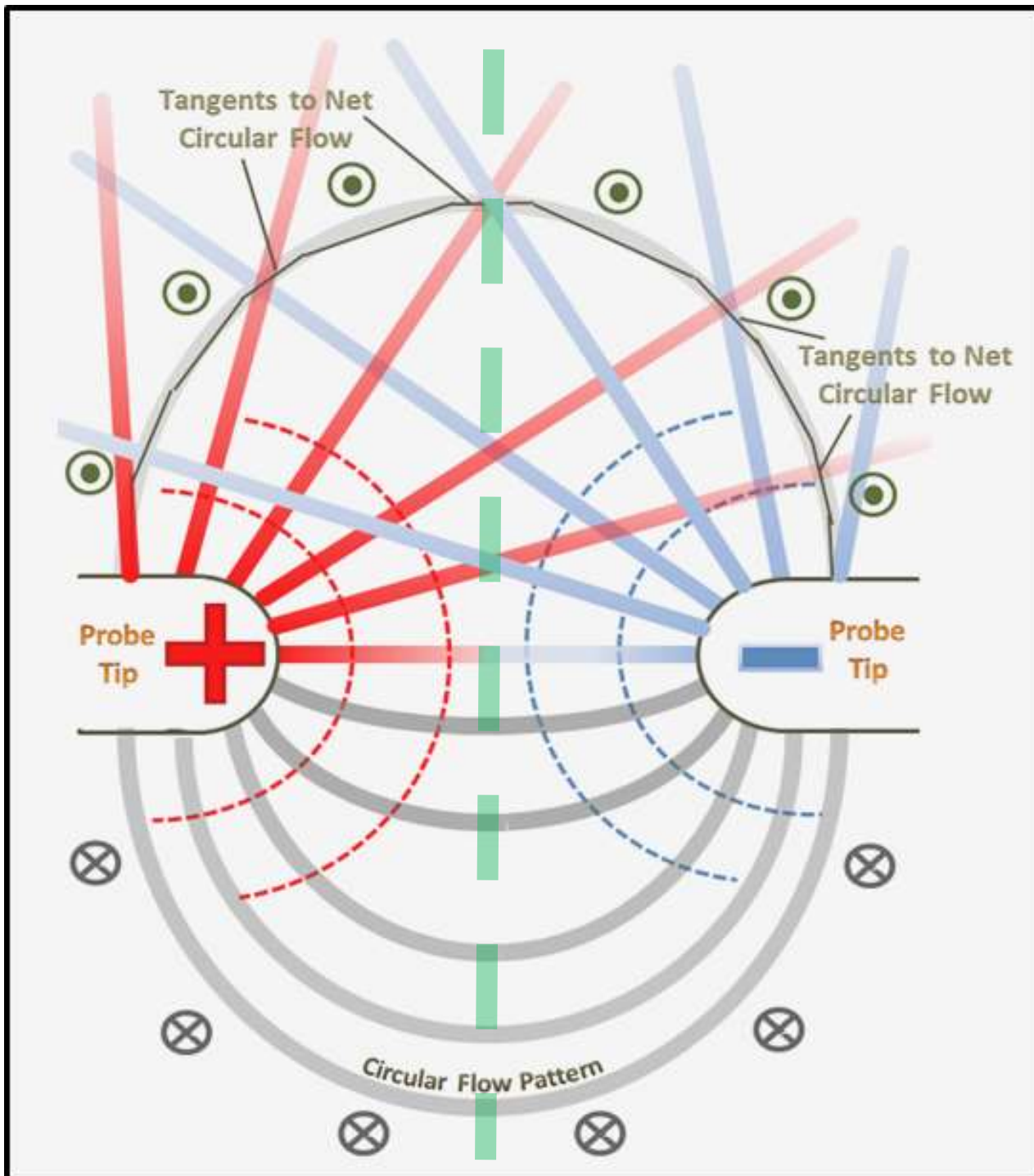


Figure 18: Circular Magnetic Field and Pseudo-Thread Formation

The ‘Tangents to Net Circular Flow’ of figure 18 represent the tangential direction of the **circular magnetic field** component of the electric field between the probes, which is analogous to the circular magnetic field produced around a current-carrying wire. The grey arrow-heads indicate that the circular magnetic field flows out of the page, and the arrow-quills a flow into the page. It is worth noting that in the 1860’s **James Clerk Maxwell** identified the circular magnetic field component within an electric field, but incorrectly attributed it to a non-existent [displacement current](#): no such displacement current was ever found but the terminology has persisted.

The **locus of the tangents** shown generates an elliptical arch connecting the probes, shown as banding in the lower-part of figure 18, grey-scaled to highlight the reduced electric field intensity moving away from the centre line between the probes. These elliptical arches have a similar geometry to conventional Science’s electric lines of force

(see figure 17), and they join opposite polarity electric charges (here the pair of probes) and are called **threads**. Threads are **notional** rather than physical but, unlike abstract lines of force, they are not directional because there is no net transfer or purposeful exchange of field energy (i.e. energen) between the probes (or any pair of electric charges).

Figure 19 is a composite representation of the key aspects of the electric field between a pair of probes as a lead-up to a discussion of the behaviour of free CC within the electric field.

Field energy is pumped out from the probes via wisps at a rate that is in excess of the more gentle retrieval rate of their inflows. Consequently, field energy accumulates centrally between the probes in the area labelled '**Central Accumulation Region**' in figure 19, with the dark grey dashed graph providing an indication of the field energy distribution profile between the probes. With an equal flow from each probe, there is no transfer of field energy across the plane between the two probes, with the electric field being zero within this plane. This corresponds to the conventional Science view that, at the central plane between a positive charge (+1e say) and an equal negative charge (-1e say), the electric field is zero.

Realistically, minor amounts of field energy is leaked to the outside world and thus become lost from the probes, but there is no net transfer of field energy flows between the two probes (or any corresponding electric charges). This means that the field energy of the circular magnetic field (its direction is once again indicated by the arrow-points and arrow-quills in figure 19) consists of a denser concentration of field energy centrally. The central concentration of field energy is also the reason why the circular isoclines indicating equal field energy distribution (see figure 18) have been removed from figure 19: such isoclines are only meaningful for an isolated monopole electric charge.

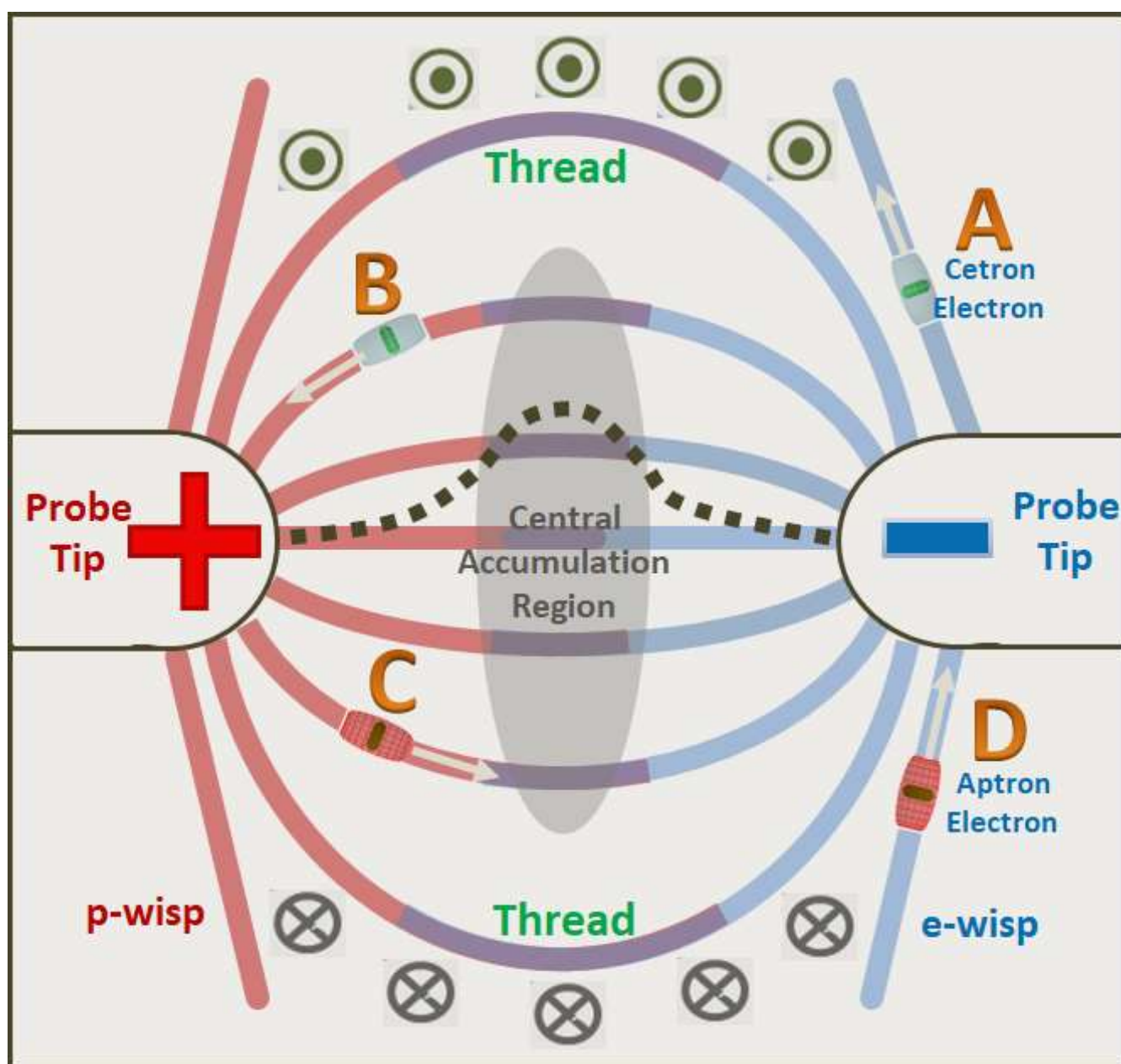


Figure 19: Thread/Wisp and Circular Magnetic Field Patterns for a Pair of Probes

The spin axis of **free CC** within an electric field are aligned to the circular magnetic field, which means that their orientation corresponds to the direction of the thread in which they find themselves, as shown in figure 19. This, however, does not mean that they keep in or move along any particular thread because their movement is controlled by the wisps they encounter, the circular magnetic field, and the effect of the central concentration of field energy between the probes.

With its outflow vortex foremost, the poloidal and toroidal components of the field energy flow of **cetron A** in figure 19 would correspond to that of the e-wisps from the negative probe tip, causing it to move away from the negative probe tip in the e-wisp outflow direction. The movement of this negative CC is like that of a leaf moving within a stream, and is attributed to **like-charge repulsion**. As the e-wisp flow rate and chirality dissipates outwards away from the probe, the like-pole repulsion effect reduces.

Cetron B also moves with its outflow vortex foremost, and is under the influence of p-wisps. As its toroidal flow component is compatible with that of the p-wisps, its outflow field energy is readily drawn in by p-wisp inflows (i.e. the inflow of p-strands within the positive charge probe tip), which causes it to be pulled towards the positive probe. Such movement towards the positive probe accelerates the closer the cetron is to the probe tip and is attributed to **opposite-charge attraction**.

Similar explanations apply to the movement of aprons C and D, but with their toroidal flow component being the reverse of cetrons, free aprons behave as if repelled from the positive probe and attracted to the negative probe.

Keep in mind that 2D diagrams of electric and magnetic fields are a cross-section of a 3D structure, with the circular magnetic fields, threads and central field energy distribution profiles being curved 3D surfaces (e.g. ellipsoids, cubic spline surfaces etc.). Wisps, on the other hand, are lines that each has a different orientation that is perpendicular to the part of the probe surface from where they are generated, with those shown being only a representative sample of those within the cross-sectional plane. Along similar lines, the free electrons (cetrons and aprons) shown in figure 19 would move in the direction of the circular magnetic field as well as laterally, and would thus follow a spiral trajectory.

Whenever two **electric charges** are brought reasonably close to each other, wisp outflow energen causes a central accumulation region. When **opposite charge** probes are brought close, as shown in figure 19, the central energen circulates as a circular magnetic field that is derived from the combined toroidal flow component of the e-wisps and the p-wisps. This flow direction movement is compatible with and amenable to being retrieved by the inflows of the static strands responsible for the wisps. The combined pull by the strand inflows on the denser central accumulation of field energy draws each probe inwards which is interpreted as **opposite-charge attraction** (or mutual attraction) between the two probes. The closer the probes get to each other, the denser the accumulated field energy becomes, and thus the mutual attraction increases accordingly.

As the probes get really close to each other, wisp field energy from each probe can reach and be drawn in more directly by the inflow of other probe, resulting in very strong attraction. When the probes are about to touch, the central field-energy outflow of each probe is almost fully taken up the inflow of the other probe and, should the emf of the power source be high (in the order of 1000 plus volts), the energen outflow can be so strong that some outer cetron electrons in the static strands of the negative probe prematurely jump the gap. As they jump the gap these cetron electrons ionise air and water molecules along the way, so generating heat and light that ranges from an **electric spark** to an **electric arc**.

Due to apron electrons having a higher work function than cetron electrons, they require more forceful coercion to leave the host medium in comparison to cetron electrons. Consequently, it is only cetron electrons that prematurely jump the gap from the negative to the positive charged probe. However, with a setup such as DC+ welding, enough energy can be supplied to coerce an apron electron arc to be generated.

By the time that the two probes are in physical contact with each other, there is suddenly zero electrical resistance and, unless there is an adequate resistance in the circuit attached to the probes, a rapid and un-moderated energy transfer occurs which is called a **short-circuit**

When two electric charges with the **same charge** are brought close together, their wisp outflow field energy has the opposite toroidal flow direction to each other which results in an accumulation of central energen that is **stagnant** (i.e. it has no significant circular flow movement). Wisp outflows from each pole (or probe) thus push against the central concentration of stagnant field energy, so pushing each other further apart, which is interpreted as **like-charge repulsion**.

Although the phenomena like-pole repulsion and opposite-pole attraction for electric and magnetic fields may appear similar and all involve the interaction of field energy; however, the mechanisms involved are subtly different,

Experiment STEM claims that for a pair of electric charges there is a central accumulation of field energy centrally. When the pair are of opposite charge, it is claimed that a circular magnetic field builds up centrally but, for same charge pairs there is no circular magnetic field, although there could be a slight circular field moving in opposite directions detectable near to each charge. This can be easily tested by attaching two probes (effectively in parallel) to each terminal of a DC power source to provide two positive and two negative probes, and checking both situations.

Should the probes be replaced by a pair of copper plates that are held parallel and close to each other, a **capacitor** is created. The gap between the plates results in no current (i.e. CC) flow between the plates, but a wisp-based electric field and associated circular magnetic field are created between them. Capacitor electric energy charge and discharge is described in more detail in the [Capacitors and Inductors](#) chapter.

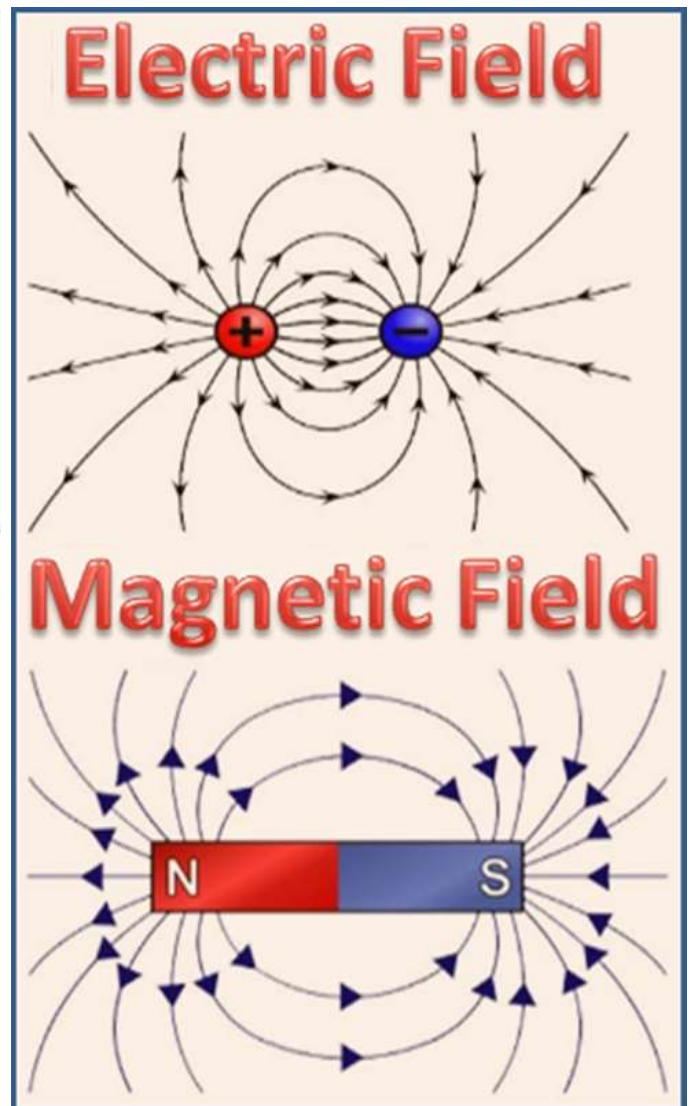
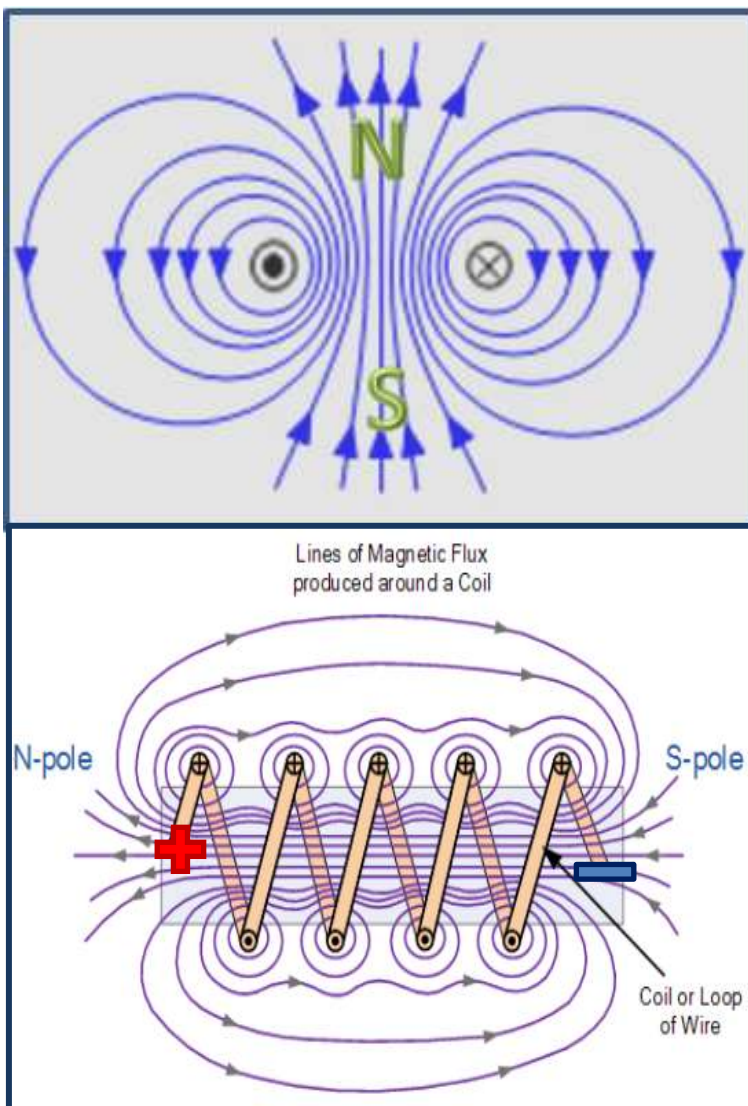


Figure 20: Magnetic Field Induced by a Current Loop

Figure 21: Electric and Magnetic Field Patterns

When an electric current is passed around a looped wire, a **loop current** is created with the duplex movement of cetrans and aptrons around the loop generating a circular magnetic field that passes through the centre of the loop. Assuming a conventional positive-to-negative current flow for figure 20, Maxwell's Right Hand Fist Rule provides the circular magnetic field direction which concentrates centrally so as to generate **implied** North and South poles as shown. The magnetic lines of flux so produced are similar to those that form around a bar magnet (figure 21). Multi-loop **coils** increase the intensity (or flux) of the generated magnetic field for each added loop. An increase in the electric current flow rate within the coils will also increase the flux levels.

A significant difference between a magnetic and an electric field is that a magnetic field has no net poloidal flow component whereas an electric field has distinct poloidal and toroidal flow components. Also, a magnetic field involves divergent flow of field energy away from a North pole and convergent flow into a South pole, albeit via implied poles. An electric field, on the other hand, has no net flow of field energy between electric poles, but does have a circular movement of field energy between poles in the form of a magnetic field. Small wonder that electric and magnetic fields are considered to be closely inter-related as encapsulated by the term ‘**electromagnetic**’.

As for an electric field, in a perfect world, no field-energy flux is lost from a magnetic field, with the field-lines being closed loops which never begin or end as shown bottom in figure 21. But unlike electric fields for which wisps are straight, magnetic lines of flux are always curved and never straight, and the net magnetic flux through any closed surface (i.e. enclosed and that flowing in and out) is zero (i.e. $\Phi_B = 0$).

An explanation has already been provided for attraction and repulsion for positive and negative charge, and for free charged particles within an electric field. The explanation of attraction and repulsion are similar for electric and magnetic poles, but are certainly not the same.

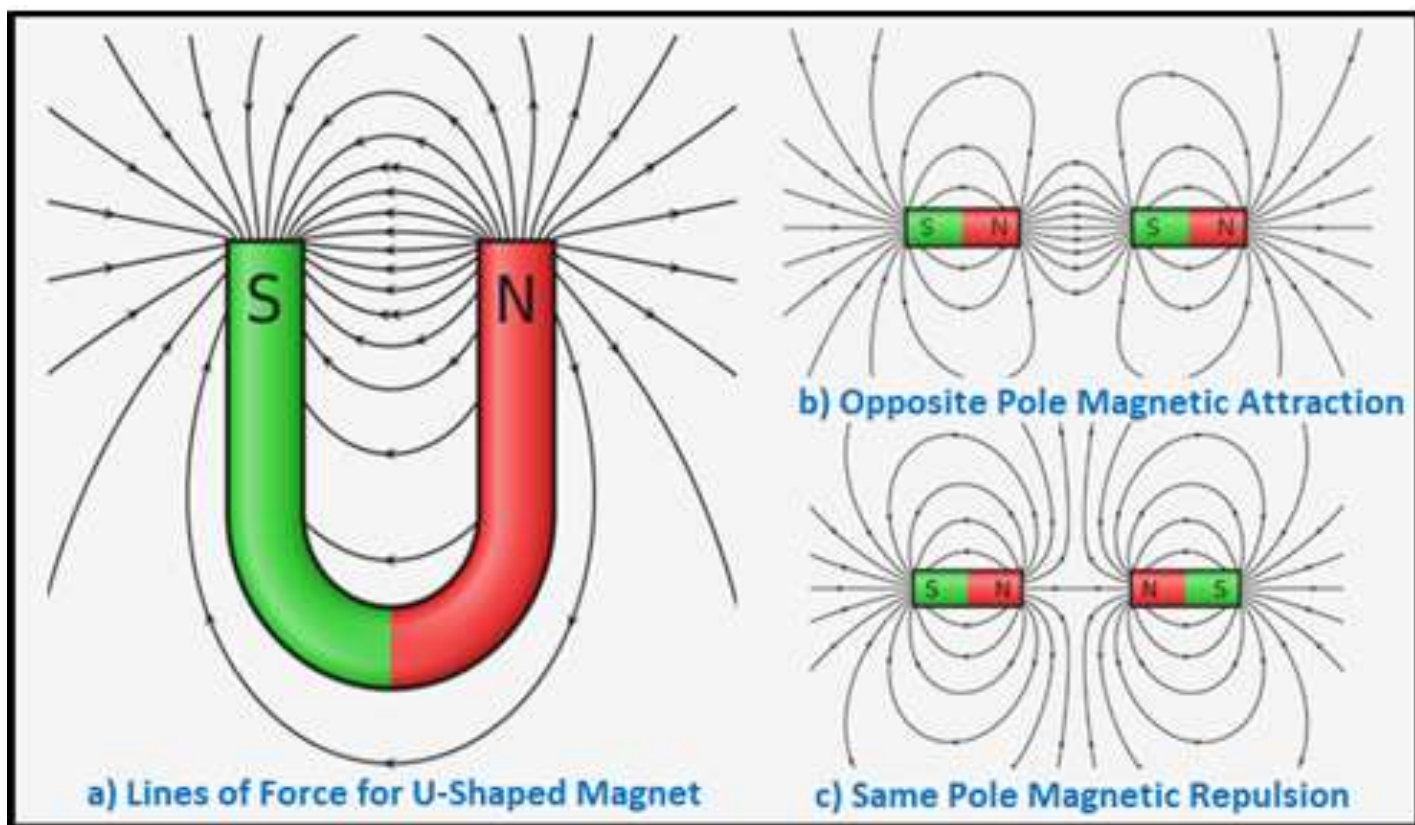


Figure 22: Opposite Pole Attraction and Like Pole Repulsion for Magnets

With magnetic flux flow from a North pole into a South pole, as shown in the field-energy lines of figures 22a and 22b, the South pole acts like a fishing-reel that pulls or draws the North pole towards itself, which is interpreted as opposite-pole attraction.

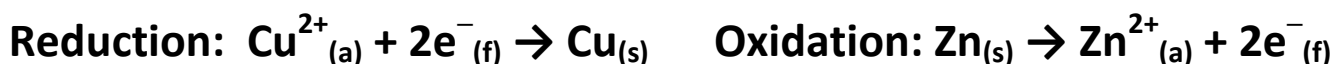
When both poles are North poles, the magnetic flux (field energy) outflow from the North poles push against each other and have nowhere to go except outwards as shown in figure 22c, which is interpreted as magnetic like-pole repulsion. When both poles are South poles, the only way that field energy can be obtained is sideways between the South poles, which becomes compressed to produce a similar flow line pattern to like North poles, except that the flow direction is reversed; however the result is the same, and that is magnetic like-pole repulsion.

To recap, STEM’s notional threads and conventional Science’s electric lines of force are similar but not equivalent. Diagrams for conventional Science’s lines of force (e.g. figure 17 or top in figure 21) are quite misleading because they clearly suggest a one-sided flow of field (or electromagnetic) flux from the positive to the negative charge which, if true, would lead to a charge imbalance. For STEM, there is an accumulation of field energy centrally that has a circular flow that presents as a magnetic field for a pair of opposite charges; or is stagnant, with no circular flow or magnetic field, for a pair of like charges. In neither case is there a net transfer or exchange of field energy between the charges.

Chemical Battery Power Sources

Redox reactions, involving metal electrodes immersed within aqueous solutions, lead to the operation of [galvanic \(or voltaic\) and electrolytic cells](#). Figure 23a shows a galvanic cell setup involving copper and zinc electrodes; the two electrolytes are 1M aqueous solutions of copper sulphate and zinc sulphate respectively; and a salt bridge containing sodium sulphate.

The (with standard reduction potential of -0.76 volt); thus copper undergoes reduction, which defines the **cathode**, and zinc is oxidised, which defines the **anode**. Only the copper and zinc are involved in the redox reaction, with the anions being spectator ions and can thus be left out of the equations, with the full equation (bottom of figure 23a) usually being broken down into 2 **half-equations** (as shown below) to highlight the redox reactions involved.



Whereas conventional Science provides only one source/sink pair for electrons, STEM provides for two source/sink pairs and two half-equations for each reduction and oxidation reaction as shown in the table below:

	Half Equation	Reduction Oxidation	Cathode Anode	Galvanic Cell (Battery)	Electrolytic Cell (Re-Charge)
Conventional Electron	$\text{M}^+ + \text{e}^- \rightarrow \text{M}$ $\text{M} \rightarrow \text{M}^+ + \text{e}^-$	Reduction Oxidation	Cathode Anode	Sink Source	Sink Source
STEM Cetron	$\text{M}^+ + \text{e}^- \rightarrow \text{M}$ $\text{M} \rightarrow \text{M}^+ + \text{e}^-$	Reduction Oxidation	Cathode Anode	Sink Source	Sink Source
STEM Apron	$\text{M}^+ \rightarrow \text{M} + \text{e}^+$ $\text{M} + \text{e}^+ \rightarrow \text{M}^+$	Reduction Oxidation	Cathode Anode	Source Sink	Source Sink
STEM Other	$\text{M} + \text{e}^- \rightarrow \text{M}^-$ $\text{M} \rightarrow \text{M}^- + \text{e}^+$ $\text{M}^- \rightarrow \text{M} + \text{e}^-$ $\text{M}^- + \text{e}^+ \rightarrow \text{M}$	Reduction Reduction Oxidation Oxidation			

The STEM half-equations involve both cetron (e^-) and apron (e^+) electron source/sinks, with the cetron source/sink equations are the same as those for the conventional Science half equations. Subscript **a**=aqueous; **s**=solid; **f**=free.

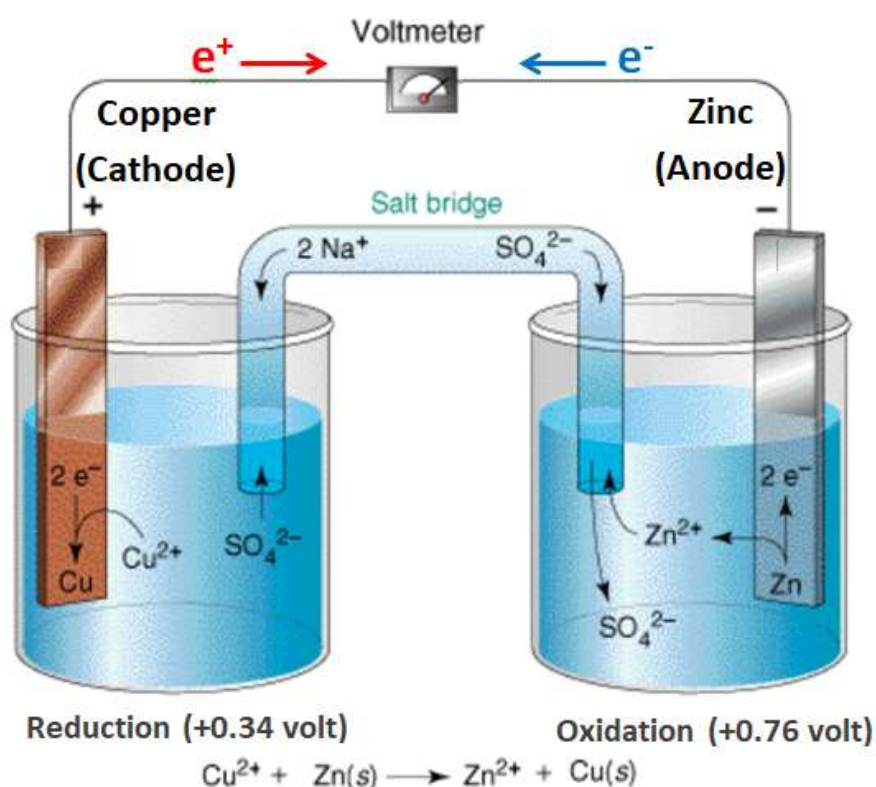


Figure 23a: Copper-Zinc Galvanic Cell

Copper and zinc atoms each have three hexadecagon (16-gon) outer layers, which means that both have a complete upper outer neutron layer and a complete lower outer neutron layer (or vice versa). As a neutral atom with no orbital ionic electrons, they can act as an **aptron sink** by acquiring one or two orbital aprtrons attached to the outer proton layer's ionic orbital. Similarly, the cations Cu^{2+} and Zn^{2+} can become neutral atoms by losing their two attached orbital aprtrons, so acting as an **aptron source**; or, by acquiring two orbital cetrons in their outer neutron layer's ionic orbital, so acting as a **cetron sink**. In the latter case, the neutral atom has two orbital cetrons and two orbital aprtrons, that has the propensity to release the two cetrons to convert into a cation, so acting as a **cetron source**.

When copper cations in solution come in contact with the copper cathode, some convert into a neutral copper atom by shedding aprtrons, so creating an **aptron source**; others in the same ionic mix take up cetrons so as to create a **cetron sink**. Both processes, acting in unison, result in the deposition of copper metal on the copper cathode, so generating an emf of approximately 0.34 volt.

On the **zinc anode** side, neutral zinc atoms on the outer surface of the anode consist of a mix of those with two orbital cetrons and two orbital aprtrons, which shed cetrons to create a **cetron source**; and those with no orbital electrons which take up aprtrons to create an **aptron sink**. Both processes acting, in unison, result in the etching of metallic zinc from the outer surface of the anode, an increase of zinc cations in the electrolytic solution and the generation of an emf of approximately -0.76 volt. The net voltage for this galvanic cell is thus 1.10 volt (calculated as $0.34 - (-0.76)$).

The two-way movement of aprtrons and cetrons serves to balance the chemically-induced charge imbalance between the electrodes, but not the chemical imbalance in the aqueous solutions; the latter results in a reduction of cations on the cathode side and build-up cations on the anode side. The salt bridge offsets ionic charge imbalance by allowing excess anions on the cathode side to move to the anode side and, conversely, excess cations on the anode side to the cathode side (albeit via a proxy of sodium sulphate electrolytic solution) to maintain the ionic balances of each cell.

With the STEM approach, positive and negative CC (aptron and cetron electrons) are generated by CC source electrode reactions, and removed by the sink electrode reactions: it is a self-sustaining system without any need for positive and negative charge to travel between electrodes via the electrolyte. The salt bridge simply provides the means for the ionic balance of the electrolyte to remain neutral and stable, rather than to repatriate electrons back to the anode from the cathode to complete the circuit.

The conventional Science model for a galvanic cell is not a balanced system. It involves the one-way movement of electrons (or cetrons) from anode to cathode, but a two-way exchange of positive and negative ions via the salt bridge. To be balanced and totally conform with the **law of conservation of energy**, only a one-way movement of negative charge (in the form of sulphate anions in figure 23a) from the cathode to the anode side via the salt bridge would be required to compensate for the one-way movement of negative charge through the connecting wire; or, **alternatively**, the electric current could consist of a two-way movement of positive and negative CC (which is the STEM approach) and a matching two-way movement of ionic charge in the other direction. In terms of energy transfer, the STEM approach has a distinct advantage.

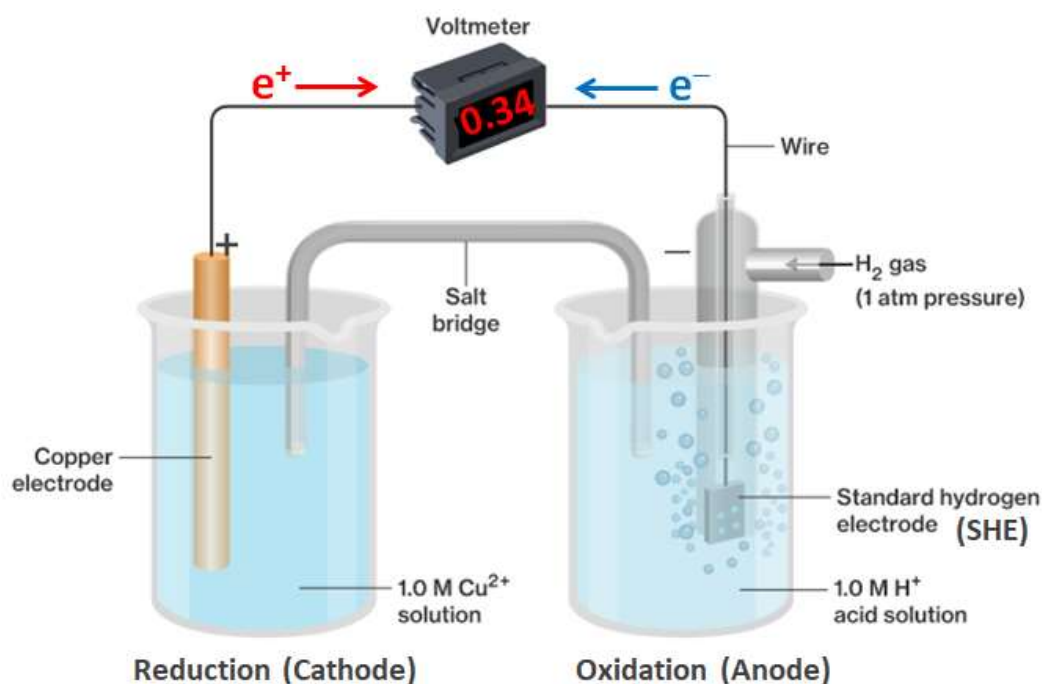


Figure 23b: Standard Reduction Potential (E^0) Cell

Bitron Bond Primer

STEM introduces a bond between atoms called the **bitron-bond** (or **b-bond**), which have a length in the region of 100 pm long (or less). A detailed description of how b-bonds form is beyond the scope of this paper, but details can be found in the ‘Electrons and Atomic Bonding’ chapter of STEM’s Atomic Structure paper (reference [17]).

A **bitron**, which forms within a b-bond, is an electron-like concentration of energy that is a **pre-cursor** to the generation of an electron. A **bitron** can be bump-released by the impact of an excited free electron, or by a photon (EMR) or by radioactive particle bombardment, or via chemical reaction (e.g. Redox). Upon its release from a b-bond there is equal probability that a bitron will become a **cetron** electron (a negative charge carrier) or an **aptron** electron (a positive charge carrier) depending upon its exit-angle from the bond upon release.

Although some newly released electrons may be captured internally and become ionic orbital electrons, some cetron electrons with sufficient kinetic energy can escape as **free electrons** (high-energy processes are required to free aprons). The number of electrons associated with an atom can thus be considered to be the number active in cetron and apron ionic orbitals plus the number potential cetron/apron pre-electrons in the form of bitrons within b-bonds.

The creation of cetrons and aprons by bitron release from b-bonds provides an alternative process to pair production. Another electron creation process is the high-impact type-conversion of cetrons into aprons, although low-energy release of cetrons from electrical conductors involves pre-existing electrons rather than being electron-creation.

A **standard hydrogen electrode (SHE)** is used to determine the **standard reduction potential (E^0)** of other elements. A SHE consists of a chemically **inert electrode**, typically a standard size and grade of platinum (Pt) plate, immersed in a 1M hydrochloric acid (HCl) solution with H_2 gas is bubbled in at a pressure of one atmosphere and a temperature of $25^\circ C$. Because the SHE electrode is inert, it does not participate chemically in the redox process, but the chemical reaction between the hydronium (H_3O^+) of the acid electrolyte and the hydrogen gas provides a ready supply of positive and negative CC.

The positive charge of hydronium results from the single b-bond attachment of a proton (H^+) to a water molecule, as opposed to the attachment of an apron electron. When one of the three hydrogen atoms attached to the oxygen atom of a hydronium molecule is released to convert hydronium back into water, **the b-bond breakage** has an **equal probability** of releasing the bitron as a cetron or an apron: the process thus acts as both a cetron source and an apron source, as reflected in the half equation below:

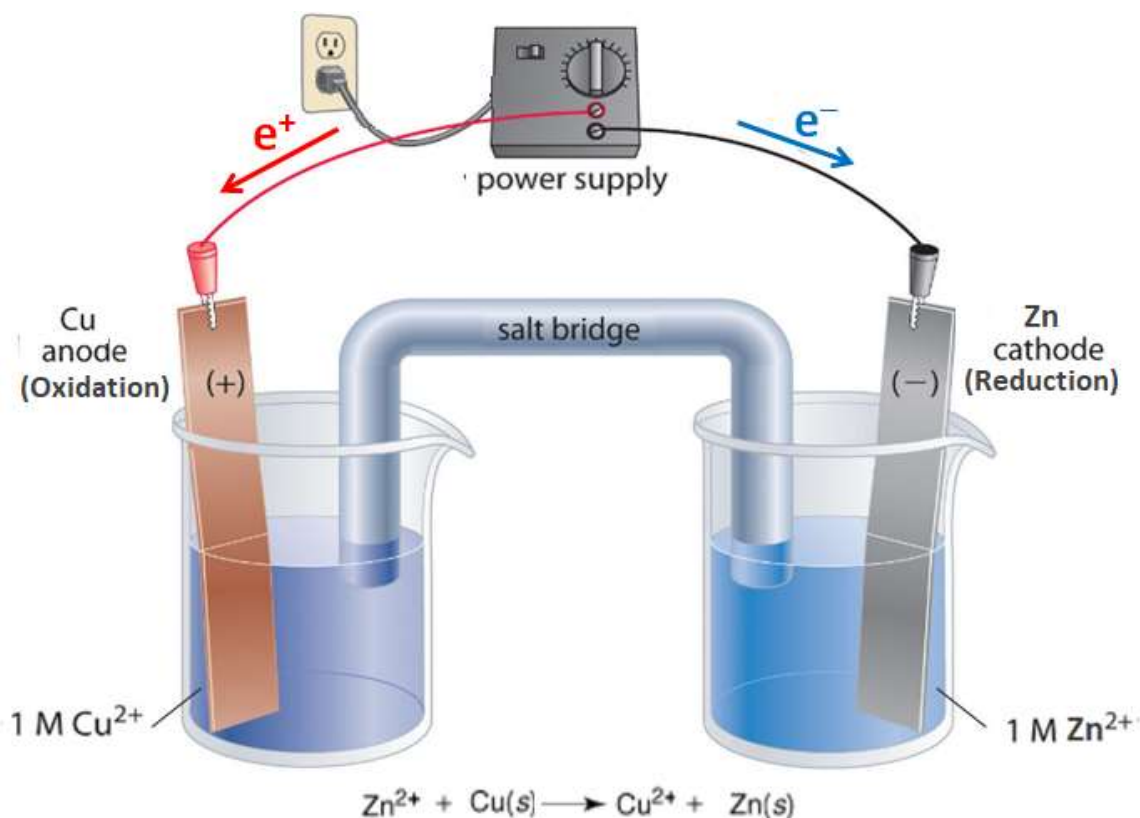


Figure 24: Copper-Zinc Electrolytic Cell

In order to maintain the chemical equilibrium of the electrolyte, the b-bond of hydrogen gas molecules (H₂) break to release two protons (H⁺), with the b-bond breakage also having an equal probability of releasing the bitron as a cetron or an apron, as reflected in the half equation:



The reactions represented by these two inverse processes provide a ready supply of both positive and negative CC for the SHE cell, but generates no electrical potential because of the net neutral charge and lack of a positive or negative CC sink. Thus, when connected to a cell with an electrode made from a different material, the only emf generated is that of the attached cell. For a copper electrode cell such as shown for figure 23b, the copper electrode acts as an apron (i.e. positive CC) source and a cetron sink, it generates a **positive voltage** of +0.34 volt that indicates that it is a **reduction** process. For a zinc electrode the current direction is reversed, with the zinc electrode acting as a cetron (i.e. negative CC) source and an apron sink: it generates a **negative voltage** of -0.76 volt which is indicative of an **oxidation** process. [Wikipedia provides a list of the standard reduction potentials](#) for an extensive range of materials.

Redox reactions are **reversible**, which allows (partially) exhausted chemical reactions of a galvanic cell to be revived by applying an appropriate voltage across the cells to generate a current in the opposite direction, effectively re-charging a galvanic battery cell. Thus, although chemical imbalance and crusting can reduce their effectiveness, galvanic cell based batteries can be re-charged using an [Electrolytic Cell](#) setup such as that shown in figure 24, which can be used to refresh the galvanic cell setup of figure 23a..

The electrolytic cell also involves cetron (e⁻) and apron (e⁺) sources and sinks, as shown in the equations below:



Electromagnetic Induction

Faraday's Law of electro-magnetic induction states that whenever a conductor is forcefully moved in an electromagnetic field, an emf is induced which causes a current to flow. The direction of the induced emf is defined by the **Fleming's Right-Hand Rule**, which has been modified for STEM: it now becomes the right-hand rule for aprons (corresponding to conventional Science's current flow direction) and the left-hand rule for cetrons (corresponding to conventional Science's electron flow direction), as shown in figure 25: it should not be confused with [Maxwell's Right-Hand Grip rule of figure 15c](#).

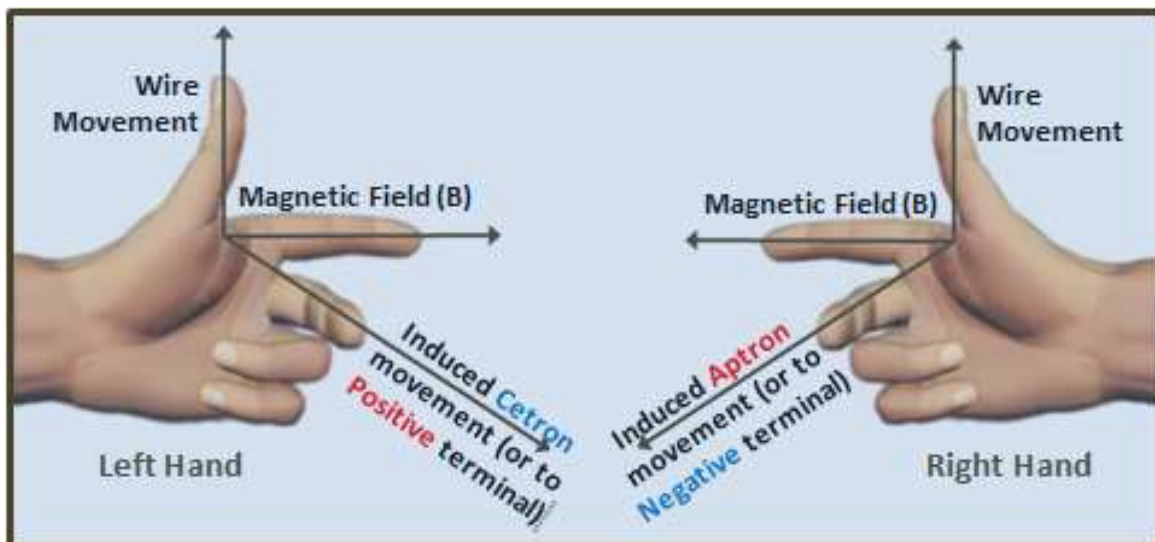


Figure 25: Fleming's Right Hand Rule and Modified Left Hand Version

When a copper wire is moved through a uniform magnetic field, and is orientated 90° to that field, Fleming's Right-Hand rule indicates the location of the implied negative pole, and thus the direction of apron movement (i.e. the direction of conventional Science's current flow). Referring to the right side of figure 25a, with the **index finger** of the right hand pointing in the direction of the magnetic field (B), and the **thumb** pointing in the direction of wire movement, then the **middle finger**, held perpendicular to the thumb-index finger plane, points to the implied negative terminal (which is the movement direction of aprons).

Consider the example of the moving a copper wire (PQ) through a magnetic field (B) as shown in figure 26. When PQ is used to close a U-shaped circuit, the conventional current (I) flows one direction (anti-clockwise in figure 26a) when the area of circuit-U is increased; when the area is decreased it flows in the other direction (clockwise in figure 26b). As determined using Fleming's rule, the **implied polarity** across the wire PQ is indicated by the green plus and minus signs.

Referring to figure 26a, the aprons move away from P (the implied positive) towards Q (the implied negative), and then continue to move in an anti-clockwise direction towards the resistor. However, when considering PQ to be a **power source** that supplies the electric current (as for electricity generators) to the U-shaped circuit, the apron source is Q, and thus Q is the power source's **positive terminal**; similarly, as a power source, P becomes the **negative terminal**, which corresponds to the equivalent circuit diagram embedded bottom-left in figure 26a. Thus, when an induced current is used as a power source, the power source polarity is the opposite of the implied polarity.

Having Fleming's rule to determine the current flow direction is one thing, but providing a logical explanation for the induced current flow is another. The real question here is 'why does the movement of a wire through a magnetic field would induce an electric current to flow?' To answer this question we need to consider the interaction between the ionic orbital CC and the magnetic flux when the wire is moved through a magnetic field.

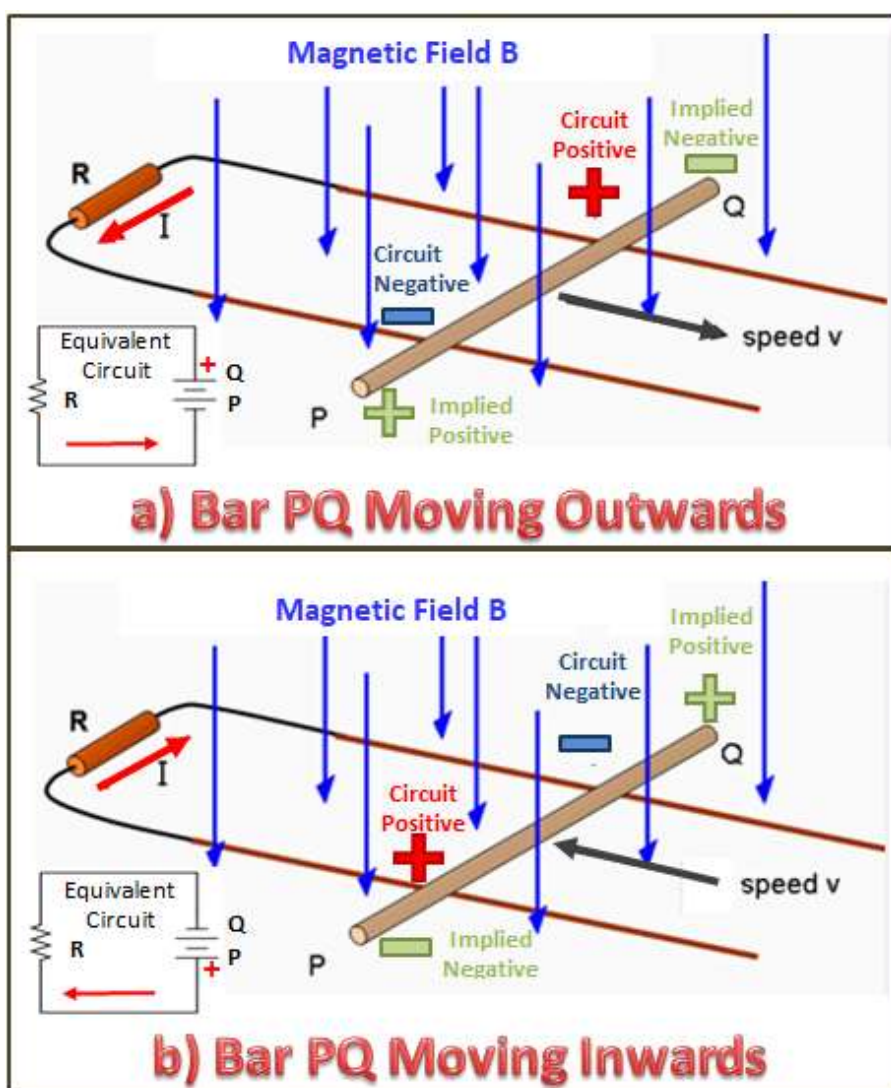


Figure 26: Current Induction by Moving Wire through a Magnetic Field

Figure 27 represents the interaction between the ionic orbitals above and below copper nuclei within a wire moving through a magnetic field flowing out of the page, which corresponds to the PQ wire movement of figure 26a. The four main locations within the ionic CC orbitals are identified by the circled numbers 1 to 4. Enlarged versions of these CC

are correspondingly numbered 1 and 4 for **negative CC**, and 2 and 3 for the **positive CC**. They show the **chiral flow** pattern of the outer energy field of the CC, with the **toroidal field energy flow** component being indicated by the curved **grey** arrows. The **applied magnetic field** is indicated by the downwards-pointing **indigo** arrows and the **wire (PQ)** containing the CC is considered to be moving out of the page.

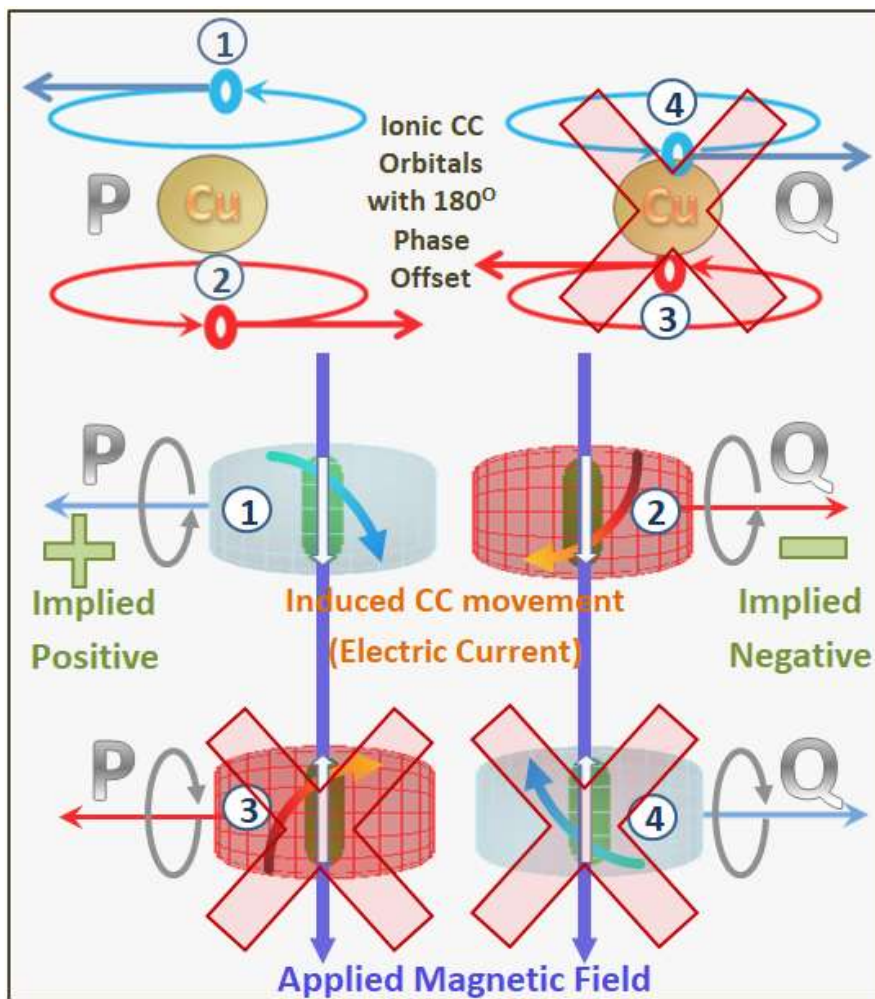


Figure 27: Strand-Level Explanation of Induction due to Wire Movement

As the wire is moved outwards through the applied magnetic field, the flow of the magnetic field energy is in the same direction as the toroidal flow direction of the CC (highlighted by the white arrow) when they are in locations 1 and 2 within their orbitals. The increase of energisation causes an increase of CC at locations 1 and 2, which is sufficient to cause them to leave their orbitals, with the negative CC (1) moving **left** towards an **implied positive** terminal and the positive CC (2) moving **right** towards an **implied negative** terminal.

The flow of the magnetic field energy is in the opposite direction to the toroidal flow direction of the CC (highlighted by the white arrow) when they are in locations 3 and 4 within their orbitals. The decrease of energisation causes a slight reduction of orbital velocity when the CC pass through locations 3 and 4, which causes their orbital radius to increase marginally, but they certainly do not represent the orbital departure locations, as emphasised by **the large red crosses**. However, the increased orbital radius sets the CC up to leave the orbital when they become re-energised upon rotating 180° to locations 1 and 2.

With billions of orbital CC being induced to skip out of their orbitals by the effect of the applied magnetic field, they all head towards their appropriate implied terminals, forming positive and negative strands as an **induced electric current** compatible with that of figure 26a. The **modified Maxwell's rule** (figure 25) can be used to confirm that the direction of the implied polarity and induced electric current flow so generated.

Should just the direction of the magnetic flux be reversed, then CC locations 3 and 4 become active exit points, which results in an induced electric current in the opposite direction; similarly, reverse just the direction of wire movement, and the electric current will be in the opposite direction (as in figure 26b). So, electric current induction process is all very **logical** and **consistent**. However, conventional Science provides no explanation of why magnetic induction works. It provides rules that apply to its generation, and provide simple ways to predict the current flow direction via techniques such as Fleming's Right Hand rule, but otherwise magnetic induction would seem to happen by magic.

Another phenomenon similar to the induction of electric current by moving a wire through a magnetic field, is that when a **bar magnet** is moved through a **wire loop**, an electric current is induced. The top half of figure 28 shows the North pole of a magnet being moved towards and away from a wire loop. The topmost yellow circle represents the wire loop as viewed from below and looking upwards, and the larger central bar magnets show the cross-sectional view of the wire loop across A-to-B and C-to-D, with the arrow quills and tips indicating the conventional current direction (i.e. the direction of aptron movement) around the loop.

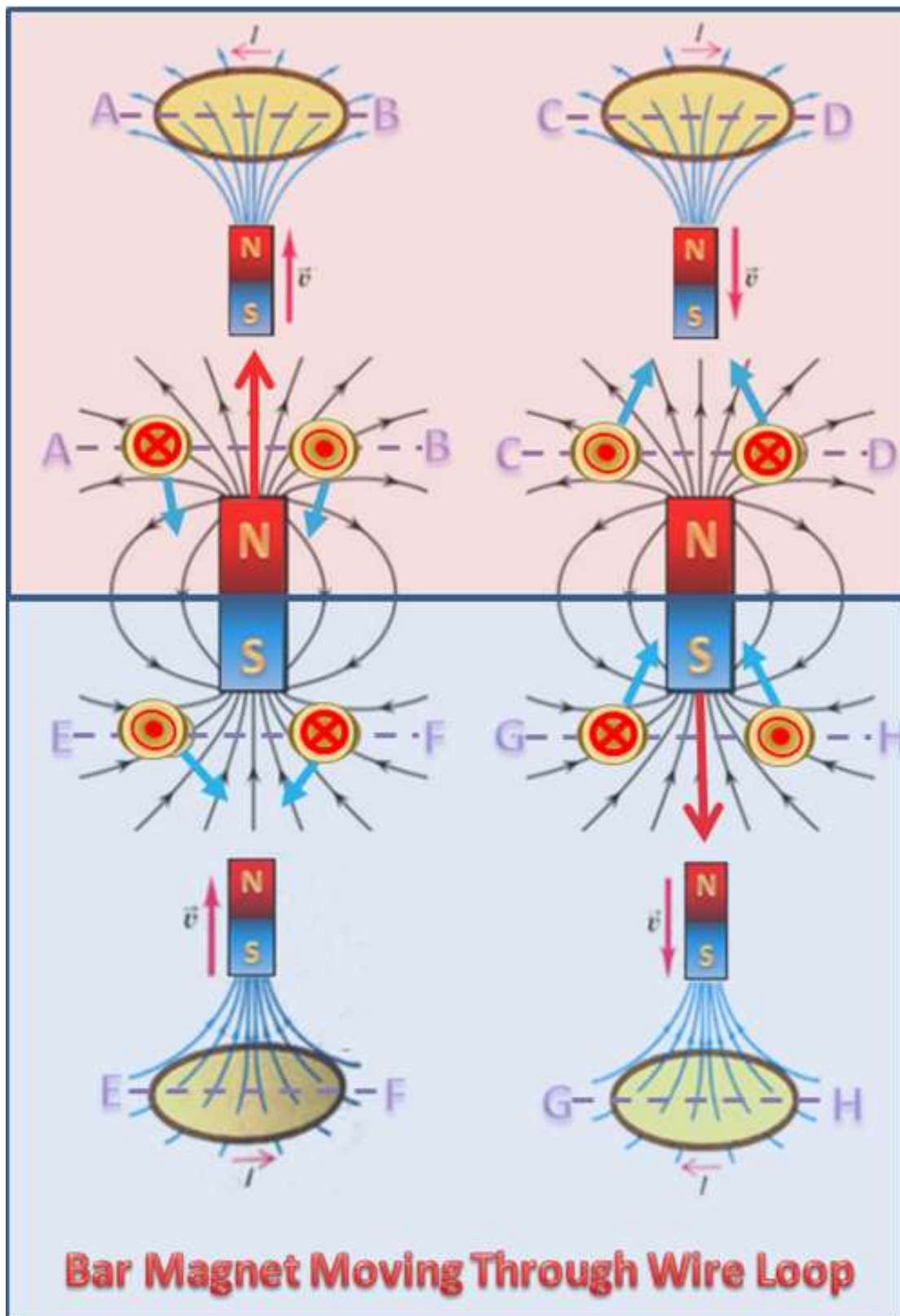
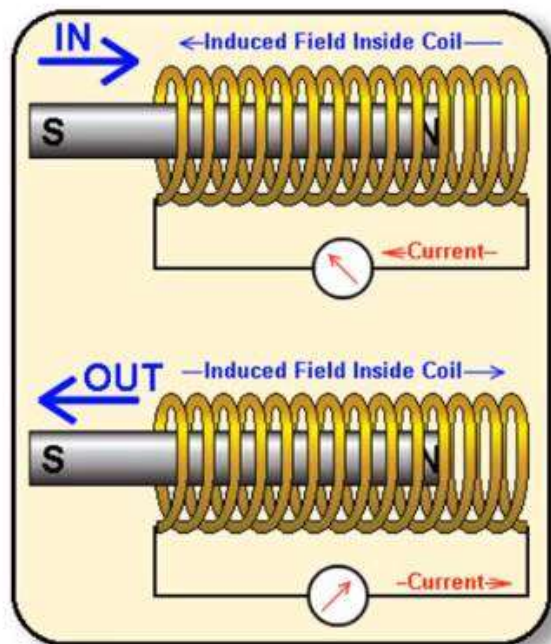


Figure 28: Induced Current in Wire Loop due to Magnet Movement

The light blue arrows indicate the relative movement of the wire loop to the magnetic flux: it is relative because the magnet is actually moving (as indicated by red arrows) with the loop remaining stationary. **Fleming's modified Right-Hand rule** (figure 25) can be used to confirm that the current (I) is correct for each of the four configurations represented.

Note that as the magnet moves into the loop (e.g. top-left in figure 28) the induced current flows in one direction, but as it moves out of the loop (bottom-left in figure 28) the current flows in the opposite direction. Assuming that the magnet is kept moving, when it is at the half-way point, there is equal flux on either side of the plane of the loop and no current flows at that point in time.

The strength of the induced current can be increased by increasing the number of coils. The change in current direction as a bar magnet is moved into and out of a solenoid (or multi-loop) coil, as shown in the graphic right. Should the magnet be kept moving in the same direction through the solenoid, the induced current flows in one direction as it enters; there is no current when it is at the half-way point, and there is equal flux on either side of the solenoid at that point; and then the induced current flows in the opposite direction as it leaves the solenoid.



The induced current generates its own magnetic field through and around the solenoid that acts in the opposite direction to the magnet's field. Thus, as it enters leading with its North pole, its central flux is into the solenoid and the generated flux is out in the opposite direction, with both being reversed as the magnet leaves the solenoid. When there is no significant change of magnetic flux (i.e. $d\Phi_B dt \approx 0$), there can be no induced movement of CC. Thus when a magnet and the conductor are stationary with respect to each other, no electric current is induced: when either moves, the magnetic flux experienced by the conductor changes, and induced current can be generated.

Electromagnetic (Motor) Force

The **force (motor or Lorentz force)** that acts upon a current-carrying wire when it is placed within a magnetic field, as shown in figure 29a, is due to the circular magnetic field (that is generated by the electric current within the wire) interacting with the externally applied magnetic field. The two magnetic fields interfere with each other as shown in figure 29b, with the clockwise circular magnetic field around the wire merging with the externally applied field.

The combined merged fields result in a concentration of magnetic field-energy on one side of the wire, and less on the opposite side, as indicated by the distorted magnetic lines of force of figure 29b. Thus a region of concentrated field-energy forms on one side of the wire and a region of low field-energy concentration on the other side, the combination of which generates an upwards-directed **motor force** on the wire. The change of energy (magnetic flux) concentrations due to a merging of circular and transverse magnetic fields is considered to be the cause the motor force effect rather than pressure changes due flow rates per [Bernoulli's principle](#) as applies to the [Magnus Effect](#).

The **open-palm** version of [Fleming's right-hand rule](#) can be used to work out the direction of the **motor force (F)** on the **stationary wire**, as shown left in figure 29c. Alternatively, the partly **closed-fist** version shown right in figure 29c but the motor force (F) acts in the opposite direction to that pointed to by the thumb (the thumb points to the direction of the **wire movement** in the **current induction** situation shown right in figure 25). Note that the current direction shown is the conventional electric current direction, which corresponds to apron movement: cetrons are simultaneously moving in the opposite direction (i.e. out of the page in figure 29b).

The force (F) on a stationary wire is similar to the force that needs to be applied, and the mechanical work done, to push a wire through an external magnetic field to induce an electric current (as shown in figure 26) is the basis for electric **power generation**, whereas **motor force** is the basis of **electric motors**.

It should also be noted that an electric current is induced by the **movement** of magnetic flux, or the movement of the wire through the flux of a magnetic field, interacting with cetron and apron electrons within ionic orbitals within the wire; **motor force**, on the other hand, results from the magnetic fields generated **outside** a current-carrying wire, which requires no movement of the external magnetic field or the wire. This is an important distinction.

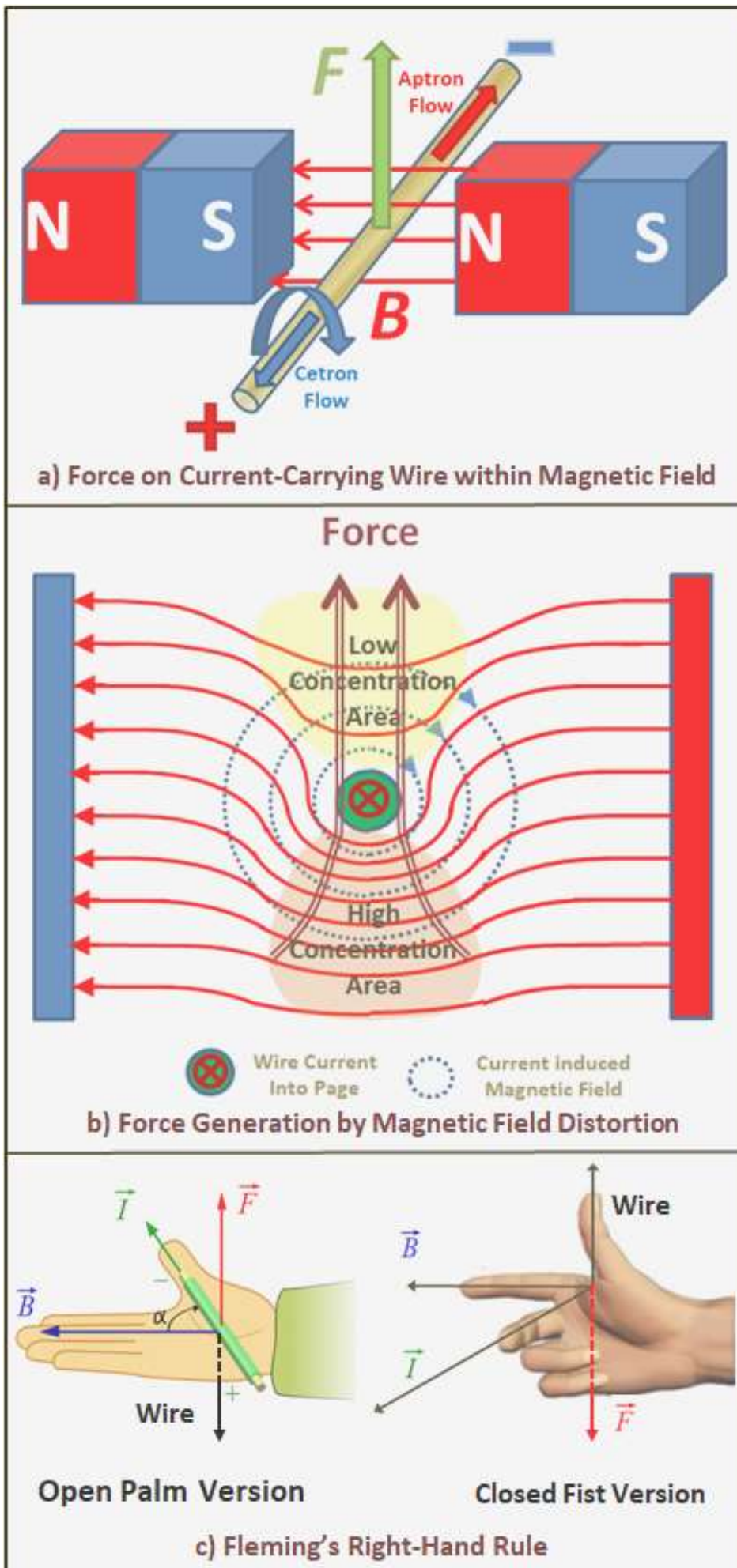


Figure 29: Motor Force on a Current-Carrying Wire in a Magnetic Field

Eddy Currents and the Hall Effect

Within **thin flat sheets of copper plate**, due to the pounding, rolling and annealing processes used in its manufacture, the copper atoms are aligned in planar single layer structures that are parallel to the plate faces. Thus the CC orbital spin axis is nearly always perpendicular to the plate surfaces. Also, they do not have the lateral constraints that wire conductors have, which allows strands to dynamically form in response to movement of an applied magnetic field.

Eddy currents are magnetically induced **circular currents** which flow in **closed loops** within a sheet of a metal conductor. The size of the eddy current is proportional to the strength, direction and rate of change of the magnetic field, and is inversely proportional to the resistivity of the conductor.

As for any current flowing through a conductor, an eddy current will produce its own magnetic field that, in accordance with [Lenz's Law](#), is in the opposite direction to the changing external magnetic field that created it. The opposing magnetic fields (i.e. the applied magnetic field and the one generated by the eddy current) so produced can be used in a variety of ways from the heating of a saucepan by an induction cook-top (see figure 30a) to the electrodynamic suspension of objects and a braking mechanism to stop high-torque power tools and rollercoasters.

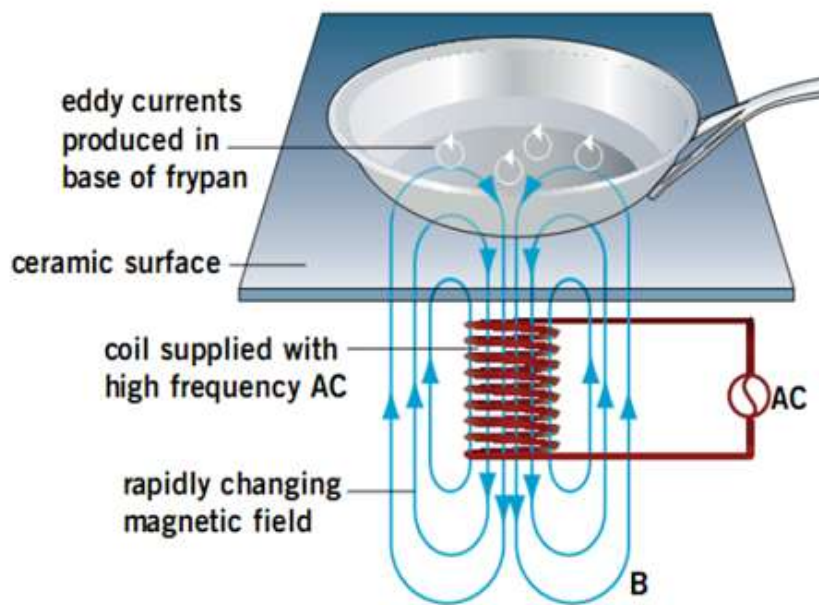


Figure 30a: Eddy Currents and Induction Cook-Tops

Induction cook-tops utilise eddy currents to heat-up cookware containing food or beverage, but the cookware needs to be made from a metal with high electrical resistance (e.g. Iron instead of copper) so that the eddy currents generated within its base will rapidly dissipate as heat energy (energy loss rate = $I^2 \cdot R$, where I is the average, or root mean square current per AC cycle). The cookware can remain stationary on the cook-top because AC electricity generates a continually changing magnetic flux via a solenoidal coil. Figure 30b shows the eddy currents formed by one such cycle as well as the opposing magnetic fields of the coil and the eddy current.

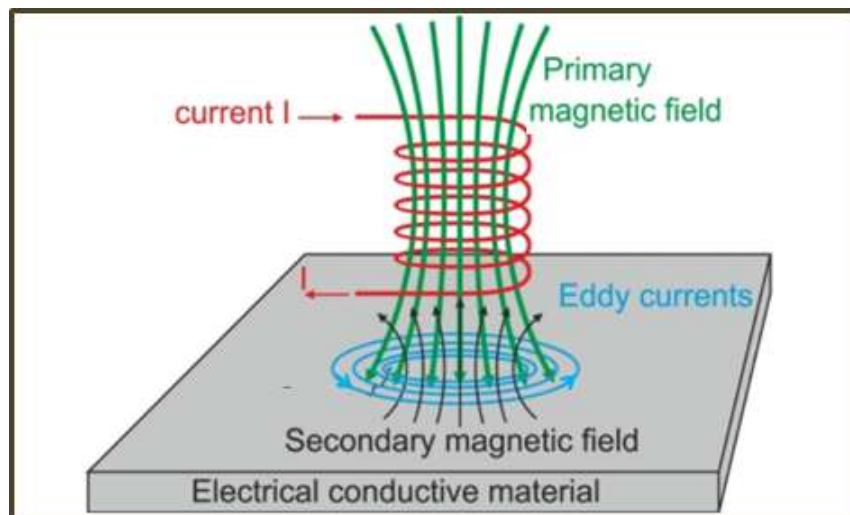


Figure 30b: Eddy Currents for Increasing Primary Magnetic Field

A super-cooled **superconductor** (e.g. vanadium, technetium, and niobium composites) becomes [superconductive](#), the thermal energy the orbital CC is zero, which means that they are no longer in orbitals. They are free to move and offer **zero internal resistance** in response to any externally applied electromagnetic field. Thus, when a magnet is moved towards a superconductive surface, the now free CC form dynamically induced eddy currents that, in turn, generate their own magnetic field that is equal in strength and opposite in direction to that of the external magnet.

The dynamic nature of eddy current formation can suspend a small magnet above a super-cooled superconductor as demonstrated by [Walter Lewin's video MIT Lecture 19](#). Walter's presentation is both informative and entertaining, and makes for excellent viewing. As well as demonstrating electrodynamic suspension (levitation), Walter covers a range of related topics including the use of eddy currents to suspend high-speed trains, which allows them to move without their wheels making direct contact with the track, so reducing frictional drag.

Within a **flat copper plate**, due to the pounding, rolling and annealing processes used in its manufacture, the copper atoms are aligned in planar single layer structures that are parallel to the plate faces. Thus the CC orbital spin axis is nearly always perpendicular to the plate surfaces which is most important to the formation of eddy currents.

A **static setup** with the metal sheet or the magnet not physically moving, but with a magnet's magnetic field varying as shown in figure 30b, results in a single eddy current pattern. However, when a metal sheet is moved past a fixed constant magnetic field as shown in figure 30c, opposing pairs of eddy currents are generated.

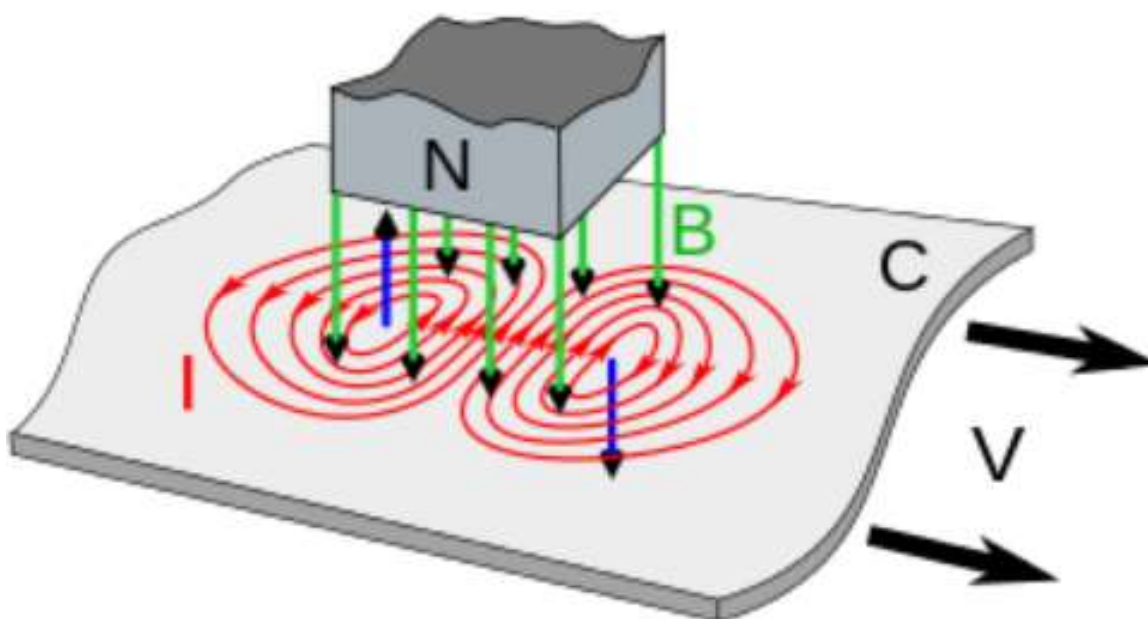


Figure 30c: Eddy Currents in Metal Sheet Moving past a Magnetic Field

The formation of the pair of reverse-flow eddy fields is analogous to, when a magnet is moved into a solenoid, an induced current and associated magnetic field are formed, which both reverse as the magnet passes the mid-point and continues to move out of the other end of the solenoid (see the [Electromagnetic Induction](#) chapter). For eddy currents, the leading edge of the plate entering a downwardly directed magnetic field induces electric eddy currents in a clockwise direction, which generate a downwards magnetic field centrally; and the trailing half induces anti-clockwise electric eddy current which generates an upwards magnetic field centrally. Should the external magnetic field or the direction of travel be reversed, then the eddy fields' flow direction also reverses.

Note that between the two eddy currents of figure 30c, the flows are in the same direction and thus combine: this is important for understanding the **Hall Effect**, which is the next topic.

In 1879 E. H. Hall discovered that, should a small flat rectangular-shaped metal conductor (called a **Hall element**) with an electric current flowing in its long axial direction be placed in an external magnetic field, then a measurable transverse voltage and current is generated. The phenomenon is called the [Hall Effect](#) in his honour. The Hall Effect has many useful applications related to the detection of movement and the measurement of the spin speed of turbine blades and high spin-speed wheels, and, as a probe, it provides a means to measure the relative directional strength of magnetic fields.

Although the Hall Effect has been much studied and used, conventional Science explanations involve the movement of positive and negative charge to opposite sides of the Hall element to appear either as **static charge** (the lower example of figure 30d), or as **curved strand-like streams** of positive and negative CC (the upper example and in [this](#)

[YouTube presentation](#)). The build-up of positive and negative charge on either side of the Hall element is considered to provide the emf to produce the Hall current. Possibly in the recognition that holes are not positive CC, some conventional Science explanations, such as that [provided in Wikipedia](#), show the one-way deflection of a strand-like stream of electrons: an animated form of this approach can be found in [this YouTube presentation](#) but, be warned, the musical accompaniment can be a little annoying.

The conventional Science explanations for the Hall Effect rely upon negative charge and positive charge travelling in opposite directions being deflected to opposite sides of the Hall element. However, when free electrons (negative charge) and positrons (positive charge) travel in the **same direction** through a magnetic field, they are deflected in **opposite directions** and thus become separated. This means that when, as an electric current, negative and positive CC travel in **opposite directions** through a magnetic field, they would be deflected in the **same direction**: this can be confirmed by [Fleming's Left-Hand rule](#) (or the modified Right-Hand or [Palm rule](#) of figure 29c). Thus, assuming that positive-holes can act as the much needed mobile positive CC, it is difficult to see how the magnetic field can cause electrons to move to one side of the Hall element and holes to the other side.

Another problem with the conventional Science explanations is that the attraction between the positive and negative charges on opposite sides of the Hall element: they should immediately drift back to the middle where the holes would be fixed. And then there is the **response time** problem: Hall Effect probes adjust instantly to changes of magnetic field strength and/or direction, which does not seem feasible for the sideways charge-push approach suggested.

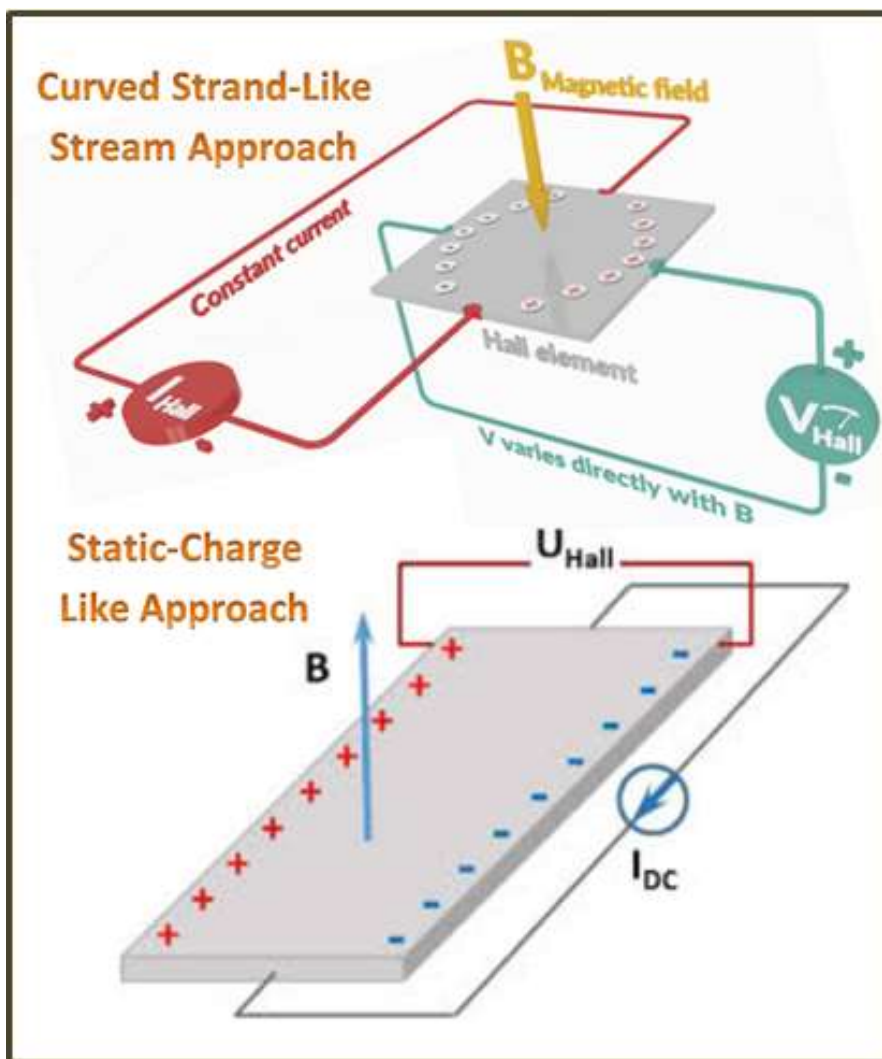


Figure 30d: Typical Conventional Science Explanations of the Hall Effect

STEM contends that the Hall Effect is due to eddy currents that form when a Hall element moves in a magnetic field. Figure 30e shows the eddy currents generated as the Hall element moves in the opposite to the applied current (the Hall element moves upwards in the long-axis direction as shown). With the magnetic field directed into the page, two identical pairs of eddy currents are generated: one pair on either side of the strands that carry the charge for the applied current, which are located centrally. The combined flow of apron flow between the eddy pair is to the left (as shown) so as to form an **implied positive terminal** on the left side of the Hall element; and equivalent cetron stream forms **an implied negative terminal** on the right side: their combined charge flow represents the **Hall current** and the implied terminals define an equivalent **Hall voltage**.

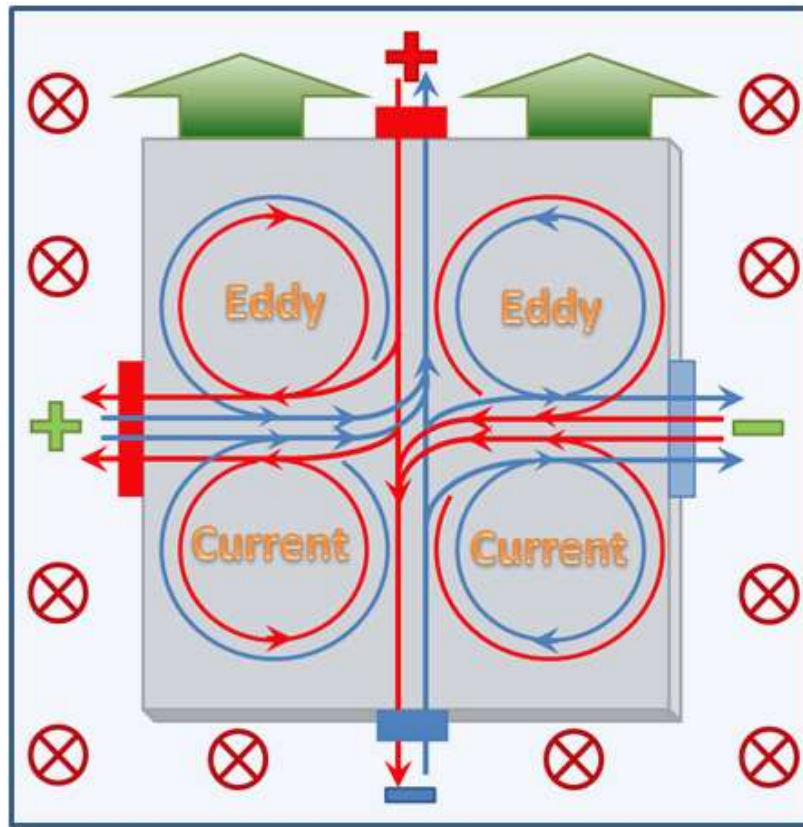


Figure 30e: Eddy Fields and Hall Current with Upward Movement

When Hall element is moved sideways to the left as in Figure 30f, a single pair of eddy currents is generated, which straddles the strands supporting the applied current: it produces implied Hall terminals with the same polarity as for the vertical movement shown in figure 30e. Whenever either the direction of movement of the Hall element reverses, or the direction of the applied magnetic field reverses, so does the Hall polarity.

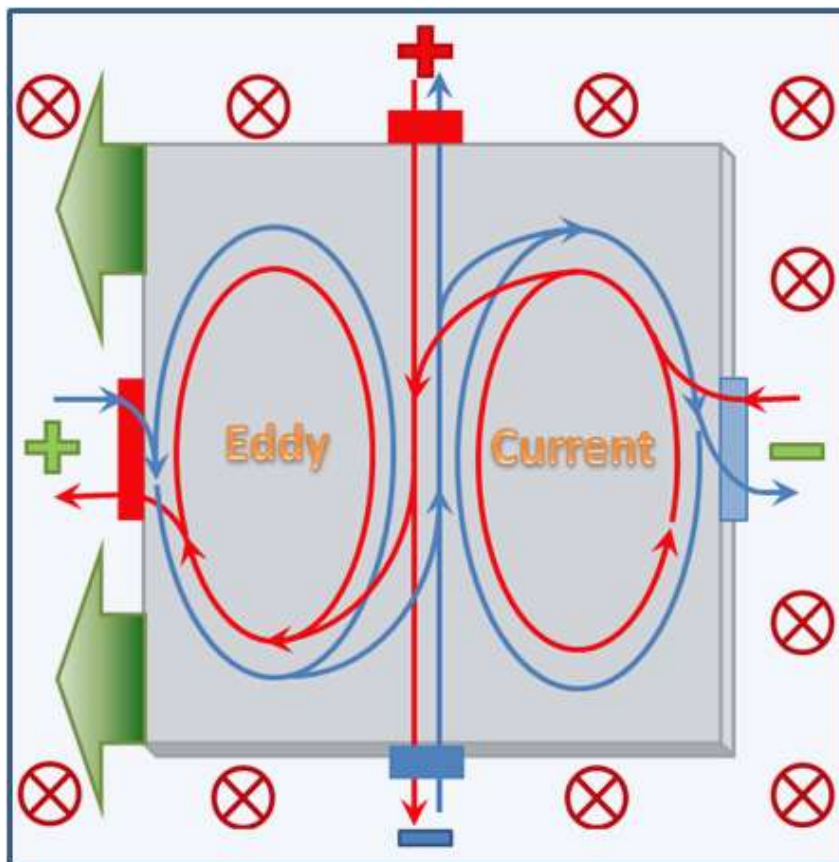


Figure 30f: Eddy Fields and Hall Current with Movement to the Left

Rather than the formation of a single pair of eddy currents as shown in figure 30f, it is highly likely that four eddy pattern of figure 30e would be present at all times, with each being dynamically strengthened, reduced and/or reversed without disappearing, as the Hall element is moved and applied magnetic field changes. And when the Hall element is

stationary in a fixed magnetic field, due to internal resistance within the Hall element, the eddy fields quickly subside and the Hall voltage and current drop to zero.

Note that the applied current combines and merges with the eddy currents, so contributing to the **emf** that generates the Hall current. Should the applied current not be present, the eddy currents would remain within the hall element with little incentive to flow into the Hall circuit: in this situation the Hall current would be zero or very close to zero.

The other thing to keep in mind is that the Hall current only reflects the relative change of magnetic field component that is perpendicular to the Hall element surface. Some manufacturers of Hall sensors offer a 3-element Hall sensor, with each element orientated in 3 orthogonal planes, and supply software to give a better measure of magnetic field strength and direction: but most applications of Hall sensors are not so sophisticated.

Static Electricity (Electrostatic Charge)

An **electrostatic charge**, often called **static electricity (SE)** or **contact electrification (CE)**, is a surface collection of electrically charged particles that is typically generated by separating or rubbing together two **triboelectric materials**. The conventional Science explanation for solid-to-solid contact electrification is that electrons transfer from one surface to another, with the **electron acceptor** becoming negatively charged and the **electron donor** becoming correspondingly positively charged due to an electron deficiency: the donor atoms thus become temporary cations, which are analogous to positive-holes within the silicon substrate of semiconductors.

The STEM explanation for static electricity is speculative and far from complete. One line of reasoning is that, because cetrans can more readily escape a host medium than aprons, similar to conventional Science's electron-only transfer explanation, it is only **ionic negative CC (cetrons)** are lost or gained in a charge transfer between triboelectric materials. The other line of reasoning is that, in close contact, triboelectric materials readily form **bitron bonds** between their outer atomic layers. Upon separation, or by rubbing, these **b-bonds** are broken with the released bitron having equal probability of being a cetrans or an apron. With this approach, one of the materials involved retaining the positive CC and the other the negative CC. The **temporary b-bond formation** approach involves both cetrans and apron creation and acquisition by the acceptor material: this is the approach described in this chapter.

[By-pass link: Click here should you wish to by-pass this discussion and move to the next chapter.](#)

The **Triboelectric Series** is simply a list of which materials have a tendency to become positively charged, such as air, leather, rabbit fur, glass, human hair, nylon, wool, lead, cat fur, silk, aluminium, paper; and those with a tendency to become negative, such as ebonite, silicone, rubber, teflon, silicon, polypropylene vinyl (PVC), polyethylene (e.g. Scotch and Cello tape), plastic wrap, styrene/styrofoam, polyester, acetate, rayon; and those with a tendency to remain electrostatically neutral, such as cotton and steel. The degree of charge exchange between triboelectric materials varies according to the situation (e.g. contact surface area, humidity etc.), the vigour applied and triboelectric combination involved.

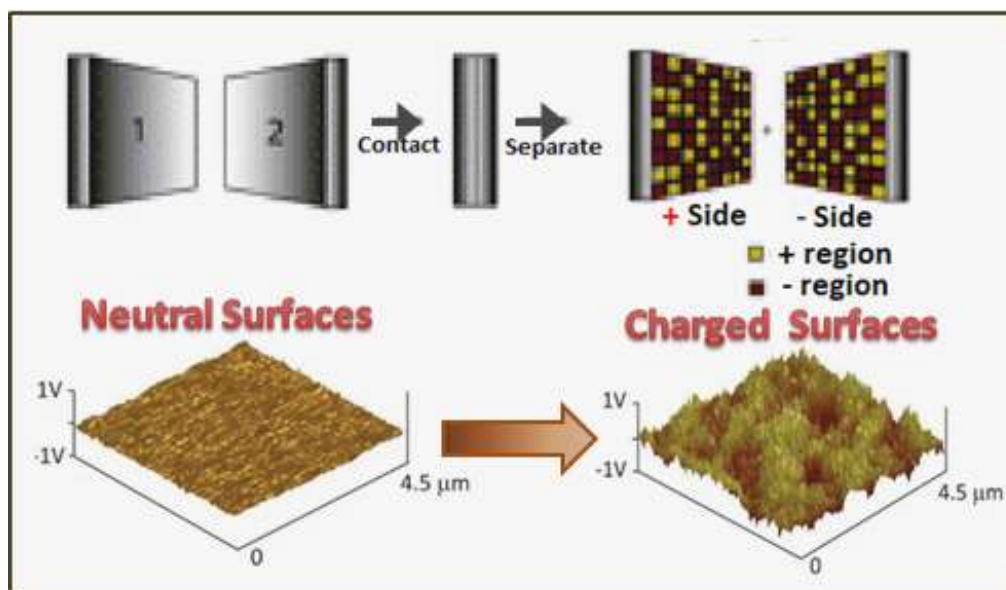


Figure 31: Nanoscale Charge Mosaic within Triboelectric Material

Unfortunately the cause of static electricity is poorly understood, and there may be several processes at work in parallel. The [2020 article by Lin et al](#) suggests that liquid-to-solid contact electrification would be due to a combination of electron and ionic transfer and the formation of an electric double layer effect that is influenced by the pH of the liquid.

The [2011 article by Baytekin et al](#) identifies a random “mosaic” of oppositely charged regions of nanoscale dimensions on each surface before and after contact electrification (see figure 31), and upon separation the size and distribution of the regions change with the negatively charged side having more negative regions (i.e. regions with an electron surplus), and the positive side having more positively charged regions (i.e. regions with an electron deficiency). Or are these mosaics more a reflection of irregular cetrion and aprtron concentrations?

The [2017 study by Musa et al](#) confirmed that triboelectric materials form a dipolar potential when in contact and unipolar potential (i.e. positive or negative charge) after separation: thus there is the distinct possibility that the dipolar pull might cause or contribute to CC transfer between surfaces. This report is more supportive of the STEM approach.

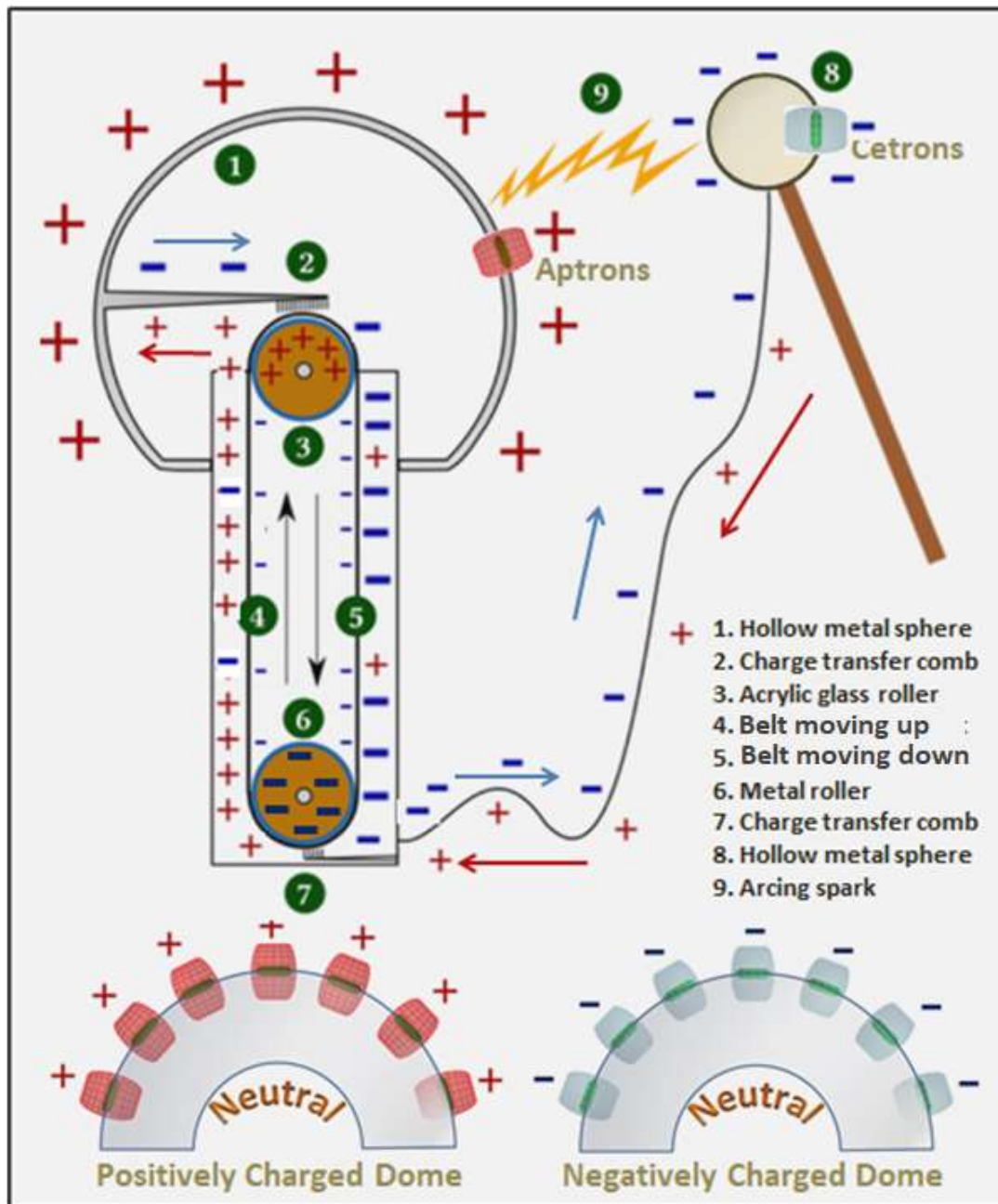


Figure 32: The Van de Graaff Generator Operation

One major problem with the conventional Science approach is that many triboelectric materials, such as rubber and acrylic glass, are also good electrical insulators, and thus do not contain many mobile ionic electrons that could be readily snatched by the acceptor side to create static electricity.

A **Van de Graaff generator** is a mechanical electrostatic charge pump that uses a moving rubber belt (an electrical insulator) to transfer charge to a hollow spherical metal structure and accumulate the charge to generate a high electric

potential up to several million volts. There are many configurational variations of the generators: single dome, double dome, earthed, unearthed or supplemented by use of electric power. For simplicity, the charging process will be explained for a double dome configuration, generating a static positive charge on the larger dome and a negative charge on the smaller.

Referring to figure 32, the upper-roller (3) is acrylic glass (another electrical insulator) or similar, that becomes positively charged by separation from contact with the inner surface of the rubber conveyor belt (5) to acquire cetrons. At the lower-roller (6), the cetrons on the inner side of the belt transfer to the metal roller, with some reciprocal transfer of aprons from the metal roller. Contact separation also adds more electrons to the lower roller and aprons to the inside surface of the belt. As the belt moves back up to the upper-roller, there are considerably less cetrons and aprons as described on the inside surface of the belt.

The charge on the rollers builds up quite quickly to generate a strong positive potential at the top transfer comb and a strong negative potential at the bottom transfer comb (7). Although it could be argued that some of the CC might work their way from the inner to the outer belt surface, with the rubber belt being an insulator, this would be most unlikely. Thus initially the initial significant build-up of charge is in terms of the positive charge in the upper-roller and negative charge on the lower roller, with some CC build-up on the inner surface of the belt but very little CC accumulation on the outer belt.

However, with the build-up of negative charge on the lower roller generates an emf that starts to push any cetrons on the outer surface to the lower transfer combs where they join cetron strands heading towards the smaller dome (8). A **sympiotic effect** caused by the build-up of cetrons in the small dome and the attraction of the lower-roller charge, draws aprons from apron strands within the lower transfer comb (7) to be deposited onto the outer surface of the belt, with the **electric current** in the wire to small dome (8) becoming a **two-way transfer** of cetrons and aprons.

While there is a cetron build up in the small dome, the aprons deposited onto the outer surface of the belt are carried to the upper transfer comb (2) where they are drawn towards the upper dome. As the positive charge of the larger dome increases, an equal number of cetrons transfers back through the combs to the outer surface of the belt. The large dome thus becomes a **cetron source** and an **apron sink** (creating a positively charged dome); and the small dome becomes an **apron source** and a **cetron sink** (creating a negatively charged dome), with the belt being a proxy carrier of CC.

In similar manner that a **capacitor** charges (see the next chapter), the electric charge build-up around the outer surface of the spheres continues until are unable to push more CC onto the compressed strands within the transfer combs. The domes hold their charge because the mechanical transfer system is not a reversible process and leakage is minimal (mainly via interaction with airborne atoms and molecules). And with increasing numbers of CC within the domes, they accumulate and concentrate around the outer surface of the domes, becoming evenly distributed around each dome's outer surface as a **static electrical charge**.

When the positively and negatively charged domes are brought close together, the large electric potential difference between the positively and negatively charged spheres ionises air and water molecules between the two, creating low-level plasma, that quickly escalates into a large-scale charge transfer as an electric arc (9), as charged particles (mainly cetrons) jump directly between spheres, electrically neutralising the surfaces.

Capacitors and Inductors

Dielectric material is an **electric insulator** that contains extremely low numbers of free charge carriers (CC) and so cannot support an electrical current: often air is used as a dielectric. A **capacitor** consists of a thickness of dielectric between a pair of conductive surfaces, which when charged, can store electrical charge that can later be released and used. The larger the cross-sectional area of capacitor surfaces, the greater is the charge that the capacitor can hold.

Similar to the pair of probes discussed earlier in regards to electric fields, a capacitor represents a circuit break in an open circuit and, during the **charge phase**, with electric current unable to flow across the capacitor, with CC concentrating within the plates and, due to their bipolar nature, forming **static strands** that generate an electric field as shown in figure 33. The cross-sectional area of the capacitor plates is considerably larger than that of the connecting circuit wire or attached probes, and with build-up of electric charge is not instantaneous.

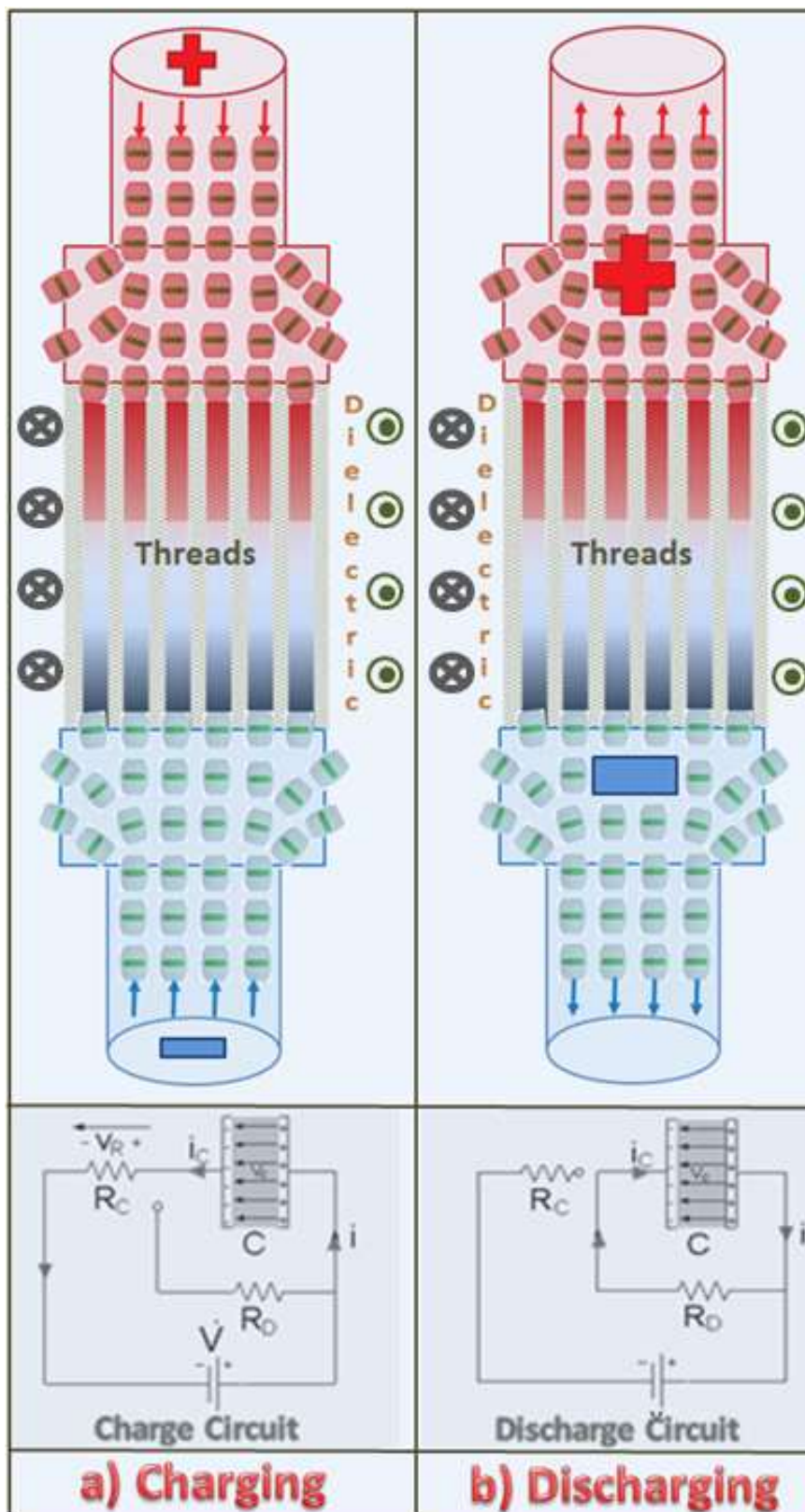


Figure 33: Capacitor Charge and Discharge Cycles

In the **charge phase** (figure 33a), there is no current flow except for an initial micro-current created by CC concentration and the formation of static strands, the degree of which is dependent upon the emf (voltage pressure) being applied by the power source. The electric field between the capacitor plates predominantly consists of **threads** derived from the compacted strands. When the applied voltage cannot push any more CC into the plates, CC movement within the capacitor ceases and the capacitor is **fully charged**.

The electric field between the capacitor plates consists of same-spin CC threads which, which, as for the probes in the [Electric and Magnetic Fields](#) chapter, generate a circular magnetic field around the gap between the capacitor plates. Due to the belief that it is the movement of electric charge as a current that generates the circular magnetic field, in the development of his famous electromagnetic equations (the [Maxwell Equations](#)) in the early 1860's, James Maxwell considered that the circular magnetic field to be due to a fictitious electric current referred to as [Maxwell's Displacement Current](#). It is now accepted that **Maxwell's displacement current** is not an electric current at all.

When fully charged, due to the small gap between the plates, the field energy stored within threads between the plates is very concentrated, and once the charging circuit is disconnected, this concentrated field energy is trapped. The only movement within the trapped field energy is in the form of the circular magnetic field associated with the electric field. And as there is only minor energy leakage in the form of ionisation of air/water molecules, capacitors can hold an electric charge for a considerable period of time after the charging power source is disconnected.

For the **discharge phase**, with the charging power supply and R_C are switched out as in figure 33b circuit diagram, the CC concentrations have a pathway to escape, which is via the newly opened circuit. As the positively charged side of the capacitor has a surplus of positive CC, the strand-bound aptron electrons start to move down the newly opened side of the circuit via the ionic orbitals of the copper atoms. The reducing CC concentration also reduces the strength of the electric field between the capacitor plates. With negative CC similarly skipping in the opposite direction between cetrion electron ionic orbitals into the newly opened circuit, the electric current now flows in the **opposite direction** to the charging current.

The driving force for the capacitor discharge current flow is the charge concentration of strand-trapped CC within the capacitor plates and their movement back to the newly opened circuit, which is accompanied by, rather than being driven by, a corresponding reduction of the electric field

For capacitor discharge, the direction of movement of CC from the capacitor is in the opposite direction to the charging circuit (i.e. the direction of current is reversed). Because the capacitor remains within the circuit, it represents a break of circuit, and thus CC start to accumulate within the capacitor but at the opposite plate. Capacitor discharge would normally result in an electrically neutral circuit, with the CC distribution to becoming evenly spread throughout the discharge circuit. However, should some of the newly moving CC be temporarily delayed or stored within the circuit, then the capacitor may be re-charged from the stored CC. An **Inductor** can provide the required **temporary storage** of CC within the circuit until the capacitor is completely discharged to allow capacitor recharge take place.

An **Inductor** is a passive two-terminal electrical component that slows down CC movement, concentrating them and thus creating a CC buffer effect. An inductor typically consists of an insulated wire wound into a coil around a core as can be seen in the figure 34 graphics. The inductor characteristics depend upon the number of coils, the coil radius, and the choice of material placed in the centre of the coil (air is suitable for some applications).

The conventional Science view is that an inductor stores energy in the current **induced magnetic field**, which is based on **Lenz's law**, which states that a change in electric current through an inductor induces a voltage which opposes the current that created it. As a result, inductors oppose any changes in current through them, and store energy in the form of the induced magnetic field.

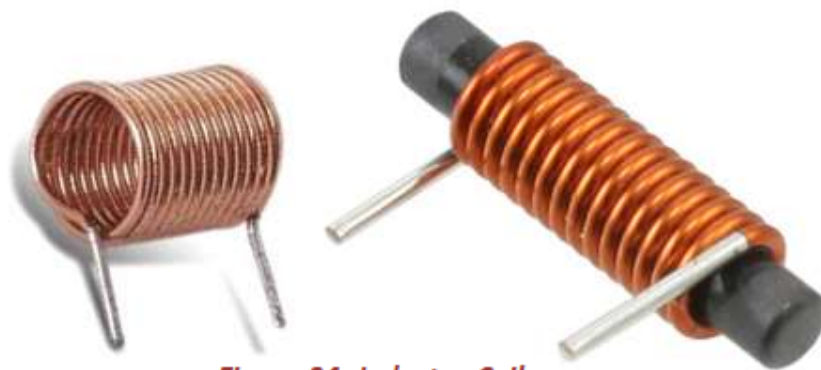


Figure 34: Inductor Coils

From the STEM perspective, while agreeing that the induced magnetic field around and through the coil acts as a buffer field and thus represents a form of temporary energy storage, another, and possibly more significant, factor is the magnetic field between adjacent coil-wires (e.g., between loop 1 and 2, 2 and 3 and so on in figure 35e). These fields, which contribute to the overall magnetic field flowing around and through the coil, are in opposite directions between each coil-loop, which slows the CC flow rate, causing a temporary concentration of CCs.

When vehicles on a busy highway have to slow down due to an obstruction, they bunch-up, so reducing their inter-vehicle gap and possibly ending up bumper-to-bumper. The reduced flow rate of CC within an induction coil similarly causes them to bunch-up and become more concentrated. Although the time taken for an inductor to reach maximum charge density is small (fractions of a second), it represents a temporal storage of charge, and by carefully matching the inductor charge build-up time to the discharge time of a capacitor, the inductor charge build-up can take place while the capacitor is fully discharging, and then be used to re-charge the capacitor.

The synchronisation of the inductor's temporal charge storage characteristics to the charge/discharge/recharge characteristics of a capacitor allows for the generation specific high frequency alternating currents (a **pure**

capacitance waveform with the current changing inversely to voltage and being a quarter of a wavelength out of phase with the voltage).

Figure 35 shows the charge/discharge/recharge cycle that generates rapid current reversals and an associated oscillating electrical current (high frequency AC). Figure 35a shows the capacitor charged and the inductor neutral (empty), with the bucket-like icons showing the relative charge content and movement of each. As the capacitor discharges, as for figure 35b, aprons (red arrows) flow from its positive plate and, in the opposite direction, cetrons (blue arrows) flow from the negative plate, to start building up charge within the inductor.

By the time that the capacitor has been discharged, the inductor charge is at its maximum and, as its stored charge is released, it continues to flow in the same direction (figure 35c) to completely recharge the capacitor (figure 35d), but now with the **capacitor's polarity reversed**. As the capacitor once again discharges, it causes current to flow in the opposite direction to recharge the inductor (figure 35e). The inductor next discharges so as to recharge the capacitor (figure 35f), to return to figure 35a status, thus completing one complete AC cycle.

It is important to note that the capacitor polarity reverses upon each charge/recharge cycle, whereas the inductor only causes a delay (i.e. a temporal storage of charge), allowing the current to continue in the same direction once it reaches maximum charge and releases it as the capacitor's discharge finishes. With well matched coil and the capacitor characteristics the energy losses are minimal, and with appropriate tuning, circuitry a wide frequency range can be achieved from inductor-capacitor pairs.

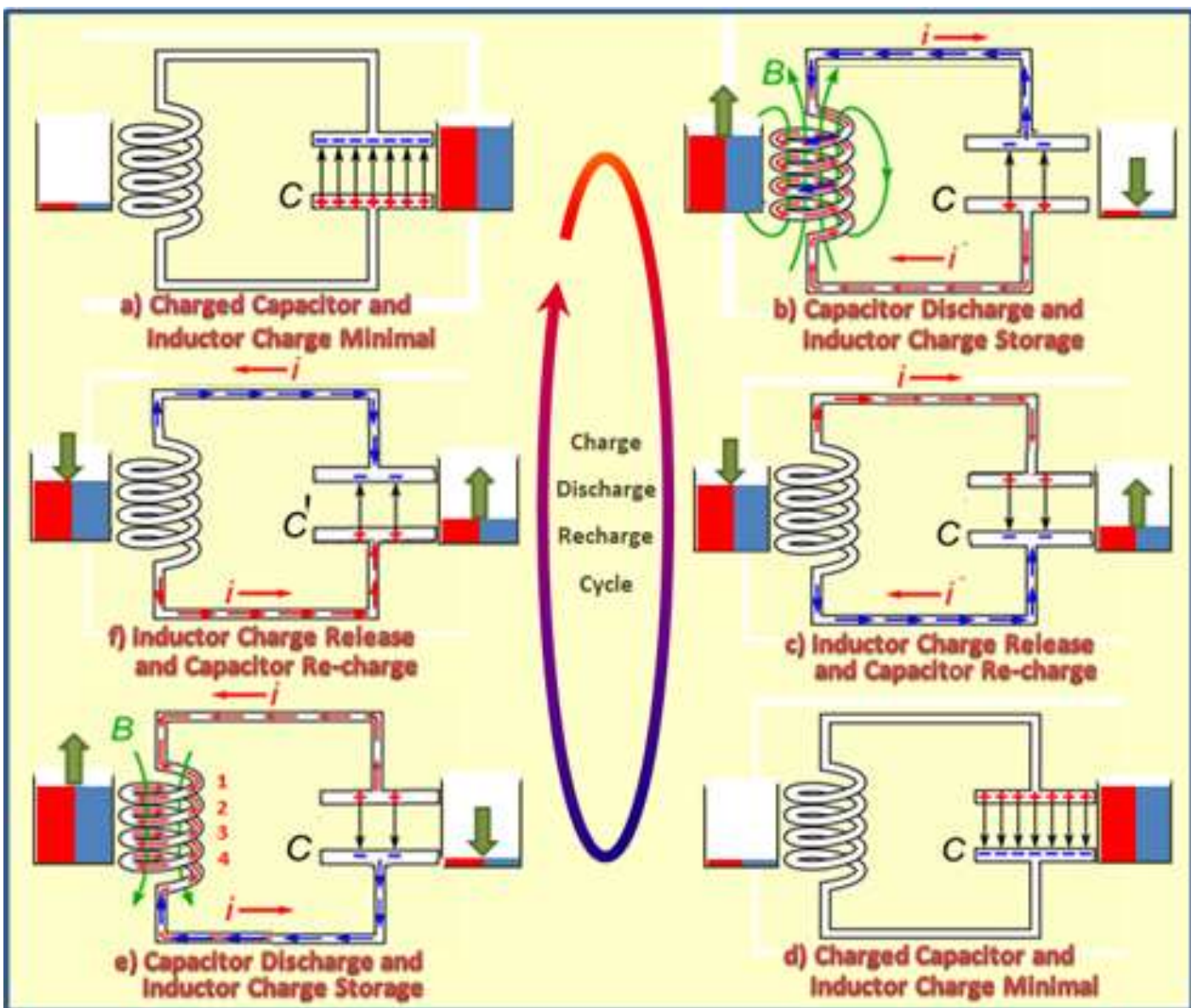


Figure 35: Oscillating Current Generation by Capacitor and Inductor Circuit

An animated gif showing the conventional Science interpretation of the capacitor and inductor combo of figure 35 can be found at this [this Wikipedia link](#) (unfortunately it is in terms of the one-way movement of positive charge). Such **oscillating currents** can be used to generate **micro and radio waves**, which are the subject of the next chapter.

Micro and Radio Waves

Man-made radar, micro and radio waves are generated by circuitry consisting of a tuneable capacitor and inductor loop circuit ([an LC circuit](#)) that delivers a high-frequency AC waveform (a 'pure capacitance' waveform) in the radio/micro wave frequency range. Circuitry can be provided to produce a range of frequencies, which can be fed to a transmitter antenna to generate radio/micro of the required frequency.

[By-pass link: Click here should you wish to by-pass this discussion and move to the next chapter.](#)

With the STEM approach, electric fields consist of **wisps** that form notional **threads** which are the equivalent of **electric field lines of force**. In order to understand how man-made micro and radio waves (which, henceforth in this chapter, will simply be referred to as **radio waves** because the same commentary applies to both) are generated, you may like to revisit the STEM explanation of the **electric fields** presented in the [Electric and Magnetic Fields](#) chapter.

A **dipole antenna** is commonly used to generate radio waves. It consists of two vertical metal rods, such as those in figure 36, connected to a high frequency AC circuit that reverses the polarity of their electric poles on each cycle.

Note that the poles of a dipole antenna face away from each other (as shown in figures 36 and 37), whereas to demonstrate magnetic attraction oppositely charged electric poles are placed to face each other in close proximity as in [figure 18b](#). This is significant because, for the generated electric field, the threads (threads represent the tangential flow direction of the electric field's circular magnetic field) connect stretch across the entire length of the antenna rods pole-to-pole. The AC oscillation frequency repeatedly and rapidly switches the electric pole polarities, and on each electric pole reversal, is associated with a renewal of rotation direction of the circular magnetic field. Examples of current and voltage distributions for a range of antennae lengths are also shown in figure 36.

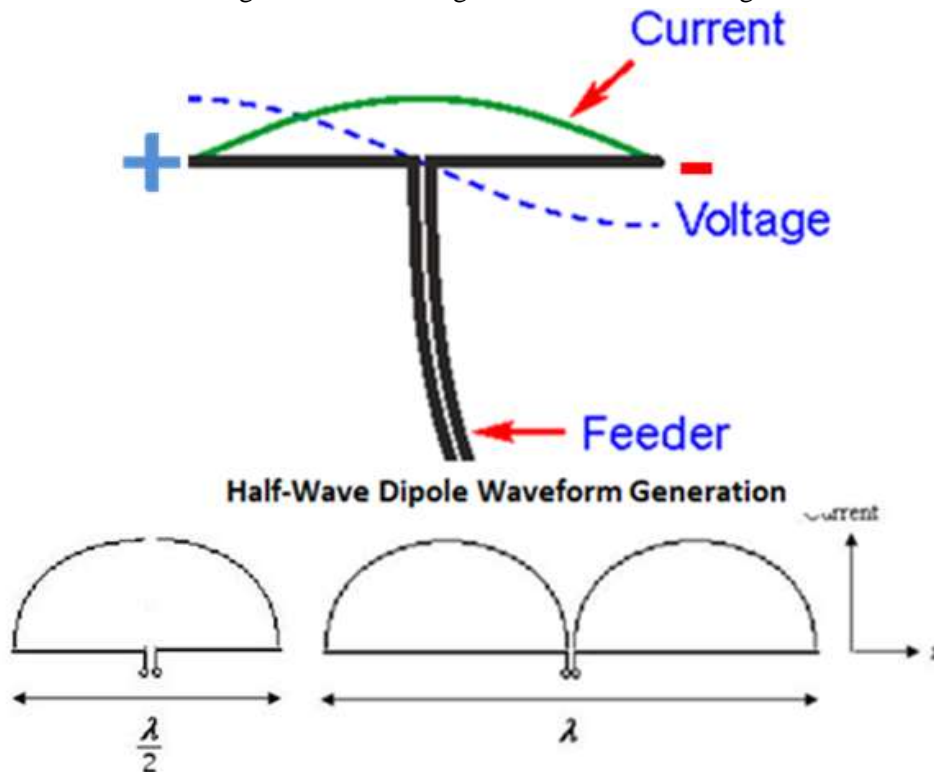
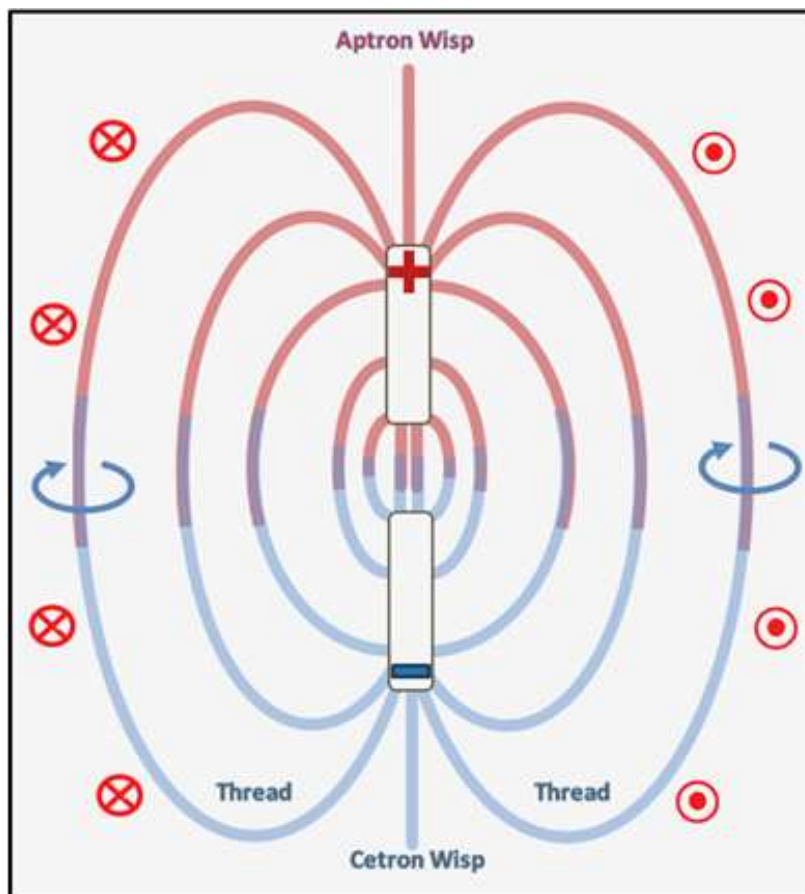


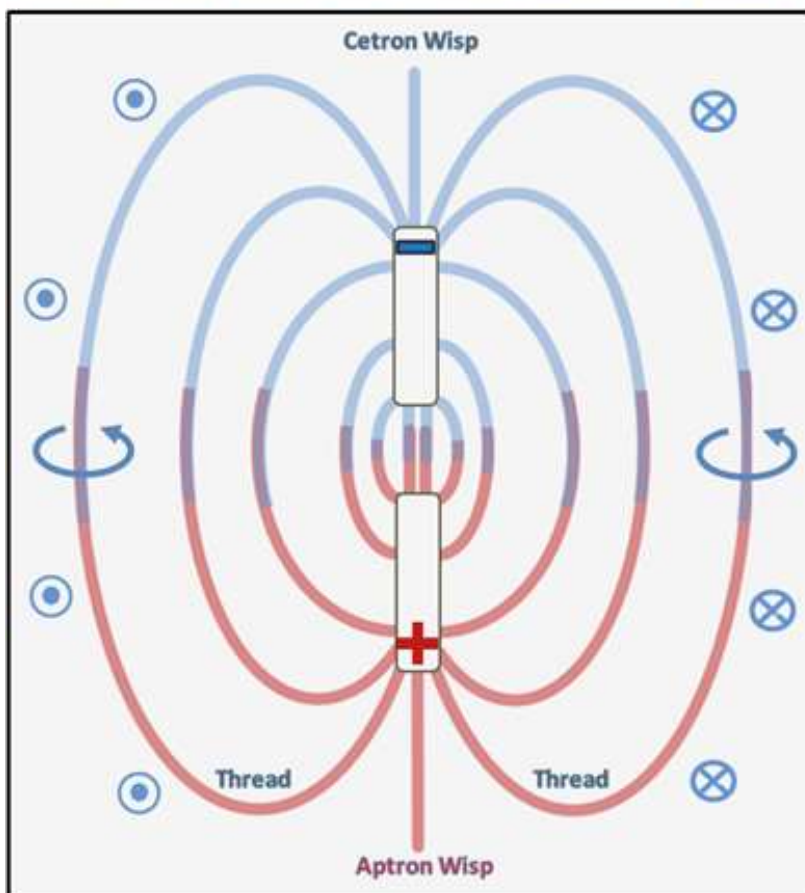
Figure 36: Half Dipole Antenna Current-Voltage Profiles

When the uppermost pole of a dipole antenna becomes positive, an electric field forms with its circular magnetic field being represented by the threads as shown in figure 37a. Upon pole charge reversal for the next AC cycle, the electric field's field-energy is summarily cut-off, and rapidly and unceremoniously pushed away from the dipole rod by the newly generated electric field that has a reversed circular magnetic field direction, as shown in figure 37b.

[This excellent video on electromagnetic radiation](#) uses an oscillating **hypothetical electric dipole** to simulate the effect of AC pole reversal in a dipole antenna. As the hypothetical electric dipole charges oscillate, their cross-over point is equivalent to the pole reversal point for an AC driven dipole antenna. The video clearly shows how the old field energy detaches with a new electric field building as the hypothetical charges separate (or the AC voltage builds); and it emphasises the need to match the antenna impedance with that of the AC source. It should, however, be noted that STEM disagrees with the explanation provided for AC electric charge build-up in terms of the one-way movement of electrons and the field flow direction indicated by the electric field flow lines.



a) Dipole Anrena Thread/Wisp Patterns (Positive Pole Upmost)



b) Dipole Anrena Thread/Wisp Patterns (Negative Pole Upmost)

Figure 37: Electric Field Patterns Generated by a Dipole Antenna

The field-energy of each successive group of cut-off concentrations of field energy (an energy **peak** or **crest**) moves away from the dipole antenna to generate an expanding torus-like electromagnetic radio wave shape. The circular magnetic field of each adjacent crest, as indicated by the **red** and **blue** bands in figure 40, has an **opposite** circular

flow direction, as indicated by the arrow points and quills. The wavelength (λ) of such radio waves is defined by a red/blue crest pair, and $\lambda = c / f$, where f = the frequency as governed by the AC frequency, and c = the speed of light.

Assuming the speed of light (rounded) to be 300×10^6 metres/second, then for radio waves with a frequency of 600 MHz the wavelength is calculated as:

$$\lambda = 300 \times 10^6 / 600 \times 10^6 = 0.5 \text{ metres}$$

Hence, the **half-wavelength** dipole antenna's length (L = total width of both arms) is 0.25 meters, which should produce the torus (or doughnut) shape antenna gain similar to that shown in figure 38. The **isotropic antenna** gain is the unachievable hypothetical perfect omnidirectional antenna.

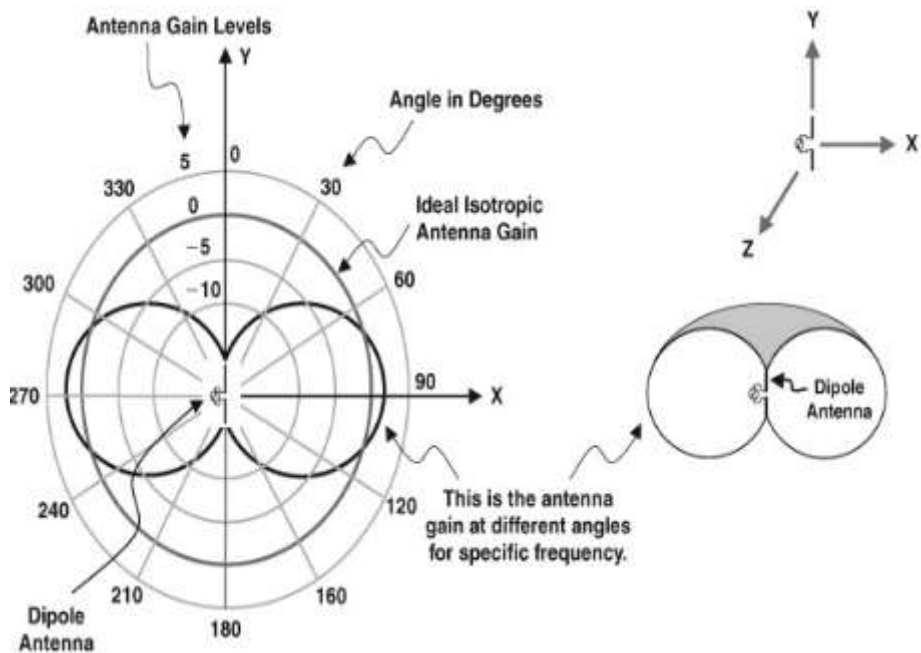


Figure 38: Directional Gain of a Dipole Antenna

Dipole antenna gain pattern (or power pattern) varies according to the length of the antenna, as shown in the directional plot of figure 39 ([source antenna-theory.com](http://source.antenna-theory.com)), which is not surprising considering the manner by which the waves are generated, as described above.

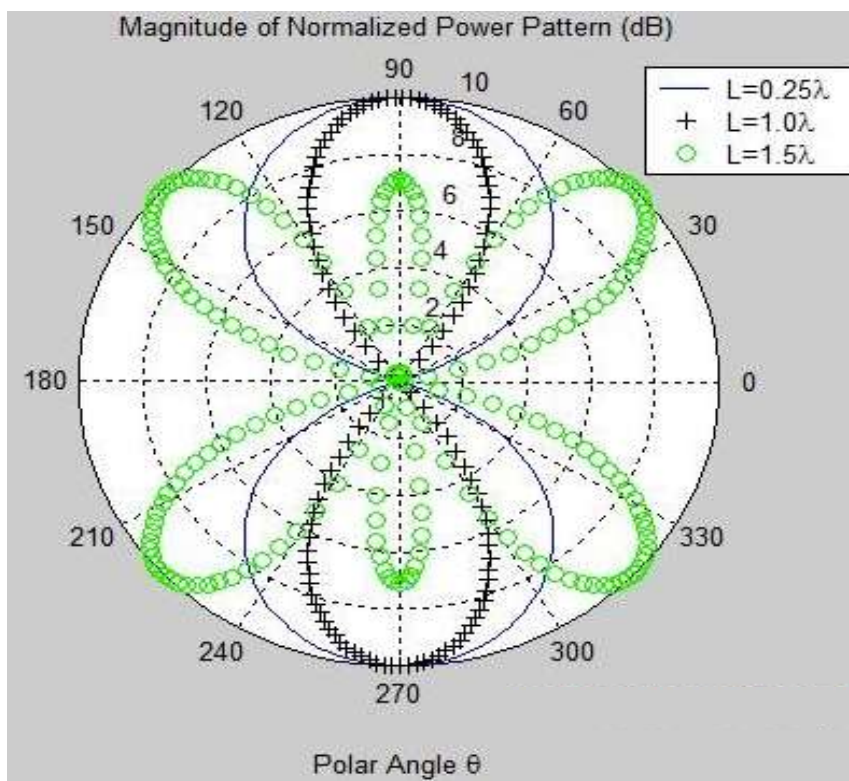
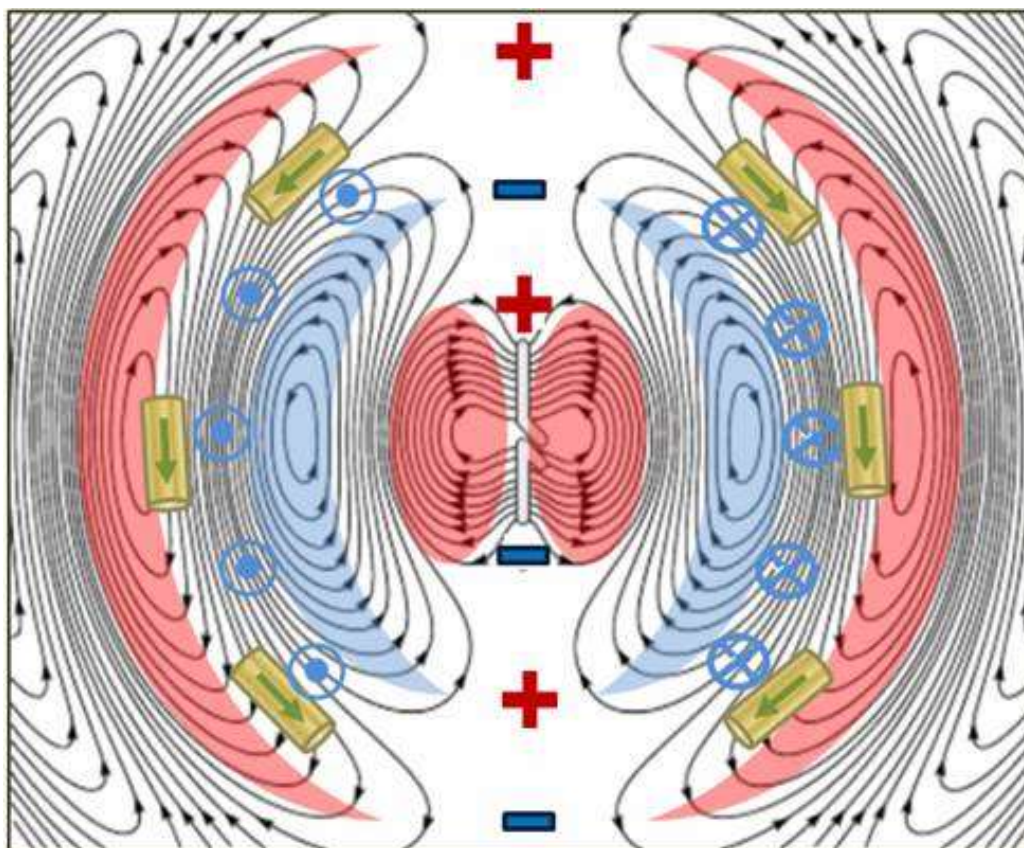
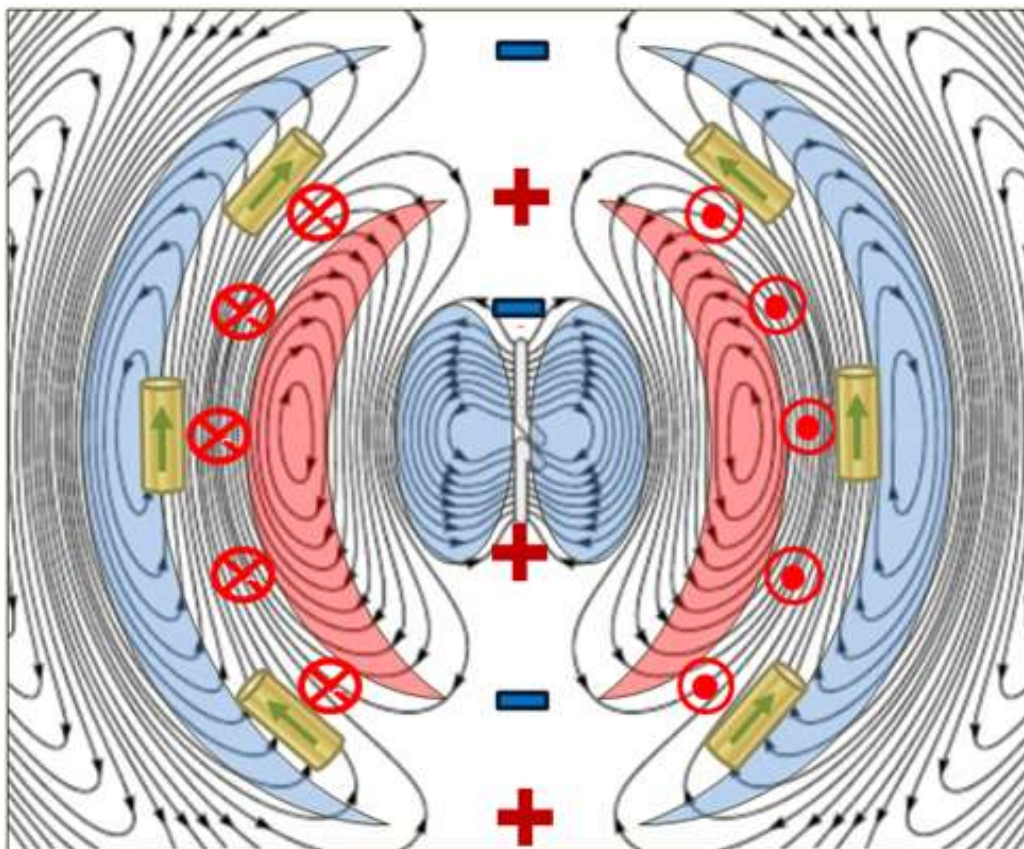


Figure 39: Directional Gain by Dipole Antenna Size

The two modified graphics of figure 40 are taken from a [Wikipedia animated gif](#). It shows a cross section through a dipole antenna highlighting the field-energy patterns being generated. The nested groups of bent ellipsoidal flowlines represent the electromagnetic radio wave crests, colour-highlighted **blue** for a **negative** crest and **red** for a **positive** crest, with the corresponding direction of the circular magnetic field highlighted by the arrow tips and quills.



a) Dipole Anrenna Emmisions (Positive Pole Upmost)



b) Dipole Anrenna Emmisions (Negative Pole Upmost)

Figure 40: Radio Wave Field Patterns for a Dipole Antenna

In its animated form, as for [the video referenced earlier](#), the **directional arrows** attached to the figure 40 flowlines imply that there is a circulation of the field-energy around the positive and negative crests which, as stated earlier, is incorrect: there is no flow of field-energy as shown. The only field energy flow within each crest is that defining its **circular magnetic field**: the flow is tangential to the outwardly expanding doughnut crests as indicated by the arrow-tip-and arrow-quill icons. These are not flow lines as shown: they are thread-like **isoclines** that map the crests and troughs of the field-energy within the radio waves.

Within the crests, the isoclines map the strength and shape of the circular **magnetic field** that move outwards from the dipole antenna: they are analogous to pressure isoclines in a weather map or elevation isoclines in a topographical map. The directional flowline arrows shown in figure 40, the animation and the video, and in many other graphics representing electric fields and radio signals, are incorrect, misleading, and should be removed.

For a piece of copper wire lying tangentially to an advancing crest, the movement of the approaching **magnetic flux** of the circular magnetic field **induces** an **electric current** in the direction of the green arrows in figure 40. The current in the wire builds, peaks and decays as the negative crest of figure 40a passes by, and reverses in similar fashion as the next positive crest passes by as in figure 40b.

The copper wire thus represents a signal-pickup **aerial** that responds with an electric AC current that is synchronised to the radio wave frequency. The current so generated may be amplified and fed to an electromagnetically driven diaphragm for **analogue sound** or to a **digital decoder** for digitised sound, pictures and/or messages.

Semiconductors and the P-N Junction

In 1939 the electrical world was reliant upon inefficient bulky vacuum tubes (thermionic diodes) for **rectification**, when Russel Ohl, working at Bell Laboratories, noticed the unexpected generation of a voltage across a cracked high-purity silicon crystal when exposed to light. This discovery led to the development of the **p-n junction** and the **n-p-n transistor** by William Shockley in 1951, which was followed by a wide range of modern-day semiconductor devices and related technologies. However, the one-way movement of electrons used to explain electric currents in 1939 could not explain the unexpected electrical characteristics of semiconductors.

A p-n junction is a semiconductor device (usually referred to as a **diode**) which is created by joining p-type and n-type semiconductor materials. The semiconductor materials are silicon (or germanium) wafers doped with small measured quantities of foreign contaminant atoms. For **n-type** semiconductors the dopant is typically **phosphorus**, and for **p-type** semiconductor material the dopant is typically **boron**.

The Conventional Science Explanation of P-N Junction Operation

Figures 41a to 41c represent the crystalline structure of a Boron-doped silicon wafer. However, it is a greatly simplified 2D representation, because the structure of crystalline silicon is far more complex: It consists of a diamond-like unit cell structure containing 18 silicon atoms, as shown enlarges as figure 41d and in situ in figure 41e.

Keeping this in mind over-simplification in mind, the conventional Science explanation for p-n junctions is as follows:

*A **neutral phosphorus atom** has 5 valence band electrons, 4 of which are used to bond with adjacent silicon atoms, each of which also have 4 valence electrons. The fifth electron ends up in the **conduction band** and becomes readily available to freely move about within the silicon substrate, with the electron-deficient phosphorous atom becoming a **cation** (a positive ion) which is locked into the n-type silicon crystal structure.*

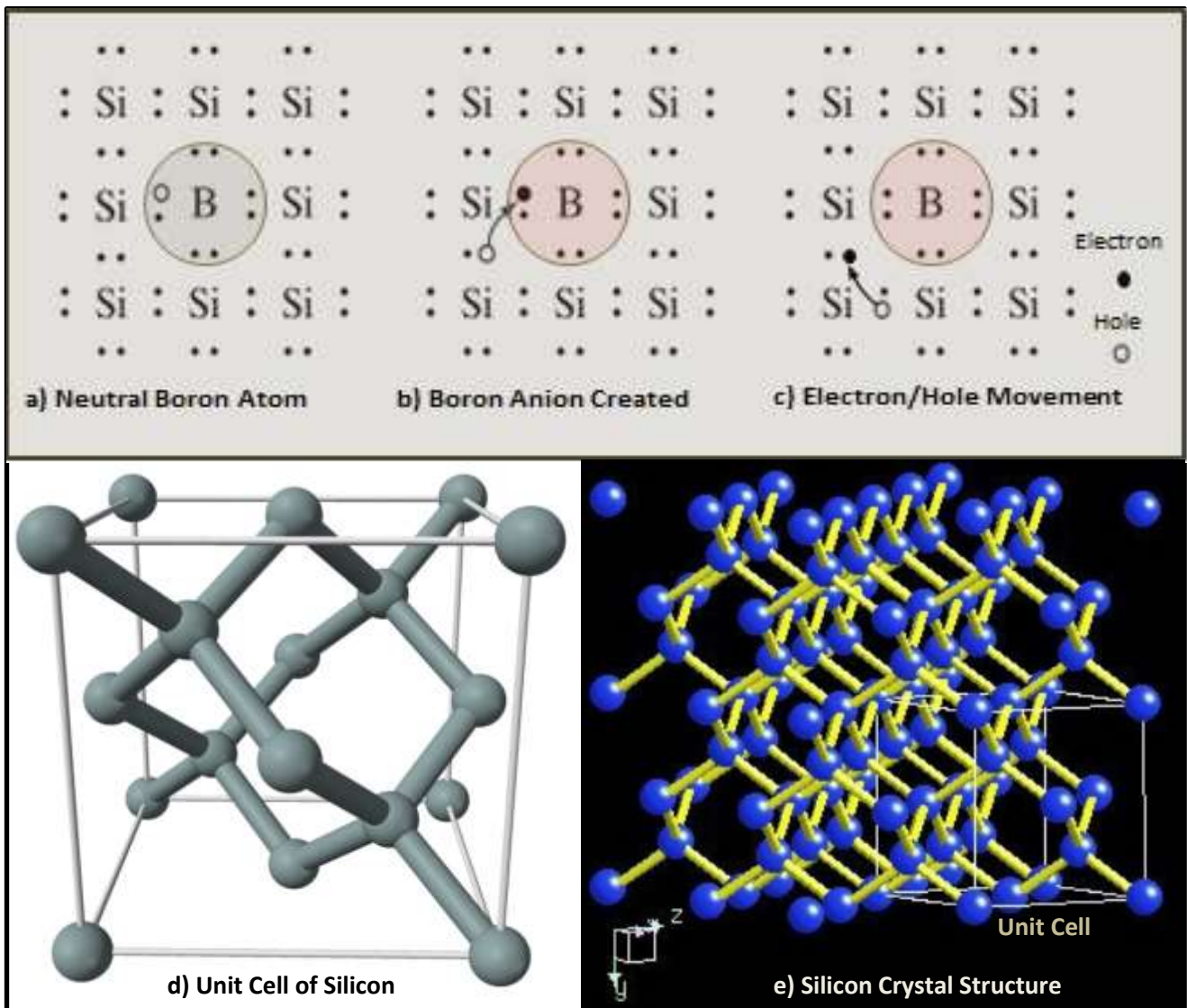


Figure 41: Silicon Unit Cell and Idealised Representation of Electron/Hole Movement in p-type Wafer

A **neutral Boron atom** has only 3 valence electrons and requires an additional valence electron to form four covalent bonds when it is a silicon dopant. When a neutral boron atom acquires the needed electron (it is called an **acceptor atom** because it accepts the extra electron), possibly from an adjacent silicon atom, it becomes an **anion** (a negative ion) and the **donor** silicon atom itself becomes a positively charged atom (i.e. a **cation**) as shown in the figure 41b.

Whereas the boron dopant acquires its electron and becomes a stable anion, the donor/acceptor exchange process is considered to continue dynamically between silicon atoms. Electron deficient silicon atoms are called **holes** and they act as **temporal cations** that play 'pass-the-parcel': the parcel (an electron) leaves a neutral atom, converting it into a hole, and the parcel passes to a neighbouring hole that accepts it to return to being a neutral atom (it is '**fixed**').

A **positive-hole** is thus a **temporal cation**: such a temporal cation is fixed and unable to move within the semiconductor substrate; but it can switch (be 'fixed') from being positive ion back into being a neutral atom. New temporal silicon cations (i.e. holes) are created from fixed-position neutral silicon atoms that become electron donors by losing an electron; and that freed electron can be acquired by a nearby hole, the electron acceptor.

When holes are created, they release electrons that can **drift** (i.e. move in a direction dictated by an applied emf), and/or **move randomly** and be subject to concentration differences in the process called **diffusion**. Thus it would seem a reasonable hypothesis that the hole-creation process could release electrons that could in turn flow from the semiconductor as an **electric current** to push other electrons through an external circuit, with an equivalent number returning to the semiconductor from the opposite direction to back-fill the holes so created.

The Problem with Positive-Holes

As alluded to in this paper's Introduction, conventional Science defines electric currents in terms of the movement of negative charge carrying electrons alone, and thus cannot explain the [Hall effect](#), the [Seebeck effect](#), and the **Brownian motion** (see the next section) of positive CC within semiconductors. For semiconductor current, **positive CC** are required, and hence the need to introduce the concept of **positive-holes**.

With a positive-hole being created by the removal of an electron from a neutral atom, it is simply a static temporary cation with any positive charge being due to an imbalance between the atom's positive nucleus and its outer negative orbital electrons. Although an accumulation of positive-holes can certainly generate a build-up of positive charge, they cannot and do not move so as to carry positive charge: it is the electrons that move away from neutral atoms leaving behind immobile entities that are conveniently termed 'positive holes'. However, clever **animations** can create the **illusion** that holes can move by having the electrons hole-hopping as they move.

For instance, in [this animated gif](#), the moving plus sign visually cues you to think that the holes are moving to the left, but it can be clearly seen that there is no physical movement of positive charge: the holes are fixed but are systematically filled (fixed) by an electron. The electrons are carefully choreographed to conveniently jump to an open hole so as to leave behind another hole that is ready to catch the next jumping electron. Similarly, [this animated gif](#) also clearly shows that the positive charges (the atom nuclei) remain fixed and it is just the electrons that move. And then there are animations like this [dynamic I-Am-Technical animation of drift within a p-n junction](#), which shows holes and electrons magically moving with ease in opposite directions as CC; but without any reasonable detail or explanation of the process involved. While one can admire the magic of such animations, any cartoon-like animation can be totally divorced from reality, as would seem to be the case for these examples.

Fixed temporal cations can be created, and with the removal of increased numbers of electrons from a specific area, a **residual positive charge** can build up. However there is no positive charge movement whatsoever, with the only movement being that of electrons leaving behind the positive-charge of cations. Positive-holes certainly cannot move, represent positive CC, or participate in the Brownian motion observed in semiconductor substrate.

Because of the holes in the concept that positive-holes can be positive CC, convoluted and unconvincing [explanations involving dispersion relations, and positive and negative mass electrons](#), are used to suggest that a positive-hole is a 'positive-charge, positive-mass quasiparticle'. However, according to STEM, positive and negative CC are same-mass 'electrons' that are identical apart from the chiral pattern of their field-energy.

Brownian motion, Diffusion and Drift

Within a **p-n junction**, the CC are sourced from the dopants because the silicon substrate has few free CC: without the presence of dopant contamination, a pure silicon substrate acts as an insulator. However, **dopants** only provide relatively few CC compared to the number within a metallic conductor such as copper wire.

As can be seen in the calculations shown right (sourced from chapter 2 of 'Modern Semiconductor Devices for Integrated Circuits' by Chenming Hu), at room temperature the **thermal velocity** of electron-like CC within a silicon substrate is in the order of 2×10^5 m/sec, which is surprisingly fast, but is still about 1000 times slower than the speed of light (3×10^8 m/sec). At such velocities, because CC are so relatively sparse within the semiconductor, random buffeting and deflection takes place so as to generate [Brownian motion](#), which is analogous to the random thermal movement of molecules within a volume of gas.

Assume $T = 300$ K and recall $m_n = 0.26 m_0$.

$$\text{Kinetic energy} = \frac{1}{2} m_n v_{th}^2 = \frac{3}{2} kT$$
$$v_{th} = \sqrt{\frac{3kT}{m}}$$
$$= (3 \times 1.38 \times 10^{-23} \text{ J/K} \times (300 \text{ K} / 0.26 \times 9.1 \times 10^{-31} \text{ kg}))^{1/2}$$
$$= 2.3 \times 10^5 \text{ m/s} = 2.3 \times 10^7 \text{ cm/s}$$

Thermal Velocity of Electrons (Chenming Hu)

At such velocities, because CC are so relatively sparse within the semiconductor, random buffeting and deflection takes place so as to generate [Brownian motion](#), which is analogous to the random thermal movement of molecules within a volume of gas.

For **Brownian motion** within a gas there is no net movement of the gas molecules unless there are differences in their concentration. The movement of gas molecules due to **concentration gradients** is called [diffusion](#). **Diffusion** is described by [Fick's first law](#) which states that **Diffusion Flux (J)**, as measured in density per unit area per unit time, is proportional to the concentration gradient. For random movement of sparse numbers of free electrons within an **n-type** semiconductor substrate, Fick's law can be expressed as $\mathbf{J} = \mathbf{q} \cdot \mathbf{D} \cdot \frac{dn}{dx}$, where \mathbf{q} = electron unit charge; \mathbf{D} = the diffusion coefficient for the electrons; and dn/dx = electron concentration gradient in direction \mathbf{x} .

Drift is the movement of CC due to an applied **emf (E)**, as indicated by the expression $\mathbf{J} = \mathbf{q} \cdot \mathbf{p} \cdot \mu \cdot \mathbf{E}$, where \mathbf{q} = CC unit charge (+ for aprtrons and - for cetrons); \mathbf{p} = Charge density; and \mathbf{E} = electric-field-generated emf. Both diffusion and drift apply equally to cetrons and aprtrons.

The conventional Science approach is fully supportive that **electrons** within **n-type** semiconductor substrate are the majority mobile negative CC that exhibit Brownian motion and are subject to **diffusion** and **drift**. Required are the equivalent majority positively-charged particles within a **p-type** semiconductor substrate that are capable of similar mobility and behaviour. Even assuming that positive-holes can move via electron hole-hopping, such activity does not involve **random collisions** or deflections that could justify the use of Fick's diffusion law, let alone generate the concentration gradients needed to cause positive charge diffusion. The conventional Science approach **desperately needs** positive-holes to be physically mobile like electrons, whereas STEM has ready-made almost identical positive and negative mobile CC.

With there being strong evidence that both diffusion and drift are active within both the p and n-side of a p-n junction, you can choose to believe that they can be accounted for by the smoke-and-mirrors illusion of the reciprocal movement of electrons and static holes: this is what most texts and animations (such as those referenced in the previous section) exhort their audience to do. Alternatively, you can carefully consider the STEM approach which considers **cetrons** to be the majority negative CC within the n-type substrate, and **aptrons** the majority positive CC within the p-type substrate.

The STEM Explanation

For the STEM approach, the **cetron** fulfils the role allocated to the electron by conventional Science's 'electron': that of being a mobile **negative CC**. The **aptron** fulfils the role allocated to the 'positive-hole' by conventional Science: that of being a mobile **positive CC**.

Within semiconductors, the main charge movement mechanisms are **diffusion** and **drift** of involving electron-like negative and positive CC. To understand how both negative and positive CC become available within semiconductor substrate (e.g. silicon or germanium), we need to look at the structure and manufacturing process of the semiconductor substrate, concentrating here upon crystalline silicon, and p-type and n-type silicon wafers.

With an abundance of 92%, Si-28 is its main isotope of silicon. In crystalline form, Si-28 has a tight diamond-like crystal structure producing a unit cube (see figures 41c and d) of side length of 543 pm, compared with 357 pm for cubic diamond. However, due to the small diameter of the STEM-based diamond carbon-12 nucleus, with a minimum centre-to-centre separation of C12 atoms being 154.6 pm, crystalline diamond has a minimum the bond length is 110 pm which, although short enough to be a strong bond, is too long for C12-to-C12 b-bond (the [Bitron Bond Primer](#) provides a brief overview of b-bonds) formation.

For crystalline silicon, the minimum centre-to-centre silicon-to-silicon atom separation is 235pm. With a STEM nucleus width of about 140pm, the corresponding minimum bond length is approximately 95pm, which is within the limits of b-bond formation. Thus, although the unit cube of diamond and silicon are geometrically similar, crystalline silicon contains b-bonds whereas diamond does not: this also means that their physical characteristics are different.

Whereas conventional science considers that, in a crystalline state, silicon atoms are **covalently bonded**, STEM considers them to be **bitron bonded**. However, at about 95pm long, crystalline silicon's b-bonds are quite weak, which means that silicon is far less hard than diamond and can be easily doped and machined into thin slices to create a wide range of semiconductor devices. Also, silicon's weak b-bond means that bitrons may easily bump-released by energised free electrons or by EMR in the visible frequency range: this is important for photo-sensitive semiconductor devices (see the [Photovoltaic Cells, Photodiodes and LEDs](#) chapter).

Most silicon-based semiconductor substrate is produced commercially in bulk using the [Czochralski process](#) (named after Polish chemist Jan Czochralski who invented the technique). Measured quantities of **dopants** are added to a **silicon dioxide** molten mix at concentrations of about one dopant atom per five million silicon atoms. Within the melt, the silicon and oxygen bonds within silicon dioxide break down and release oxygen and lots of excited electrons in approximately equal numbers of cetron and aprtron electrons.

Within an **n-type** substrate, **phosphorous** atoms are **reduced** by acquiring a **cetron** (a negative CC) to become an **anion** embedded within the cooling n-type silicon crystal structure. Similarly, within the **p-type** substrate, **boron** atoms are **oxidised** by acquiring an **aptron** (a positive CC) to become a **cation** embedded within the cooling p-type crystal structure.

When the molten mix cools and solidifies as part of the Czochralski process, the number of dopant phosphorous anions within the **n-type** doped silicon crystal provides a supply of loosely bound ionic orbital **cetrons** (negative CC) not available within the chemically neutral silicon host. Correspondingly, within the **p-type** mix, the boron cations provide a supply of loosely bound ionic orbital **aptrons** (positive CC). All that needs to be done is to slice the silicon crystal into thin sheets (between 160 to 300 μm thick), cut the sheets to the required junction size, and then to glue matching pairs of each type together and add the electrical contacts to produce **p-n junctions**.

Even with doping, cetron and apron concentrations within p-type and n-type wafers are very low compared with their concentration within metal conductors. At room temperature after the silicon wafers have cooled, the CC can freely move with the thermal energy causing them to take on **Brownian motion**, randomly buffeting each other but with no net movement, which is a similar to the action of molecules within a volume of gas.

When, as part of the p-n junction manufacturing process, slithers of p-type and n-type substrates are joined by gluing them together, there is a concentration of negative CC (cetrons) in the n-side wafer that, due to the concentration of positive CC (aptrons) in the p-side, start to drift across the join. Similarly, p-side aprons drift across the join to the n-side. The two-way migration of positive and negative CC in opposite directions across the join represents electric charge movement that is referred to as a **micro electric current** (see the '[The Nature of Electric Currents](#)' chapter).

Should this migration process continue unabated, the positive and negative CC would eventually become fully intermixed, with their net charge effect becoming zero; but that is not the case. Instead, as part of the initial micro current, as more cetrons migrate into the p-side, and aprons migrate in unison into the n-side, a negative cetron-based layer forms on the p-side, and a positive apron-based layer on the n-side which, due to like charge repulsion, prevents further drift-based migration. Thus, after a short period of time, the micro electric current stops and a state of **equilibrium** is attained, as shown in figure 42a.

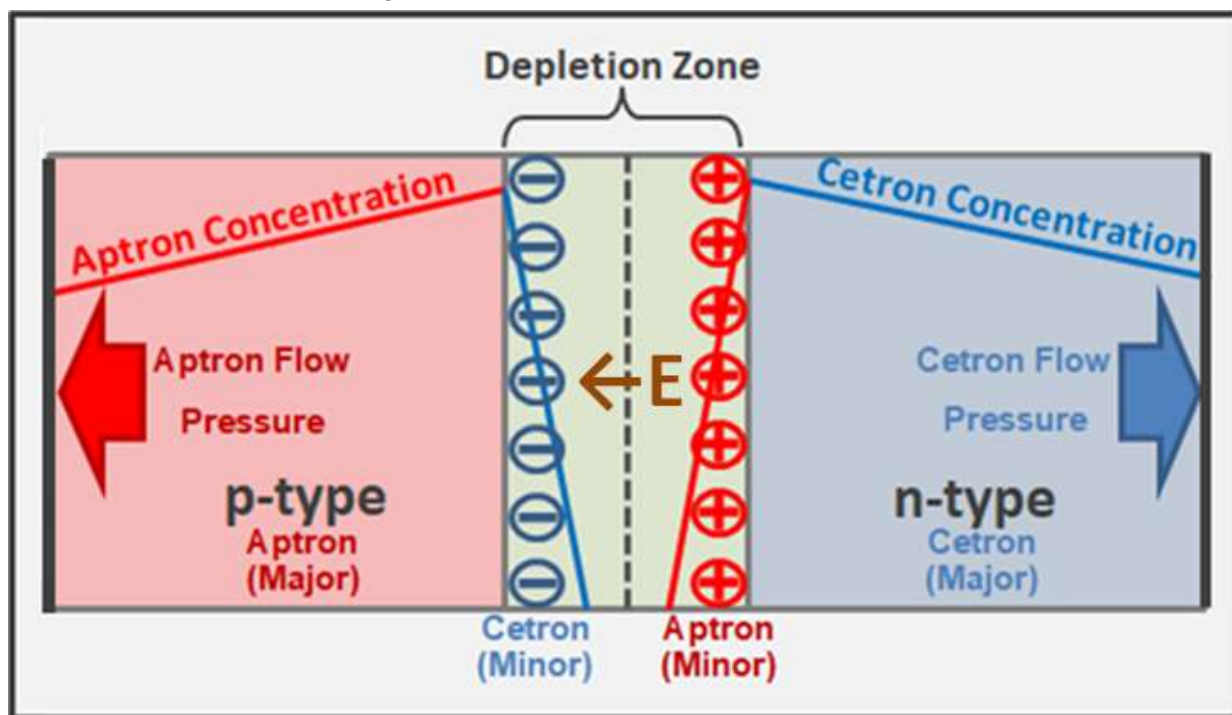


Figure 42a: Positive and Negative Charge Carriers and Depletion Zone Formation

The result of this short-lived migration and concentration process is a narrow zone (light green figure 42a) centred on the join, which is called the **space charge region** or the **depletion zone**. Within the depletion zone, the **majority CC** are depleted, because they have migrated into the other side, to the extent of being non-existent centrally, and hence use of the term 'depletion zone'. The CC concentration are in a minority on the side they accumulate, and are thus called **minority CC**. Minority CC represent two distinct charge layers that together generate an **emf (E)** across the depletion zone variously called the **contact potential** or **built-in voltage** or **junction voltage** or **barrier voltage**: as the term suggests, this 'built-in voltage' is ever-present across all P-N junctions to the extent that it can be troublesome within semiconductor circuitry.

The concentration of charge along the sides of the depletion zone, created by minority CC concentration, attracts the majority CC so as to create a **concentration gradient** that, in turn, generates a diffusion-based **flow pressure**, as shown in figure 42a. This diffusion-based cetron and apron flow pressure is quite important for the explanation of the operation of photodiodes (see the '[Photovoltaic Cells, Photodiodes and LEDs](#)' chapter).

The **depletion zone** acts as a porous barrier that separates the majority carriers: electrons on the n-side and holes on the p-side. However, the depletion zone width and associated barrier voltage is a delicately balanced equilibrium that can be affected by a change of temperature, an applied emf or exposure to light.

For instance, should the positive terminal of a DC power source be connected to the p-side of a p-n junction and the negative to the n-side as shown top in figure 42b, the diode is considered to be in **forward-bias**. The emf of the applied power source attracts electrons towards the positive terminal, and closest electrons are those minority carrier concentrated on the p-side of the depletion zone. With these electrons drifting towards the positive terminal, and similarly the minority carrier holes on the n-side drifting towards the negative terminal, the minority carrier concentrations of the depletion zone are reduced, reducing both its width and the strength of the barrier field it creates. With sufficient applied voltage, the depletion zone becomes wafer-thin to non-existent, so that it provides no effective internal resistance to forward bias current flow. In forward bias mode, the diode thus can act as an **ON switch**.

When a diode operates within the **forward-bias** region (which is often referred to as being in **photoconductive mode**), the barrier voltage initially off-sets the applied voltage but, as the depletion zone is progressively narrowed and the barrier voltage is declining, majority CC start to breach the barrier and a current starts to flow. For silicon substrate current starts to flow as the applied voltage increases towards 0.5 volts.

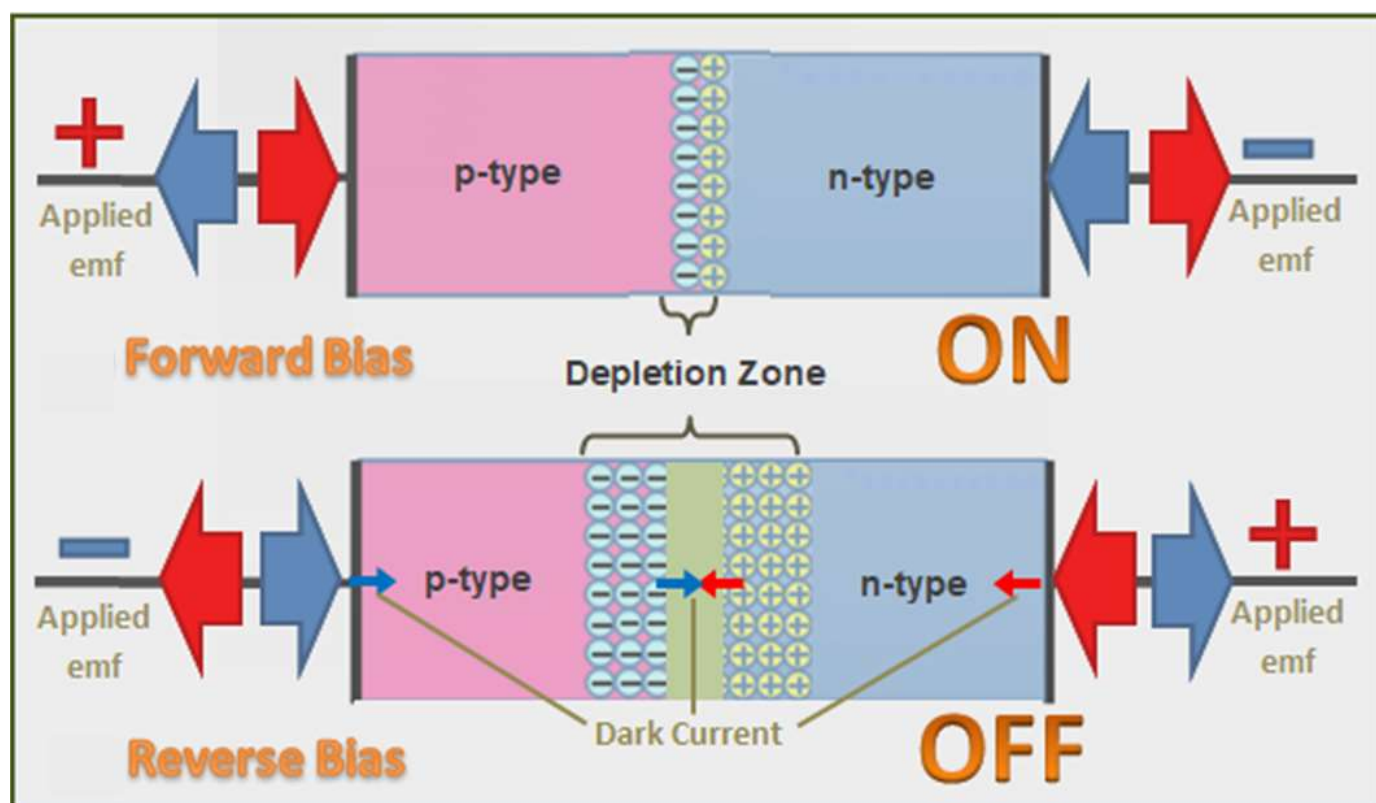


Figure 42b: Forward and Reverse Biased P-N Junctions (Diodes)

In the **knee region** of the I-V curve, the current flow rapidly increases as the depletion zone resistance continues to reduce so that, by the time the forward voltage (V_f in figure 43) is reached, the diode's internal resistance is effectively zero, and the current increases significantly for only a small increase of applied voltage. For silicon substrate V_f is 0.7 volts, and for germanium substrate it is 0.3 volts.

Should the negative terminal of a DC power source be connected to the p-side of a p-n junction and the positive to the n-side as shown bottom in figure 42b, the diode is in **reverse bias** mode. For this situation, the applied emf attempts to push electrons into the p-side, but they cannot get pass through the electron barrier of the depletion zone; instead they join and widen the electron barrier. Similarly, holes are being pushed into the n-side by the applied emf but simply end up joining and widening the hole barrier. Thus, the depletion zone widens and the barrier voltage increases, with no current associated with the applied emf able to pass through the diode, which functionally acts as an **OFF switch**.

Although reverse bias mode acts as an OFF switch, there are two subtle forms of current flow. As CC are initially pushed into the diode by the applied emf of the power source, until the depletion zone widening adjusts to the provision of CC, a micro current briefly flows in the external circuit: this ceases when the new equilibrium is in place.

In reverse bias mode, due to the **increasing barrier voltage**, there is increased attraction of minority CC on the inner surfaces of the charge barriers, allowing small numbers of them to randomly swap sides as indicated by the small

arrows central shown bottom in figure 42b. Each cetron that swaps sides causes a micro-imbalance, marginally reducing the cetron charge barrier and allowing another cetron from the negative terminal to enter the p-side and then migrate to the cetron barrier so as to rectify the imbalance. With aprtrons similarly trickling across the depletion zone in the opposite direction, a small current flow occurs in the reverse bias direction, which is called the **dark current**.

Figure 43 shows a typical I-V diagram for a diode. In reverse bias mode region, as the voltage is increased (i.e. has a larger negative value), the reverse flow of current is dark current, which increases only slightly with voltage in an almost flat linear manner, in the order of μ amps (i.e. 10^{-6} amps). This flat part of the graph is also referred to as the **photoconductive mode**. As the applied reverse current increases, the gradient of the I-V curve starts to increase significantly as the breakdown voltage (V_{br}) is exceeded and the **Zener breakdown** (or **avalanche**) zone is entered.

In the breakdown zone, with the depletion zone having significantly widened, the confinement space of the majority CC has been significantly reduced, with the number of minority CC approaching that of the majority CC on each side of the diode, the depletion zone collapses, causing the CC to intermix and to flow as a current with the diode offering zero resistance, resulting in a short circuit that cause the diode to overheat and be irretrievably damaged so that the depletion zone cannot be re-established.

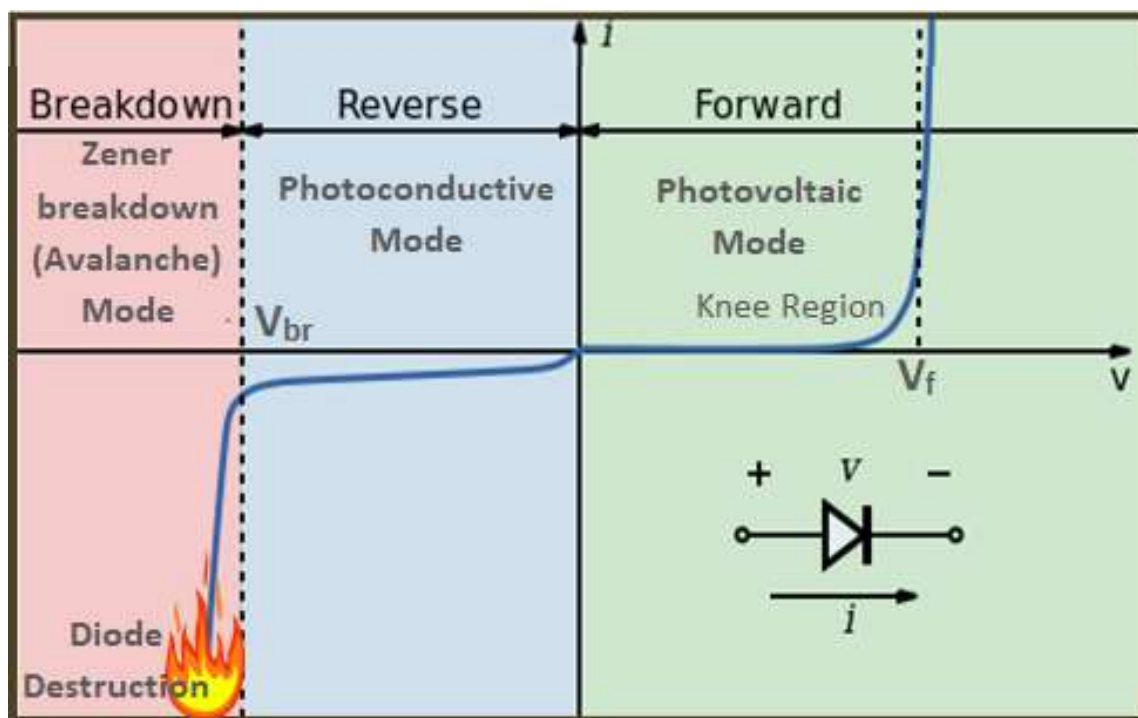


Figure 43: Forward, Reverse and Breakdown Regions of a Typical Diode's I-V Curve

Photodiodes and transistors are important applications of P-N junctions, but an explanation of their operation is complex, and will be covered later in the [Photovoltaic cells, Photodiodes and LEDs](#) and [NPN and PNP Transistors](#) chapters. Next is a discussion about the nature of electric currents.



Photovoltaic Cells, Photodiodes and LEDs

A **photovoltaic cell** provides an alternative source of electrical power to chemical batteries and magnetic induction. For a photovoltaic cell, CC are released from silicon atoms within the P-N silicon wafer by the bombardment **electromagnetic radiation (EMR)** within the **visible light frequency** range, which provides sufficient internally generated emf to generate an electric current.

A typical P-type photovoltaic cell structure is shown in figure 44a. It has a large light collection surface area and, to allow light to penetrate the lower p-type wafer, the upper n-type wafer is usually considerably thinner than the p-type.

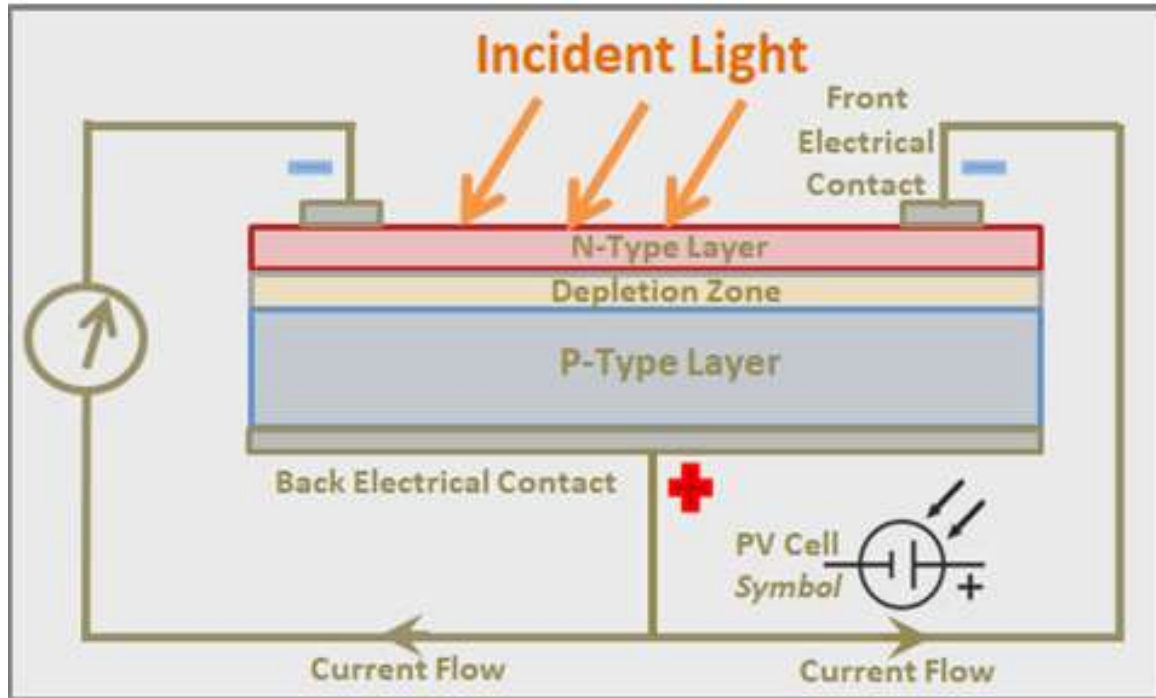


Figure 44a: A Typical P-Type Photovoltaic Cell Structure

Conventional Science's approach considers that silicon atoms within the crystalline structure of the wafer are **covalently bonded** to four other silicon atoms or an occasional dopant atom. EMR with sufficient energy is considered to knock electrons from a covalent bond is considered to release free electrons and leaving behind a **positive-hole**, which represent a pair of positive and negative CC. However, as [discussed earlier](#), a free electron is mobile, but not so a positive-hole: it represents a fixed **temporal cation** within the semiconductor substrate, and certainly does not, and cannot, act as mobile positive CC as claimed.

The STEM approach considers that the bonds between silicon atoms (and the sparse dopant atoms) are **b-bonds (bitron bonds)** rather than covalent bonds. Bitrons consist of concentrated field energy that is quantized to that of the energy core of an electron: it is thus a pre-electron.

There are two schools of thought related to the release of bitrons from b-bonds and their conversion to a cetron or apron electron.

One school of thought is that EMR simply energises existing CC, increasing their kinetic energy, and it is energised CC that collide with b-bonds, so releasing the bitron as a new CC. In this scenario it is likely that cetrons would cause released CC to have the chirality of a cetron, and aprons would likewise generate another apron. Thus in the n-type side of the photovoltaic cell there would be an increase of cetron concentration (the majority CC), and on the p-side there would be a similar increased concentration of apron CC.

The other school of thought is that EMR of sufficient energy knocks a bitron from a b-bond and, as a pre-electron, it has equal probability of becoming a negative CC (a **cetron**) or a positive CC (an **aptron**). Thus additional mobile negative and positive CC are generated in approximately equal numbers from the semiconductor substrate by EMR bombardment. This is the assumption made in all the diagrams, explanations and discussion from this point onwards.

Note also that when a bitron is removed from a b-bond, in an environment wherein the atoms are firmly held in a rigid crystalline structure such as a silicon substrate, another bitron quickly forms to re-establish the b-bond. In this manner b-bonds essentially become cetron and apron breeders: they certainly can produce sufficient CC to generate an electric current and power up a micro-circuit. Newly generated CC are notated as 'photon created' in figure 44b.

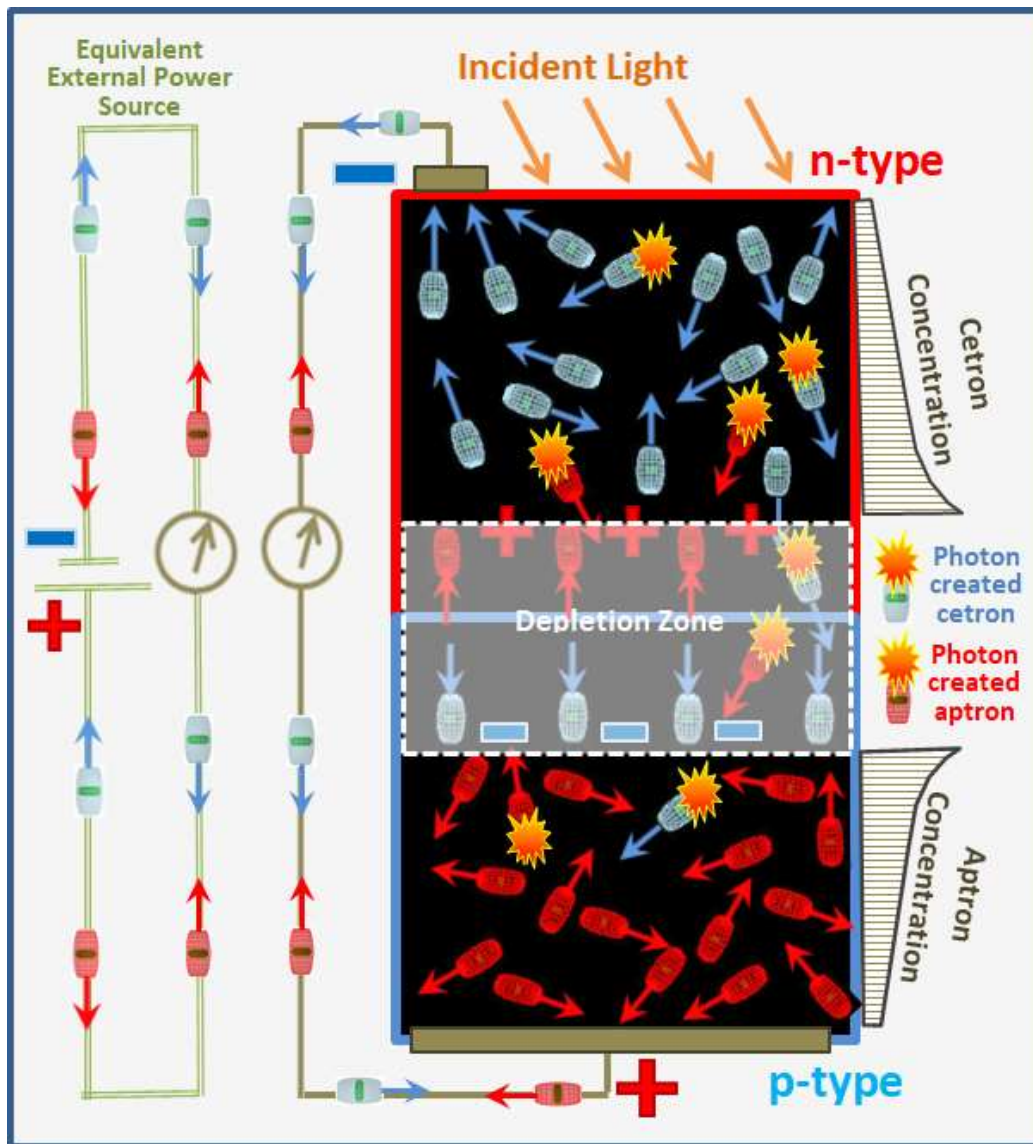


Figure 44b: Plateau Region Dynamics for a Photovoltaic Cell

As for any diode, the number of CC resulting from the manufacturing process is sparse within a photodiode, as determined by the number of dopant atoms in the mix. Typically a phosphorus dopant determines the level of negative CC in the n-type, and boron the level of positive CC in the p-type. As described earlier in the ‘[Semiconductors and P-N Junction](#)’ chapter, without exposure to light or an applied emf, the CC adjust to form a **depletion zone** and an associated **reverse-bias (barrier) voltage** that generates **dark current** within an electric circuit.

With the silicon substrate being semi-transparent, light can penetrate through to the lower n-type zone, with light of different frequencies capable of penetrating to different depths. In order to help equalise the photon hit rate of bitron bonds in the upper n-type and lower p-type layers, the n-type wafer thickness is usually made considerably less than that of the p-type. As photons of sufficient energy to release bitrons to generate equal numbers of extra positive and negative CC, the diode’s electrical dynamics change.

The photon b-bond hits increase the number of CC in all three layers (n-type, depletion zone, p-type), and that has several effects. In all zones of the diode, the CC become excited and gain kinetic energy from the incoming light and heat energy. Specifically, newly released CC increase the majority CC concentrations and gradients in both sides of the diode which, in turn, increases the **flow pressure** from within both the n-side and p-side. Newly created minority CC soon become attached to, and thus widen, the depletion zone. The increase of majority CC increases the voltage difference between the diode’s terminals and the widening depletion zone increases the diode’s resistance. Both drift and diffusion thus contribute to the diode’s changing dynamics.

Initially, the voltage and depletion zone resistance both increase at about the same rate, and thus, according to **Ohm’s Law** ($V = I \times R$), the current flow remains constant, as reflected by the **plateau region** of the I-V curve of figure 44c.

However, by the stage that the **decay region** is entered (at about 0.4 volts for silicon substrate), the diode resistance starts to outstrip the voltage increase, causing a drop-off of current. **Cetrons** entering the p-type from the circuit wire

connected to the lower contact encounter increased resistance as they attempt to migrate back to the n-type; and similarly, **aptrons** moving in the opposite direction from the upper contact encounter increased resistance to their migration back to the p-type side. With the **depletion zone resistance** increasing at faster rate than the voltage, by the time the voltage approaches 0.6 volts (for silicon substrate), the current flow ceases.

Of importance for the commercial use of photovoltaic cells, the power ($= I \times V$) curve for a photodiode peaks just over half-way into the decay region, well after the current flow starts to reduce.

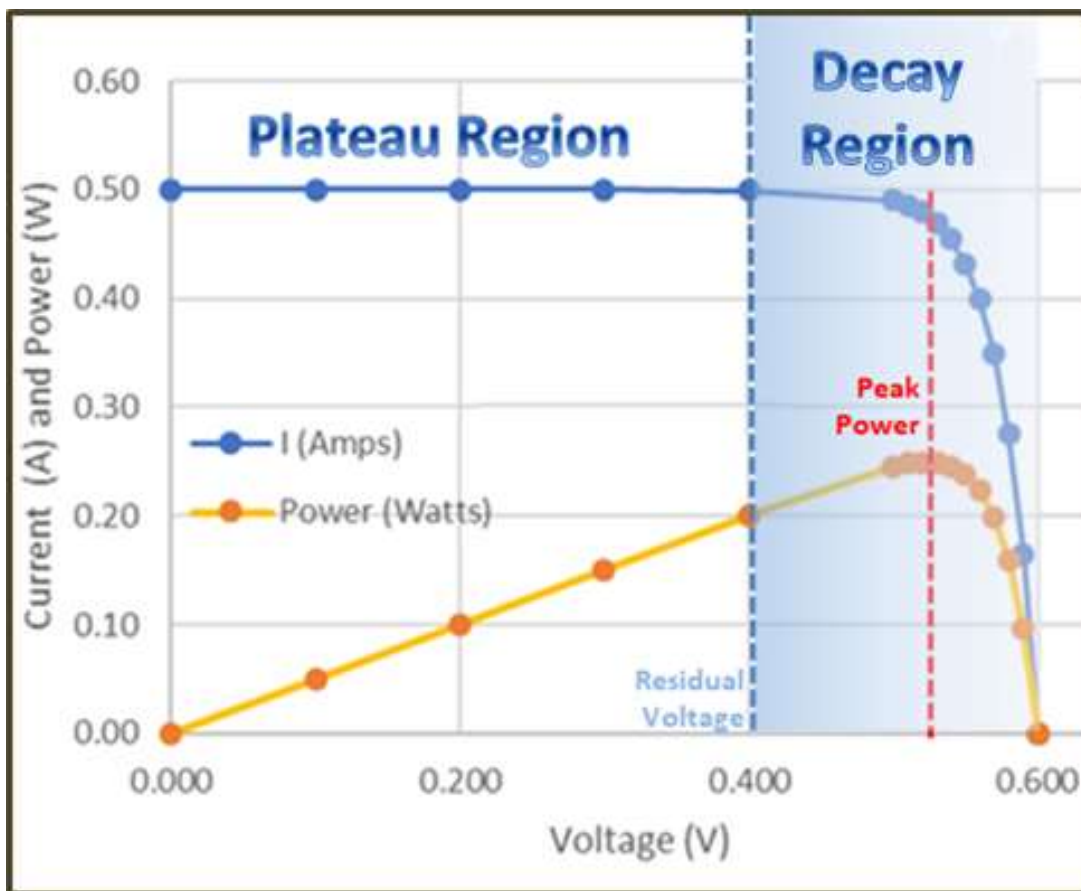


Figure 44c: Photovoltaic Cell I-V and Power Graphs

The orientation of an **equivalent power source** to replace a photovoltaic cell is shown to the left of figure 44b. A photovoltaic cell acts as a low-voltage power source that, when hooked up in series, can be used to create a **solar panel** to generate commercial levels of **solar power**. Interestingly, the cell structure of the P-type photovoltaic cell of figure 44a can be reversed to create an N-type photovoltaic cell as shown in figure 44d.

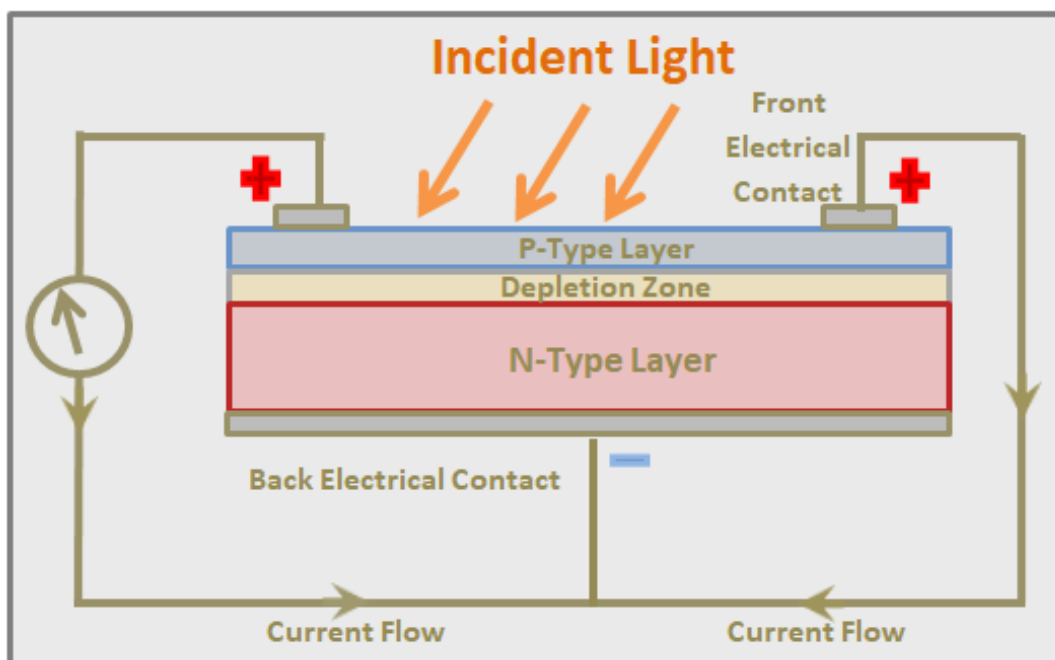


Figure 44d: Typical N-Type Photovoltaic Cell Structure

A **photovoltaic cell** works in reverse because the positive and negative CC migration directions are simply reversed. The operational characteristics of the two types are very similar, but commercially n-type cells are more expensive to manufacture, but with the n-type silicon being of a higher purity, which enables higher efficiency, lower losses and much lower cell degradation over time. These aspects generally outweigh the additional upfront cost over the life of the panel. However, there are many technologies that improve cell efficiency and, particularly with increased production volumes, the cost versus efficiency equation will most likely continue to change.

Whereas the **photovoltaic cell** is a **diode** that has a large light collection surface area, a **photodiode** is a compact diode with a small light-access window (see photo in figure 46), with the p-type uppermost exposed to incoming light as for an N-type photovoltaic cell. With no light exposure (i.e. in the dark), a photodiode acts as an ordinary diode and, when it is connected to a power source, it has the three distinct diode regions: the **breakdown**, **reverse-bias** and **forward-bias** regions as shown earlier in figure 13.

When exposed to light, a photodiode's I-V curve has a similar shape and consists of the same three regions, but is shifted downwards in the negative current-axis direction dependent upon the **intensity** and **wavelength** of light-exposure. A typical photodiode I-V plot is shown in figure 45. It consists of a series of curves P0, P1 and P2 representing different incident light intensities (**lumens**), with P0 representing zero exposure (i.e. in the dark) and thus corresponding to the figure 13 plot for a diode..

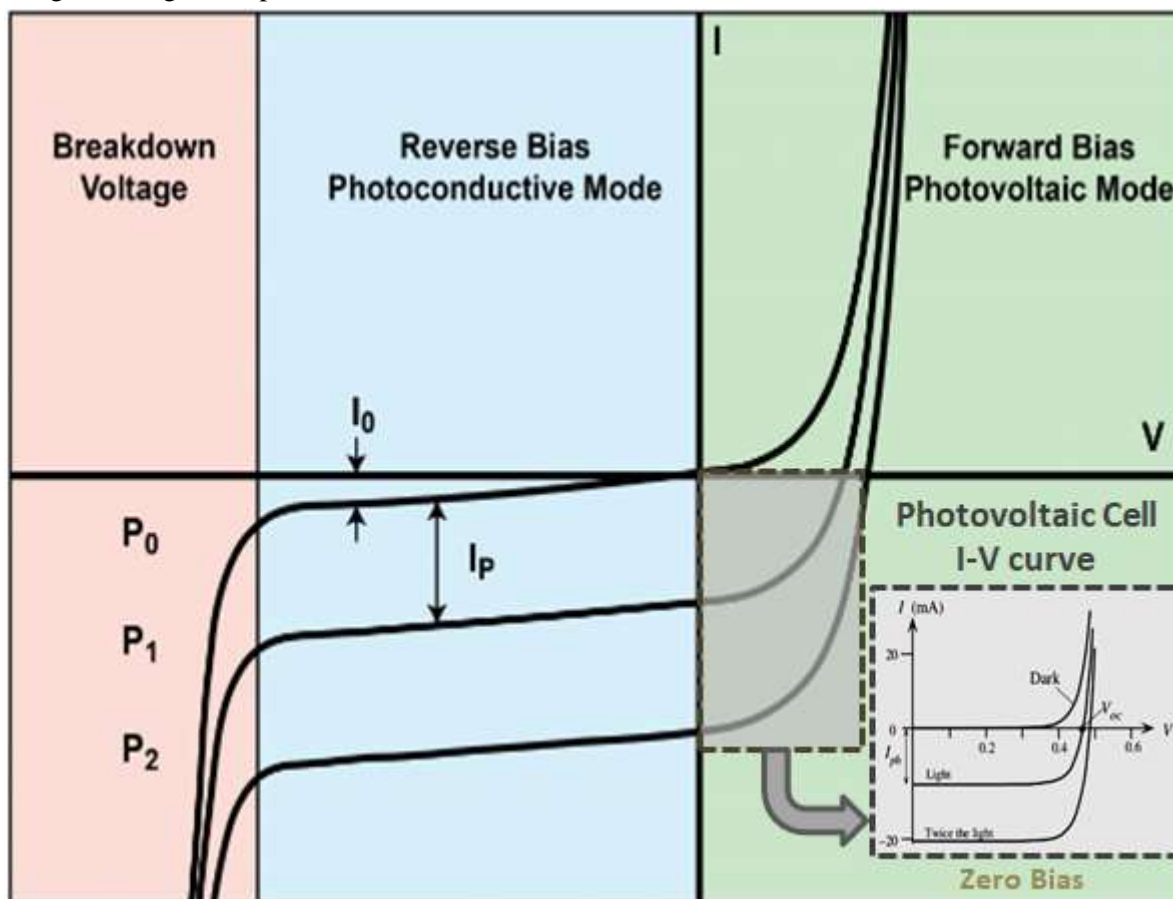


Figure 45: I-V Graph by Light Intensity for a Biased Photodiode

In **photoconductive mode** (i.e. reverse-bias), the I-V plots are almost linear and almost horizontal, and paralleling each other with increased light exposure. It is worth noting that in the forward bias region for negative current flow (the grey area of figure 45): allowing for differences in physical size and design between photovoltaic and photodiodes, the curve is quite similar to that of the photovoltaic cell (compare figure 43 versus the light grey '**Zero Bias**' insert), which is not surprising, as the same CC-related processes are involved for both diode configurations.

Figure 46 shows the physical structure of a typical top-window photodiode: it is operated in **photoconductive mode** to act as a light-detection device. Light is allowed to enter the top of the p-type side, which is usually kept thin to enhance performance by increasing light penetration into the depletion and n-type regions. With no light (i.e. in the dark), the photodiode blocks current flow, apart from the μA dark current, so registering the **light-OFF** condition. When exposed to light (**light-ON**) the current flow in the reverse bias direction depends upon the light intensity, and thus represents low to high light exposure.

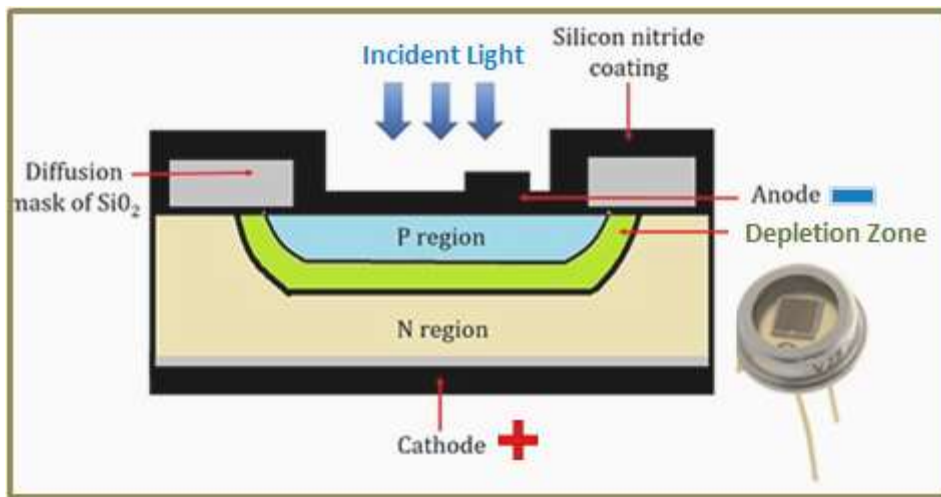


Figure 46: A Typical Top-Window Photodiode Structure

Figure 47 represents the operation of a **photodiode** in **photoconductive mode**. It is basically an N-type photovoltaic cell but with a smaller light exposure window and it has been wired up in reverse bias to a power source.

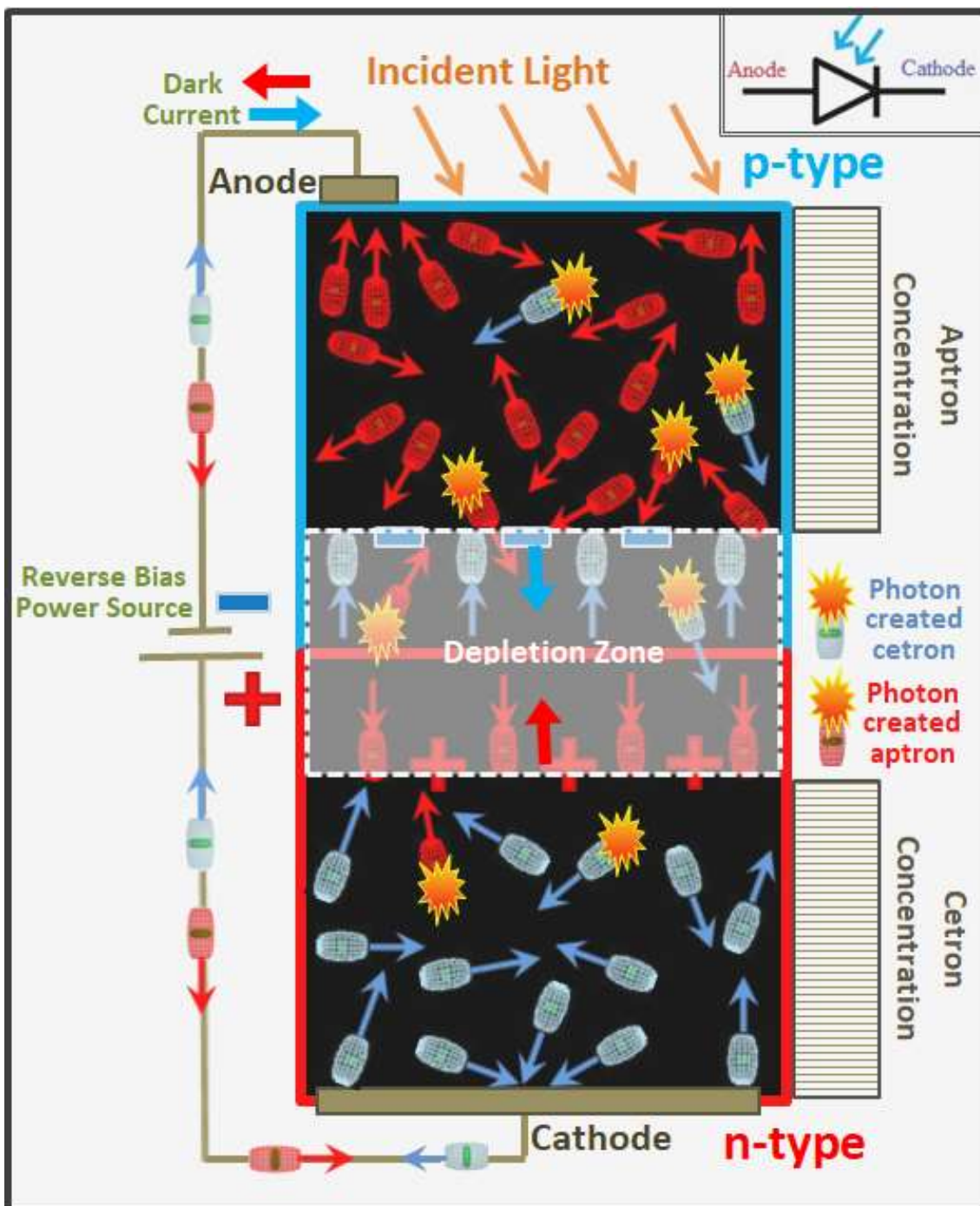


Figure 47: Operation of a Photodiode in Photoconductive Mode

The reverse bias power supply causes a **widening of the depletion zone**, and with the barrier charge being close to the applied voltage, there is a negligible concentration gradients in the majority CC. Consequently, there is no current flow apart from a trickle of dark current in the reverse bias direction.

As for all diodes, the depletion zone is a delicate and dynamic balance of drift and diffusion, with ongoing continual micro-adjustment taking place to maintain its current equilibrium. As small numbers of minority positive CC manage to break free from the inside surface of the positive charge barrier, they represent an imbalance that triggers a compensating negative CC to break free from the negative charge barrier (or vice versa). Such CC-exchanges cause minuscule variations of the barrier voltage that is responded to by minor reverse bias current variations.

With **light-exposure**, photons of sufficient energy to release bitrons to generate equal numbers of extra positive and negative CC, the diode's electrical equilibrium changes. Newly created majority CC instantly increase the majority CC concentrations and minority CC more slowly drift to the depletion zone's outer charge barriers. The increase of majority CC pushes them into the attached circuit, while the minority CC cause a migration across the depletion zone to complete the loop for CC moving as a reverse bias current. Increase exposure causes increased reverse bias current flow as indicated I-V plots for different light intensity (see the photoconductive mode curves in figure 45).

The response time for a light-sensing photodiode in photoconductive mode, which is dependent upon light-induced CC creation and energisation, is too slow for many applications. Quicker response times are achieved by photodiodes operating in breakdown-voltage (or avalanche) mode, which involves higher reverse-current flow rates. These photodiodes are called **Avalanche photodiodes (APD)**, and employ different doping and layer-bevelling techniques compared to 'normal' APDs, leading to greater voltage tolerances (more than 1500 volts) before breakdown occurs: hence they achieve greater operating gains and response times.

LED semiconductors are photodiodes that operate in **forward bias** (or photovoltaic) mode: they are encrusted in glass or translucent plastic, and doped with a mixture of exotic compounds including Gallium, Arsenic, Gallium, Phosphorus, and Indium, all mixed together at different ratios to selectively produce a distinct colour (a sample range is shown in figure 48).

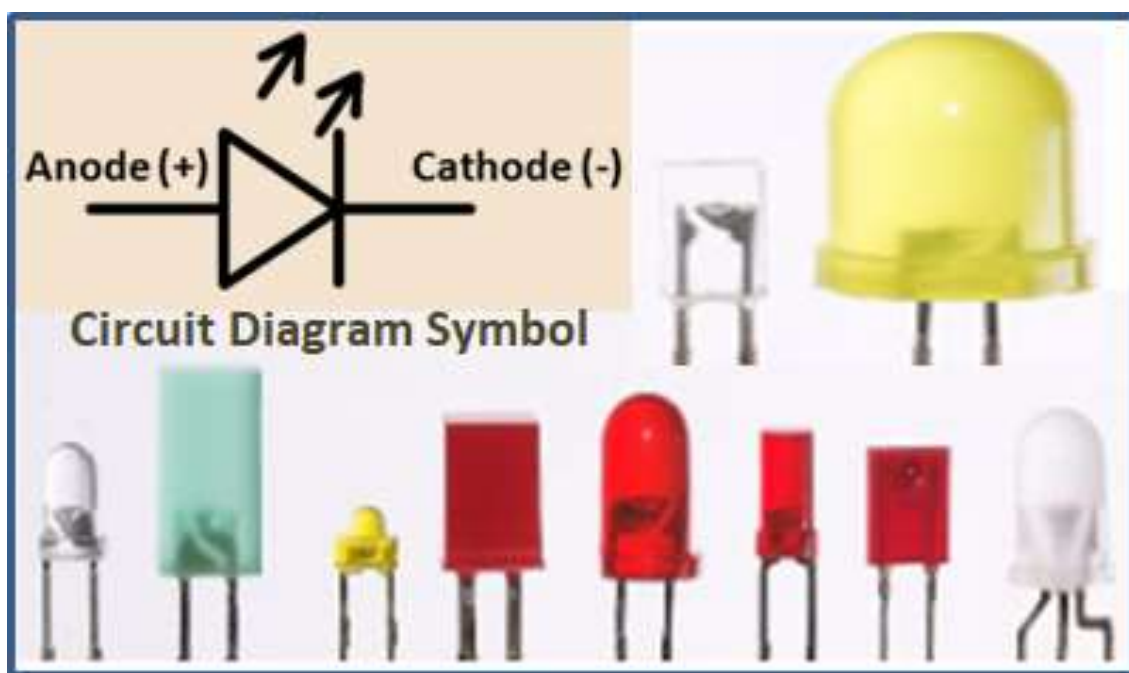


Figure 48: Light-Emitting Diodes (LEDs)

The most common LED **p-type dopant** is Gallium (Ga, atomic number 31); and Arsenic (As, atomic number 33) for the **n-type dopant**. The resultant semiconductor substrate is referred by a descriptive chemical name such as Gallium Arsenide (GaAs) or Gallium Arsenide Phosphide (GaAsP) should Phosphorus be added.

LEDs operate on low forward-bias voltages and have low power consumption. They are designed to excite the n-type and p-type mix of dopants to emit photons (called **spectral emission**) within the visible light range. The selection of the dopant mix to produce specific LED light-colours has been, and will most likely continue to be, an evolutionary trial-and-error selection process rather than an exact science.

LEDs are specially constructed to release a large number of photons outward, and are thus housed in a plastic bulb that concentrates the light in a particular direction, with most of the light bouncing off the sides of the bulb to increase emission intensity.

But even still, LEDs are simply specialised diodes: should multiple LED's be connected in parallel and exposed to sunlight, they operate as low-yield photovoltaic cells producing only a modest electric current.



NPN and PNP Transistors

A **transistor** is a three-layer double P-N junction: we shall be considering the **NPN transistor** which has a p-type layer sandwiched between two n-type layers: it has two end contacts (or pins) and a central one called the **base**. There are five main techniques to construct transistors: the Point contact, Grown-junction, Alloy-junction, Diffusion, Epitaxial techniques. Although the size, production costs and performance characteristics vary between the various forms, the cause of their behaviour within electric circuits is the same.

With no electrical loads on any of its 3 contacts, and with sufficient time to establish (or re-establish) equilibrium, the NPN transistor contains two depletion zones as shown schematically in figure 49. Out-of-the-box new NPN transistors should be in equilibrium mode.

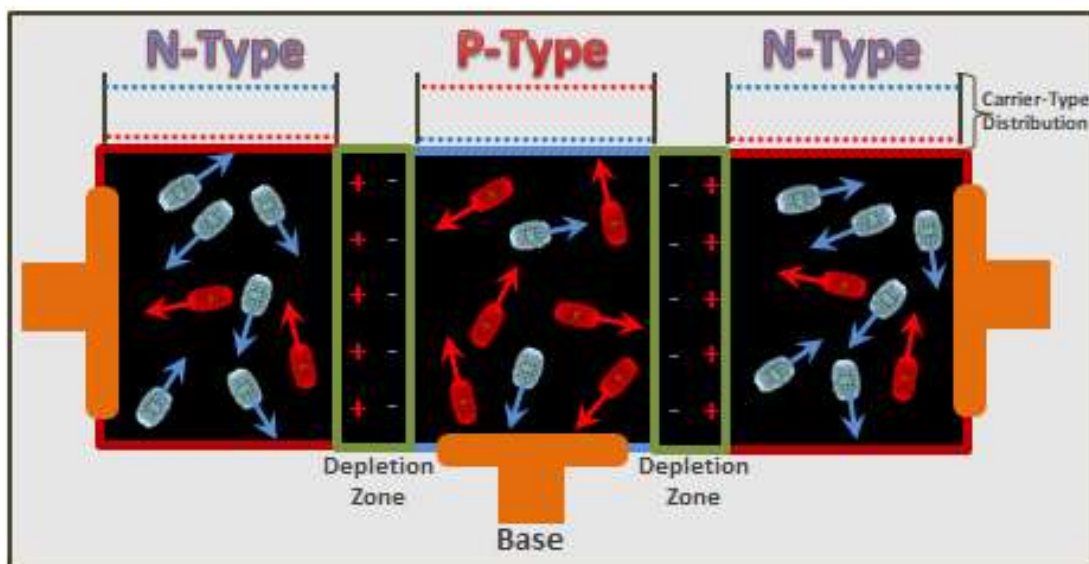


Figure 49: Un-powered NPN Transistor (In Equilibrium)

For circuit design purposes, the negatively charged end pin is referred to as the **emitter** and the positively charged pin is the **collector**, which is based upon the conventional Science concept that under 'normal' operation electrons move from the negative emitter side to the positive collector side of the transistor.

With **no emf** applied to the **base pin**, as shown in figure 50, the emitter-side p-n junction is **forward-biased** and, should the V_{CE} (voltage drop between the collector and emitter pins) exceed the barrier voltage (dependent upon doping levels, typically be 0.7 volts for silicon substrate or 0.3 volts for germanium substrate), the emitter-side depletion zone becomes negligible to non-existent.

The collector-side p-n junction is **reverse-biased** and thus its depletion zone widens and its barrier field increases accordingly, which prevents the movement of charge between emitter and collector: thus the transistor is in **off** (or **cut-off**) **mode** and acts like an **open circuit** break.

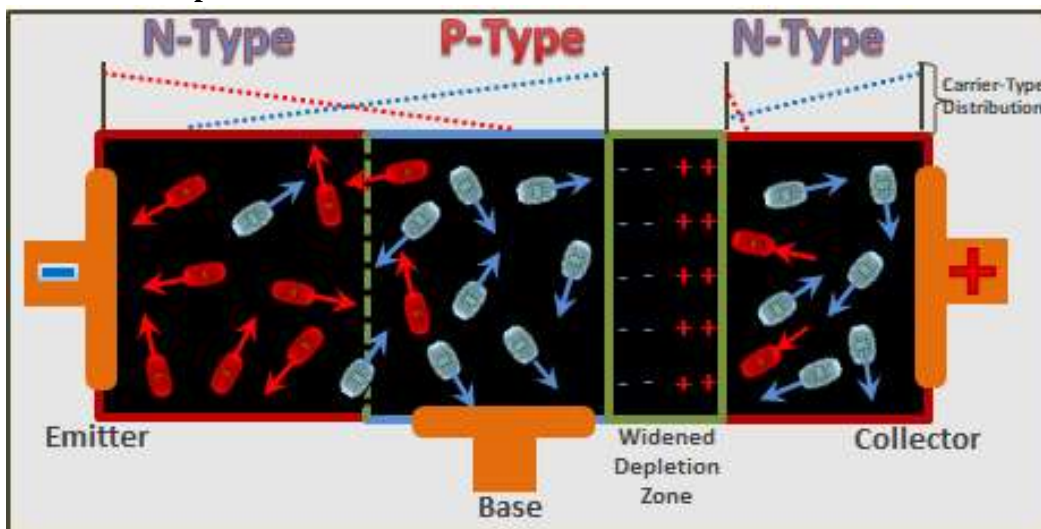


Figure 50: Powered NPN (Zero Base Load → Polarised Charge Carriers)

The applied voltage causes **aprons** to drift from the p-type to concentrate in the immediate vicinity of the negative emitter terminal, and **cetrons** from the emitter-side n-type to drift in the opposite direction to concentrate along the collector-side depletion zone. The net effect is a **reverse-polarisation effect**, with the major CC (aprons in the p-type and cetrons in the n-type) swapping sides, as can be seen in the **dot-line CC distribution graphs** by CC-type at the top of figure 50. A less pronounced polarisation effect also occurs within the collector-side’s n-type, with its major CC (cetrons) drawn towards the positive collector contact.

When a **negative voltage** is applied to the **base**, the collector-side depletion zone re-appears and widens, increasing the barrier field (no graphic has been provided for this option: it is similar to that of figure 50 except for a wider collector-side depletion zone), and thus the transistor remains in **cut-off mode**. Thus, as well as cut-off occurring when no emf is applied to the base pin, it also occurs as the base pin takes on a negative voltage.

Should a **positive voltage** be applied to the base pin, then current will start to flow and the transistor is ‘on’. When current flows the transistor may either be in **active** or **saturation** mode. For **active mode**, the transistor current is **amplified** and is proportional to the current flowing through the base pin: the current **amplification factor** (β), or **gain**, is the ratio of collector to base current (i.e. $\beta = I_C/I_B$). For **saturation mode**, the transistor current freely flows with minimal resistance (i.e. it acts like a **short circuit**).

A **PNP transistor** is structurally the reverse of a NPN transistor: it consists of an n-type substrate sandwiched between two p-type substrates. Assuming that the pin voltages are reversed (i.e. negative becoming positive and vice versa) the PNP acts with the same modal characteristics of a NPN transistor except that the conventional current flows in the opposite direction (from emitter to collector).

The mode settings for NPN transistors in terms of the pin voltage settings are provided in the table of figure 51.

Forward Modes (NPN Transistor)		Transistor Circuit Symbols
Positive Base $V_{BE} > 0$	Negative Base $V_{BC} < 0$	
Saturation $V_{BC} > 0$	Cut-Off	
Active $V_{BC} < 0$		

Figure 51: NPN Transistor Mode Settings

Due to the symmetry of the NPN transistor, the active, saturation and cut-off modes also apply should the E-to-C polarity be reversed (i.e. by applying a positive voltage to the emitter and negative to the collector), but performance is compromised by the reverse-polarisation effect and any amplification of current is reduced. The modes active,

saturation and cut-off are often prefixed by the term ‘**forward**’, indicating ‘normal’ or design polarity; or ‘**reverse**’ for the reverse-modal polarity situation in order to emphasise such performance issues.

Reverse modal situations are usually avoided in DC circuit design involving transistors because they add ambiguity and uncertainty to the design without offering any substantive advantages. Should current reversal be required then a PNP can and should be used instead of allowing a NPN transistor to enter reverse mode.

As for photodiode operation discussed earlier, in order to keep the discussion the dynamics of the NPN transistor as straight forward as possible, a **hypothetical setup** will first be considered.

*The hypothetical setup consists of making the emitter pin negatively charged, and both the base and collector pins positive as shown in figure 52. The positive polarity of the base pin contact causes a reduction of the collector-side depletion zone, which is more pronounced closer to the base contact so as to result in a **wedge-shaped depletion zone** that tapers down to nothing close to the base contact. This differential reduction of the collector-side depletion zone is aided by reducing the width of the p-type within the n-type sandwich.*

As the strength of the base pin’s positive polarity increases, the size of the wedge-shaped depletion zone reduces accordingly; and as it is reduced the wedge size increases. Thus the positive voltage can be used to control the resistance to CC movement on the collector-side.

*Because the emitter-side of the transistor is forward-biased, its depletion zone is negligible to non-existent, so that the only effective resistance within the transistor is provided by the collector-side depletion zone which, when in **active mode**, can be controlled by the charge applied to the base pin. As the base pin voltage is increased, the collector-side depletion zone wedge shrinks to the extent that it also provides little resistance and becomes ineffectual, which means that the transistor is operating in **saturation mode**. Saturation mode theoretically occurs when the base voltage is greater than the collector voltage to the extent that the collector-side barrier field is overcome.*

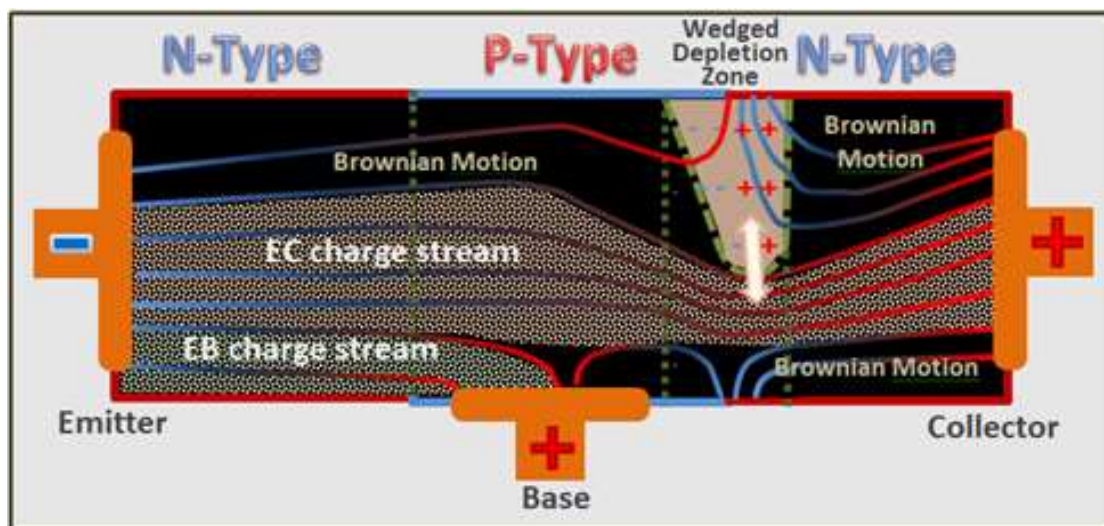


Figure 52: Powered NPN Transistor with Positive Base

Figure 52 shows an active mode hypothetical setup for a NPN transistor. The current at the emitter is equal to the sum of the flows from the base and the collector, which can be expressed as $I_E = I_B + I_C$; where I_B is the EB charge stream and I_C is the EC charge stream. The threads (electric lines of force) shown are generated by the pin polarities, and they map out the approximate geometry of the internal current flows (or CC streams). However, the set-up, as shown is only hypothetical because none of the pins are connected to each other via a power supply: thus, although there may be initial drift adjustment within the transistor, no current flow between the pins is possible.

For DC electricity to flow through a transistor, **pin pairs** must be connected to the opposite polarity terminals of a **common power source**. For instance, a current could flow if the emitter and collector were attached to a power source to generate the EC charge-flow stream, or if the emitter and base be connected to a power source for the EB charge-flow stream. However both these strategies would mean that one pin is not connected to any power source, requiring one of the three pins to be shared between two separate electric circuits, which is called the **Common pin**. For a DC application, two DC power supplies are needed; for an AC application, only the one AC power supply is needed.

The three possible shared-pin configurations are the Common Base (C_B), Common Emitter (C_E), and Common Collector (C_C) configurations. For each configuration, one circuit is considered the **driver** (the **input signal**), and the other the **respondent** (the **output signal**). Also, as we will soon discover, for each configuration the current relationship $I_E = I_B + I_C$ holds true for both DC and AC applications.

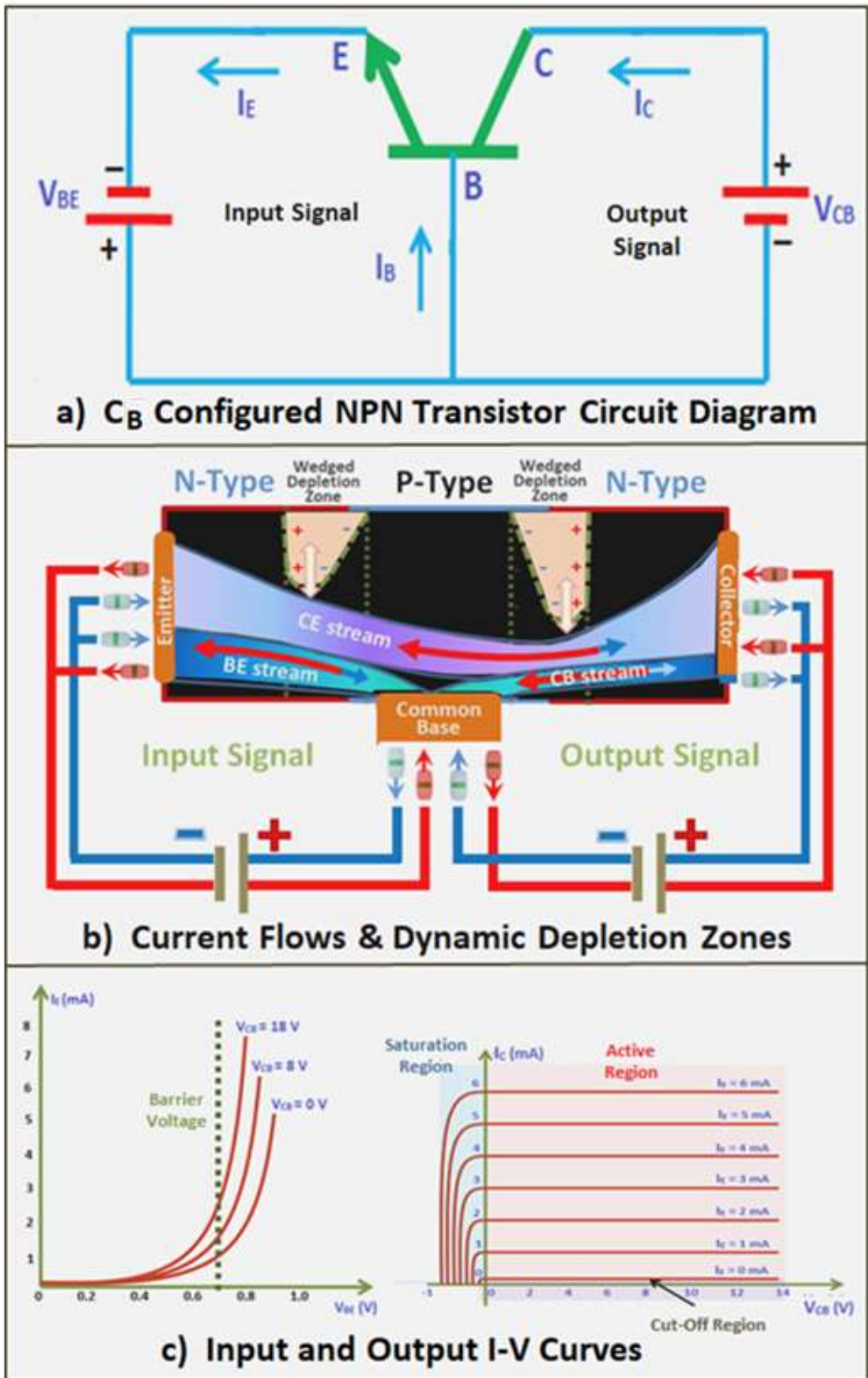


Figure 53: Common Base (C_B) Configured NPN Transistor

For the **common base (C_B) configuration** shown for figure 53a, the emitter (E) is the input terminal; the collector (C) the output terminal; and the base (B) is connected as a common terminal for both input and output. This C_B configuration represents the merging of two separate currents (or signals) moving in opposite directions, the net resultant current being I_B flowing to B via the wire-in-common.

For current flow diagrams that show the current movement for two different circuits with a **common base connection**, it is convenient show the flows in terms of **four strands**: an inflow positive and negative CC pair for flows in one direction, and another pair for current in the opposite direction. This is not intended to imply a double-duplex (quadruplex) transfer of charge. Instead, it simply shows possible CC movements depending upon the current in both circuits: there might be a flow in one particular direction or, if the circuit flows are equal in opposite directions, there may no CC movement in either direction within the **common base segment**.

Another aspect is that common base configured transistors contain two **wedge-shaped depletion zones** (see figure 53b), whereas the simplified hypothetical model with a positively charged base contains only one (figure 52). The wedge-shaped depletion zones dynamically change, each expanding and shrinking in response to input and output voltage change, so altering the internal impedance of the transistor.

As for the hypothetical setup of figure 52, it is the positive charge from the input apron strands of the base contact in the common base configuration, which is dictated by the input voltage (V_{BE}), that affects the size of the **collector-side depletion zone** (which is reverse-biased by the output circuit's voltage). Thus, as V_{BE} increases, two things happen: the forward-biased emitter-side depletion zone reduces further (if possible); and the size of the collector-side depletion zone reduces, so reducing emitter-side impedance.

Similarly, as the output voltage V_{CB} increases, the negative charge created by the output cetrion strands of the base contact increases, which marginally increases (or partly reinstates) the **emitter-side depletion zone**; and combined with the inward apron strands at the collector contact, it greatly increases the collector-side depletion zone. Thus the two internal impedances are both dynamically affected any change in strength of the voltage of either the input and/or output circuits.

The CC being pushed into the transistor by each power source combine and split to form the three internal **strand-based CC streams** shown as I_{CE} , I_{BE} and I_{CB} in figure 53b. These three CC streams are related to the pin currents by the following relationships: $I_E = I_{BE} + I_{CE}$, $I_B = I_{BE} - I_{CB}$ and $I_C = I_{CE} + I_{CB}$, from which the relationship between the three external currents (i.e. $I_E = I_B + I_C$) can be confirmed by re-grouping the terms as below:

$$I_E = I_{BE} + I_{CE} = (I_B + I_{CB}) + (I_C - I_{CB}) = I_B + I_C.$$

Because the emitter-side is partially to fully forward-biased, its depletion zone is always considerably smaller than that on the collector-side: the significantly larger depletion zone means increased collector-side resistance. The CB configuration thus provides a **high voltage gain** (see output I-V curves of figure 53c, which were sourced from the [Physics and Radio Electronics web site](#)) combined with an **attenuation of electric current** rather than its amplification. Note that in the output I-V curves, when the voltage is negative (i.e. $V_{CB} < 0$, which corresponds to $V_{BC} > 0$ in the table of figure 51), it means that the system is in the **saturation region**, and in the **active region** when it is positive, which corresponds to $V_{BC} < 0$ in figure 51.

A consequence of the emitter-side being forward-biased is that it could very well be short circuited unless a resistor (not shown) is added to the input circuit as a safety-measure: such a resistor is called a **base resistor**.

There are many web sites and textbooks that provide excellent description of the characteristics and applications utilising the three transistor configurations, but precious few provide detailed and/or logical explanations of their performance characteristics from a conventional Science perspective. Those that do attempt to explain, rely heavily upon the dubious assumption that positive-holes can move like electrons, but in the opposite direction, to act as positive CC. Examples from two of the better web-based explanations found are provided in figure 54: the reference link for 54a is the [ExplainThatStuff](#) site, and for 54b and 54c (note that this relates to a PNP transistor, so all the currents are reversed) is the [Physics and Radio Electronics](#) site.

For a **common collector (or emitter follower) configuration**, the base is the input terminal, the emitter is the output terminal and the collector is the common terminal for both input and output, as shown in figure 55a. Whereas the common base configuration has double-duplex charge flow at the base contact, the common collector configuration has double-duplex flow within the collector contact and connection. This configuration produces low voltage gain and high current gain, and is thus often used as a **voltage buffer**. Note that as both the emitter and collector sides can be forward-biased, an output circuit load (R_E) is required to prevent a short circuit situation occurring.

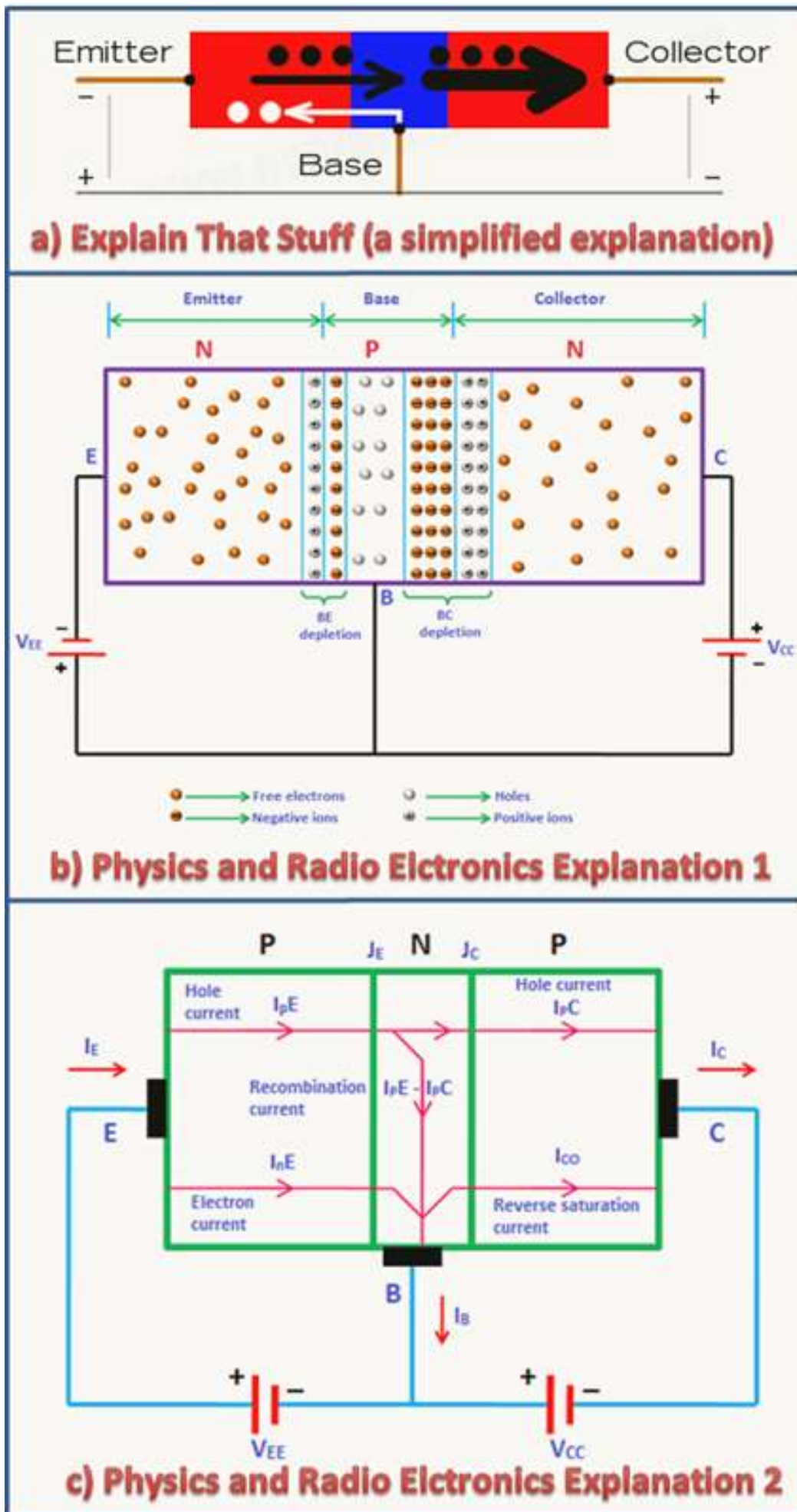


Figure 54: Conventional Science Explanation of C_B Configured Transistors

For a **common emitter configuration**, the base is once again the input terminal, the collector is the output terminal and the emitter is the common terminal for both input and output, as shown in figure 55b. As the polarity of both the input and output signals at the common emitter are the same (negative), this configuration does not have or require double-duplex current flow. The common emitter configuration produces both current and voltage gain that can be described as medium, but for AC applications (see figure 56) the output is the inverse of the input (i.e. there is a 180° phase change). It provides a good overall performance and would seem to be the most used of the three possible configurations.

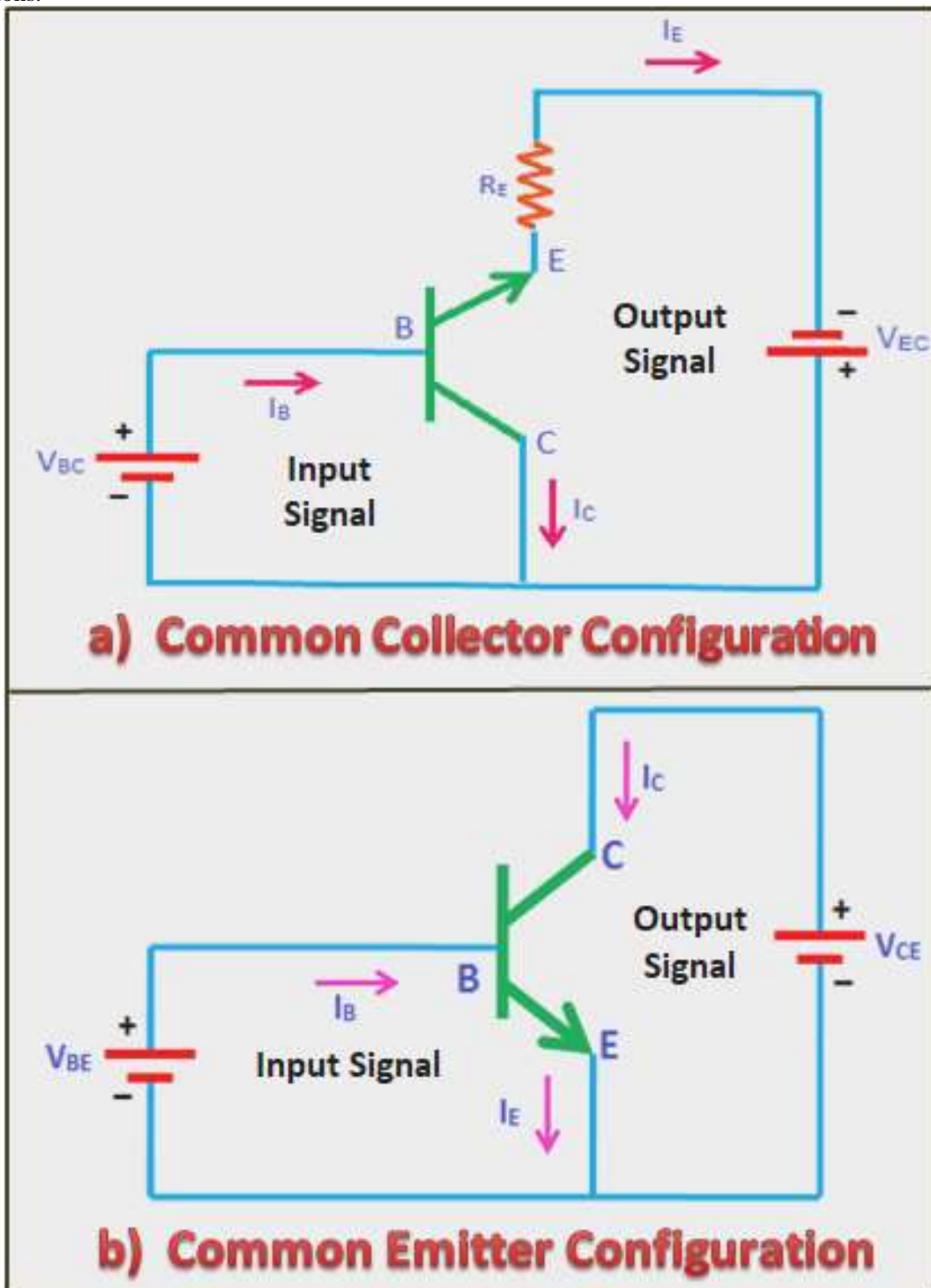


Figure 55: Common Collector and Emitter NPN Transistor Configurations

The dynamics of the three common pin configurations become more complicated for **AC circuits** than for DC circuits: this is because, as there is no power supply connected to the output circuit, there is no initial voltage or current associated with the output circuit. Also, whereas resistance remains fixed and current varies with voltage for a conventional DC circuits (i.e. those not involving transistors), for AC circuits, both the voltage and current are inversely related and sinusoid, with the input circuit polarity reversing upon each half-cycle.

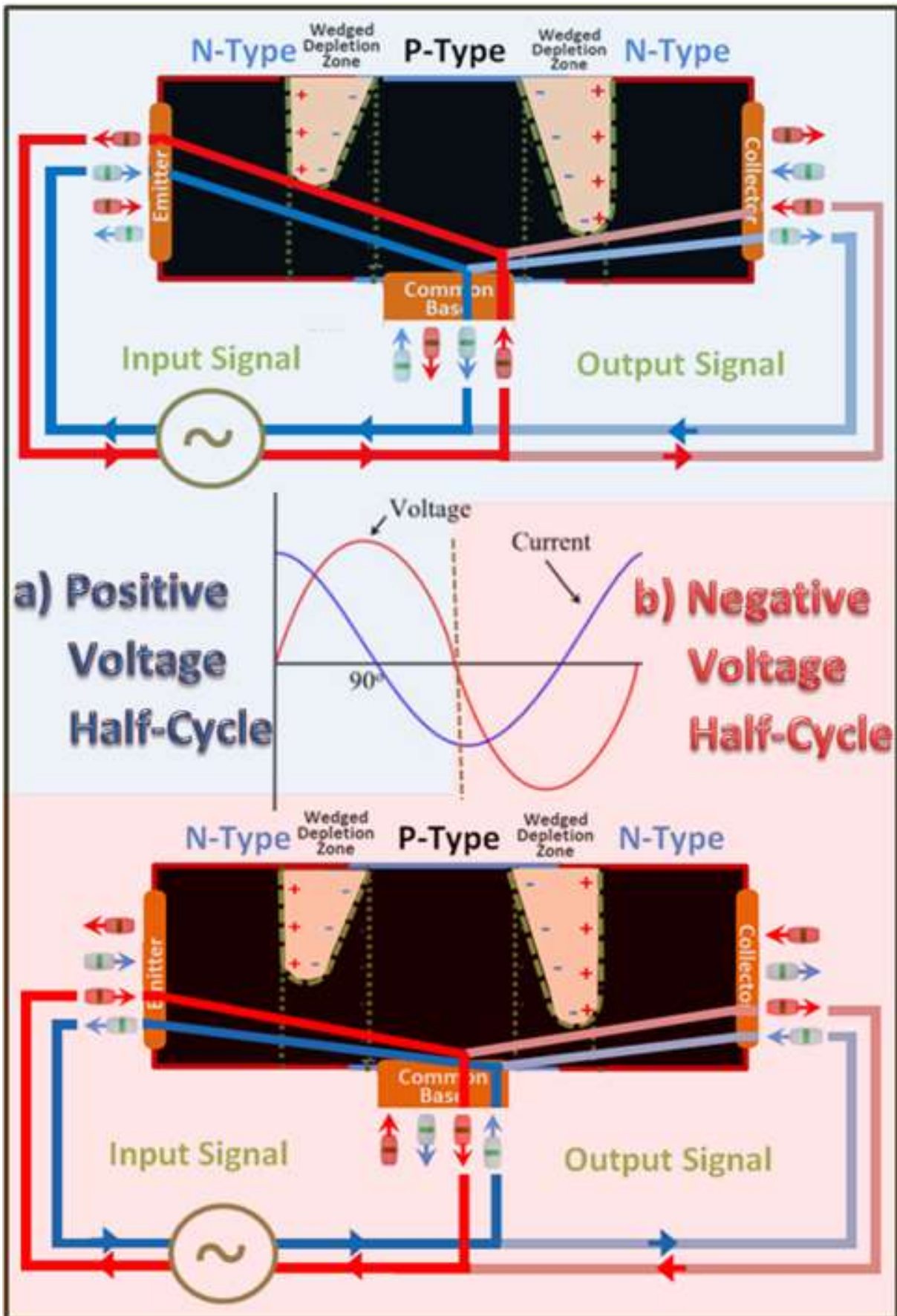


Figure 56: Common Base Configuration AC Charge Flow Patterns

Another complication is, with the rate of voltage change (50 to 60 Hertz) associated with the AC input signal, that the wedge-shaped depletion zones within the transistor, which dynamically vary in size depending upon the changing voltage, have insufficient time to completely adjust. A depletion zones thus neither fully disappears nor fully forms so as to prevent all CC movement. However, on the **positive voltage half cycle** (figure 56a), the emitter-side is forward-biased whereas the collector-side forward-biasing effect on the **negative half-cycle** (figure 56b) is considerably

weaker. The net effect is that, although both depletion zones expand and shrink with changing voltage, the collector-side depletion zone always remains significantly larger than that of the emitter side, which results in a significant voltage gain for the output signal.

Figure 56 highlights the schematic electron and proton flow directions and strand-group usage for each half cycle of an AC input power supply. The current passing through both input and output circuits is the same shared current and, as would be expected for pure capacitance AC power source, is a quarter of a wavelength out of phase with the voltage and changing inversely with voltage. However, because of the increased resistance provided by the larger collector-side depletion zone, the output signal has significant voltage gain, as summarised in the first column of the table and graphics of figure 57.

For the common base configuration, each pin connection utilises only one pair of strand groups, but different pairs for each half cycle. Also, although each depletion zone is continually adjusting to changes in voltage, the relative size of each depletion zone remains approximately the same for each part of each half cycle, thus maintaining a constant gain across the entire output cycle.

A summary of the AC characteristics of each of the three transistor configurations is provided as figure 57. The only other mystery remaining relates to why, for the **common emitter configuration**, the input and output signals are a **half-cycle (180°) out of phase**. The answer to this question is quite simple: it is because the CC (i.e. electric currents) move in the opposite direction within the input and output circuits, as can be clearly seen in the DC setup of figure 55b, which in AC terms, means the input and output signals are a half-cycle (**180°, π or $\lambda/2$**) out of phase.

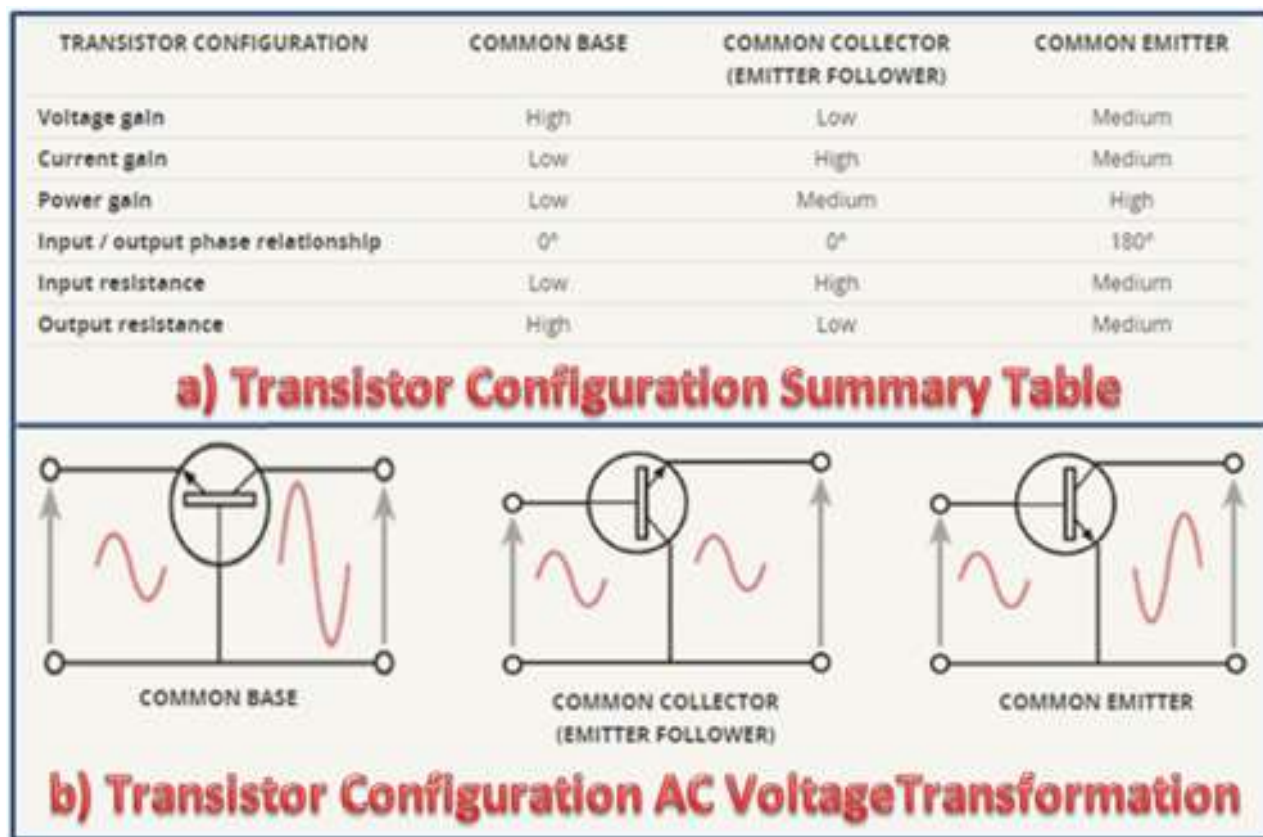


Figure 57: Transistor AC Common Configuration Comparison

Based upon electrons, and even assuming that positive-holes can move as positive CC in a manner similar to electrons, conventional Science still struggles to explain the dynamics of P-N diodes, photovoltaic cells and transistors. Furthermore, the explanations provided are unduly complex, involved and are not well grounded. Although the performance characteristics of the three configurations are well documented and [quantified mathematically](#), no satisfactory practical explanation of the diode dynamics is forthcoming from the conventional Science area.

On the other hand, although the STEM explanations might not always be simple, they are not unduly difficult to follow and to understand. The STEM approach is logical and consistent across all forms (DC and AC) and sources (chemical, induction or photovoltaic) of electricity, and across all transfer media (metal or semiconductor) and devices (resistors, capacitors, inductors, diodes and transistors).

Concluding Remarks

Since Benjamin Franklin's 1759 discovery of electricity, electric currents have been considered to be due to the one-way movement of electrons, and that explanation has not been re-assessed or changed since. Neither the 1932 discovery of free **positrons** in cosmic radiation, nor the mysterious performance characteristics of semiconductor technologies in the early 1950's caused a re-assessment of the nature of electric currents. For semiconductors, there was a recognised need for a positive charge carrier of mobility equal to that of the electron to explain the characteristics of electric current within semiconductors. Instead of re-assessing the nature of electric currents, fixed **temporal cations** were re-branded as '**positive-holes**' and touted as the new positive charge-carriers. However, even with the specious 'positive-hole' approach, many aspects of semiconductor behaviour cannot be adequately explained.

STEM is an energy-centric model predicated upon the hypothesis that '*there is only one source of energy*': and that source is **energen**. The STEM electron consists of a torus-shaped **energy-core** of concentrated energen, and an outer torus of less concentrated energen that is called its **field-energy**. The STEM electron can have one of two chiral forms: the **cetron electron**, which has **left-handed** (or clockwise) **chirality** (or helicity) of its field-energy, and acts as a **negative** charge carrier (**CC**); and the **aptron electron**, which has **right-handed** (or anti-clockwise) chirality, and acts as a **positive** CC. With the appropriate boundary condition settings, the STEM electron satisfies the Schrodinger and Dirac wave equations, and thus the QM equations that piggy-back onto the wave equations.

The only difference between cetron and atron electrons is that of having different chirality of their energy-field. Their energy-field provides them with dipole-like characteristics and their different chirality causes their behaviour to be subtly different to each other: hence the use of the term '**Duplicit Electron**' in this paper's title,

Within a **metal conductor**, such as copper wire, CC are quite plentiful, occupying **ionic orbitals** of the conductor's atoms. An **applied emf** causes CC to skip from their ionic orbitals, with the negative CC moving towards the positive terminal and the positive CC moving towards the negative terminal. As the CC move in opposite directions within a wire conductor, they form same-charge **strands**, and the net toroidal flow component of their field-energy combines to create a **circular magnetic field** around the wire.

Chemical batteries, solar-cells, piezo-electric devices, thermocouple devices and magnetic induction represent a **source/sink** (or supplier-consumer) mechanism. The source/sink mechanism involves the creation of a negative CC source (the **negative terminal**) that also acts as a positive CC sink; and a separate positive CC source (the **positive terminal**) that acts as a negative CC sink. Moving within strand-like groupings as an **electric current**, the CC move with their outflow vortices directed towards the sink, which creates a strong central flow of field-energy and an outer zone of less concentrated field-energy flow back towards the appropriate source.

An **induced electric current** is generated by magnetic induction, which involves the movement of magnetic flux through a wire conductor. As the process does not involve physical sources and sinks, there are no physical terminals; only **implied electric poles**. Circular **eddy currents** also can be similarly induced by a magnetic field moving across a thin metal sheet. Eddy currents are most useful for the heat generation of induction cooktops and for the generation of the Hall Effect (an induced traverse current across a thin metal sheet).

With DC electricity and domestic AC electricity, an electric current consists of the **duplex two-way movement** of **positive** and **negative** CC. For a thin wire conductor, the current flow is distributed fairly evenly across the cross-section of the wire but, for thicker high-voltage AC transmission lines, an outer **skin** carries the bulk of the current.

When there is a break in an electric circuit that stops current flow (e.g. across capacitor plates or a pair of probes attached to a DC power source), the central energy-fields of the strands extend beyond the break-point as an **electric field**. Unlike **magnetic fields** that have curved field-energy flow from a North (real or implied) to a South pole, an **electric field** generates a weak circular magnetic field, but has no net flow of field-energy between the positive and negative charge sources.

A **capacitor** consists of a thickness of **dielectric** (insulation) material sandwiched between a positively and a negatively charged flat plates. As for the built-up static charge on the domes of a Van de Graaff generator, capacitors can build and hold charge for an extended period of time due to CC concentration. Capacitors can be **discharged** at a later time so as to act as a **power source**, generating an electric current that flows in the opposite direction to that of the charging current.

A **capacitor** and **inductor loop** can be used to generate a rapidly **oscillating** or **alternating current** (**AC**) that can in turn be used to generate and broadcast **radio waves** from an **antenna**. As voltage builds up across each rod in a **dipole antenna** (a commonly used antenna), an electric field is generated between the polar ends of the antennal rods. As the terminals are switched by high frequency AC reversal, the field energy of the previous electric field is summarily cut-

off as new opposite polarity electric field forms, pushing it away from the dipole rod as an expanding doughnut-shaped wavefront of electric field energy, with each adjacent wavefront having a reversed circular magnetic field.

The **work function** (i.e. the work required to escape a host medium) for positive CC is considerably higher than that for negative CC. Thus, for **low energy** interactions such as the photoelectric effect, electron guns and cathode ray tubes, only negative CC (cetron electrons) are emitted. The high work function of positive CC can be overcome by high energy (i.e. more than 1 MeV) events, such as impact by energised cetron, or X-ray or gamma ray bombardment; or by high voltage in the case of DC+ arc welding.

Within the electron-sparse environment of **semiconductors**, thermally-induced velocity of CC causes them to undergo **Brownian motion**, with **diffusion** and **drift** being the primary causes of low-level charge transfer (i.e. an electric current) within diodes and transistors. The cetron represents an excellent negative CC, but as an equally mobile positive CC, the positive-hole concept simply lacks independent mobility and is not up to the task. However, as for electric current within a metal conductor, the apron represents an ideal mobile positive CC, and is up to the task.

The creation of cetrons and aprons by the release of a **bitron** from a **b-bond (bitron bond)** provides an alternative process to pair production. A bitron consists of concentrated field energy that is quantized to the energy level of the energy core of an electron: it thus represents a pre-electron. A bitron can be bump-released from a b-bond by the impact of an excited free electron, or by a photon (EMR) of sufficient energy, or by radioactive particle bombardment, or by chemical reaction (e.g. a Redox reaction). Upon its release from a b-bond, there is equal probability that the bitron will become a cetron electron (a negative CC) or an apron electron (a positive CC) depending upon its exit-path from the bond upon release.

The bonds between silicon atoms (and the sparse dopant atoms) are considered to be b-bonds rather than covalent bonds of conventional Science. Should EMR of sufficient energy, and/or an energised free electron, knock a bitron from a b-bond, there is equal probability that it will become a new negative CC) or a new positive CC, thus increasing the available mobile CC that can participate in the formation of an electric current.

In an environment wherein the atoms are firmly held in a rigid crystalline structure, such as that of the silicon substrate of a semiconductor, whenever a bitron is removed from a b-bond, another bitron quickly forms to re-establish the b-bond. In this manner b-bonds essentially become self-healing, and thus they can be considered to be electron (i.e. cetron and apron electrons) breeders. Within a photoelectric semiconductor device, b-bonds can certainly produce sufficient CC to generate an electric current and power up a micro-circuit.

Another form of apron creation is the cetron-to-apron type-conversion by high-speed electron-to-electron or electron-to-nucleus collision. This form of type-conversion is more relevant to the beta decay and electron capture processes.

Static electricity is a surface accumulation of CC that are typically generated by separating or rubbing together two **triboelectric** materials. When triboelectric materials make close contact, **b-bonds (bitron bonds)** can form which, when broken by separation, release cetron and/or apron electrons which adhere to opposite surfaces so as to generate opposite surface charge concentrations on each material. Electrons may also be released by friction-based removal of some electrons from ionic orbitals, which is more attune to conventional Science's explanation.

The STEM approach provides explanations related to the duplicit nature of the electron in terms of positive and negative CC; the generation of electric current by chemical battery and induction; the formation and nature of electric fields; capacitor charge and discharge; the generation of micro and radio waves; and the behavioural characteristics of diodes, photovoltaic cells, photodiodes and transistors. It also addresses the nature and interdependency of electric and magnetic fields and explains how, rather than being different types of energy, positive and negative electric charge can be attributed to the chiral differences between cetron and apron electrons.

The ramifications of the duplicit electron approach for Science, industry and education are significant. However, the STEM approach runs counter to long and widely held conventional Science beliefs related to electricity and electromagnetism, which have become an important part of Science culture and education: herein lies a problem that could be more cultural than scientific when it comes to change.

It is quite amazing, and somewhat ironical, that conventional Science's fundamental theory and understanding of electricity and semiconductors, two of the most important accelerants of this century's world-wide computer and communication technological revolution, might be flawed and in need of updating.

References

(note: many references in this paper have been provided via direct links)

- [1] Cambier, J. and Micheletti, D. (2000) Theoretical Analysis of the Electron Spiral Toroid Concept.
- [2] Consa, O. (2018) Helical Solenoid Model of the Electron. *Progress in Physics*, 14, 80-89.
- [3] Consa, O. (2018) The Helicon—A New Preon Model. *Progress in Physics*, 14, 215-219.
- [4] Bergman, D.L. and Wesley, J.P. (2002) Spinning Charged Ring Model of Electron Yielding Anomalous Magnetic Moment. *Common Sense Science*, 1, 63-67.
- [5] Kanarev, P. (2012) Particle Resolution. Proceedings of the NPA, Albuquerque.
- [6] Kyriakos, A. (2004) Geometrical Illustration of the Electromagnetic Representation of Dirac's Electron Theory. ArXiv: quant-ph/0407071v1.
- [7] Wayte, R. (2010) A Model of the Electron. *Progress in Theoretical Physics*.
- [8] Williamson, J. and Van der Mark, M. (1997) Is the Electron a Photon with Toroidal Topology? *Annales de la Fondation Louis de Broglie*, 22, 133.
- [9] Osmera, P. (2012) Fractal Dimension of Electron. Proceedings of MENDEL.
- [10] Yao, A. and Padgett, M. (2012) Orbital Angular Momentum: Origins, Behavior and Applications. *Advances in Optics and Photonics*, 3, 161-204. <https://doi.org/10.1364/AOP.3.000161>
- [11] Sarri, G., et al. (2013) Table-Top Laser-Based Source of Femtosecond, Collimated, Ultra-relativistic Positron Beams. *Physical Review Letters*, 110, Article ID: 255002. <https://doi.org/10.1103/PhysRevLett.110.255002>
- [12] Bowen, D. (2106) The Real Reason Why the Electron's Bare g-Factor Is 2 Times Classical. *Journal of Modern Physics*, 2016, 7, 1200 -1209, <https://www.scirp.org/journal/paperinformation.aspx?paperid=67682>
- [13] Bowen, D and Mulkern, R (2015) An Electron Model Consistent with Electron-Positron Pair Production from High Energy Photons. *Journal of Modern Physics*, 2015, 6, 1334 -1342, [Article link](#)
- [14] Garaud, J. Radu, E. and Volkov, M (2018) Stable Cosmic Vortons, arXiv:1303.3044v2
- [15] Odom, B. Hanneke, D. D'Urso,†B. and Gabrielse, G. (2006) New Measurement of the Electron Magnetic Moment Using a One-Electron Quantum Cyclotron, *Physical Review Letters*, 97, Article ID: 030801 <https://journals.aps.org/prl/abstract/10.1103/PhysRevLett.97.030801>
- [16] MacGregor M. (1992) *The Enigmatic Electron*, Klurur Academic
- [17] The STEM Development Group, (pdf 2023) '[Atomic Structure: STEM and the Orbital Model](#)'
- [18] The STEM Development Group, (pdf 2023) '[The Nature of Light](#)'
- [19] Markoulakis E and Antonidakis E (2022) A $\frac{1}{2}$ spin fiber model for the electron, *Int. J. Phys. Res.* 10 (2022) 1–17. doi:10.14419/ijpr.v10i1.31874. <https://hal.science/hal-03544897>

Appendix A: Rationale for the Structure of the STEM Electron

Central to the STEM approach is that all matter and related electromagnetic phenomena consist of, or are related to, enegen. A hypothetical small daub of enegen, with a nominal radius of 0.175pm (based upon the estimate of the small radius of an electron's energy-core torus: see the [Electron Models](#) chapter) as labelled 'Core Energy' in figure 58, will be used to build up a potential structure for the STEM electron. It is hypothesised that this small daub of enegen becomes less concentrated radially outwards in all directions from its core-energy (as indicated by the widening **energy equipotential** surfaces of figure 58), and is referred to as its **field energy**. Together, the core energy and its field energy are referred to as a **hypothetical enegen particle**.

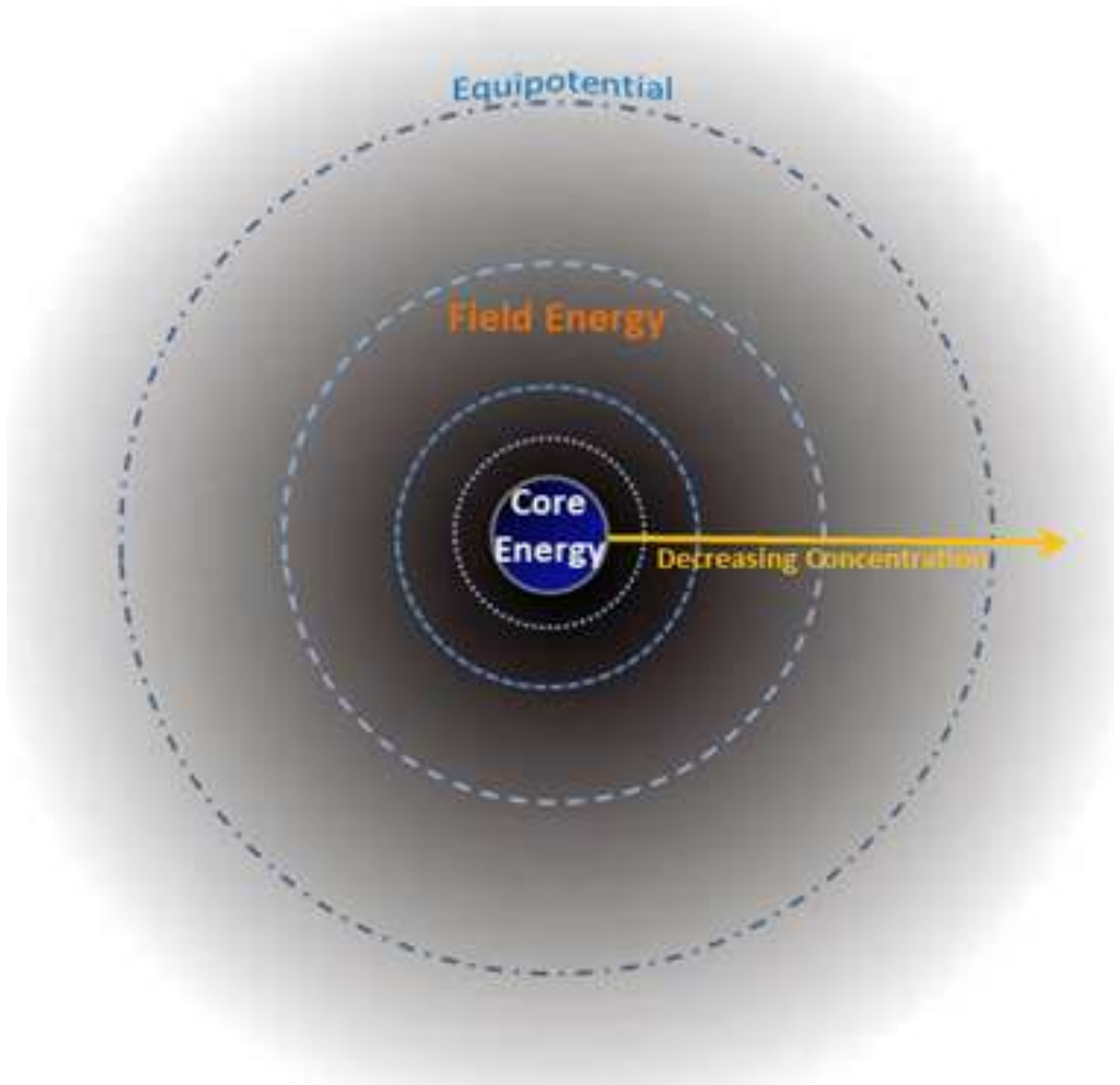


Figure 58: Structure of STEM's Hypothetical Enegen Particle

When a single hypothetical enegen particle moves at speed, its net energy-field profile has a sinusoidal wave form with wavelength λ as shown figure 59 (note that in 3D the sinusoidal energy-field envelope that is fully symmetrical around its direction of travel as shown in the graphic in the bottom right of figure 59). Thus, when moving at close to the speed of light, the hypothetical enegen particle's energy-envelope mimics a sinusoidal electromagnetic waveform.

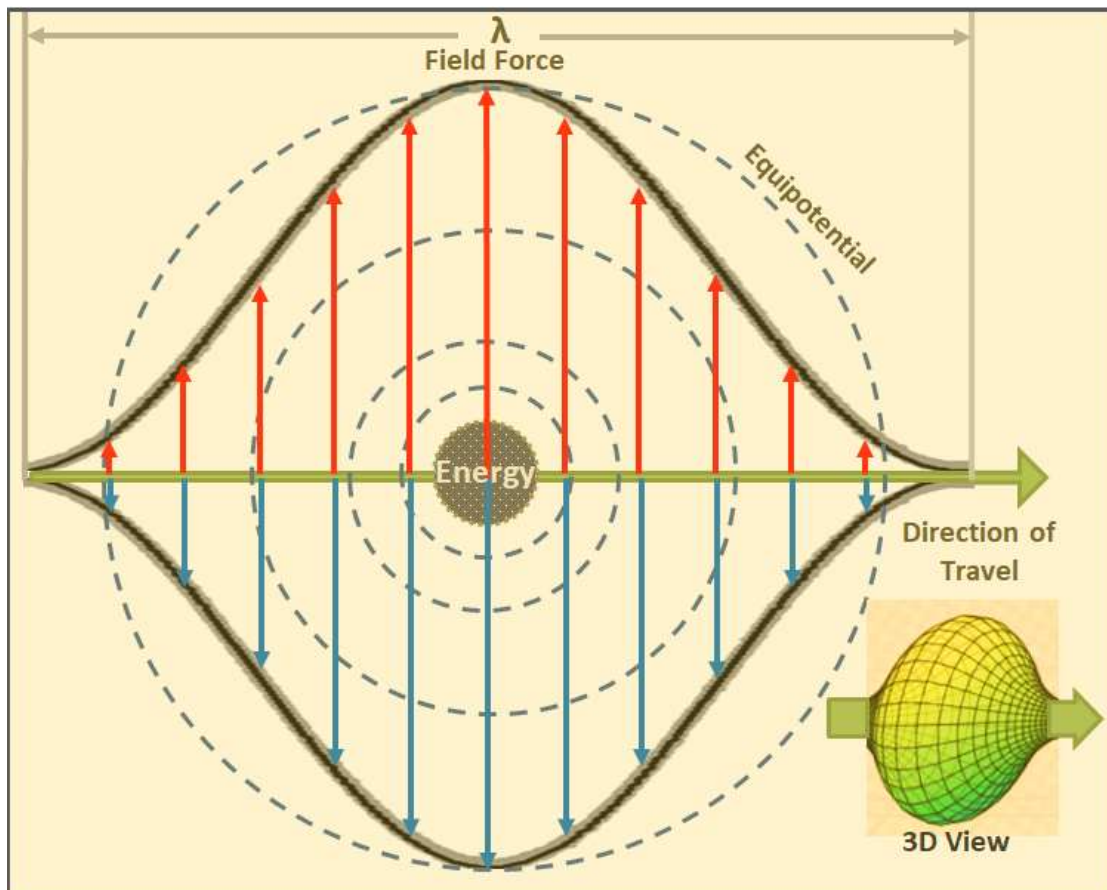


Figure 59: The Field Energy of a Moving Hypothetical Energen Particle

When a hypothetical STEM energen particle moves in a circular path at a speed close to that of light, its energy-field dynamics are significantly different to when it moves in a straight line. Figure 60 shows the hypothetical energen particle frame-frozen as it is moving on opposite sides of a circular path: the energy-field profile on the inside of the circular path (blue in figures 59 and 60) contains less energy (red in figures 59 and 60) than is outside the path.

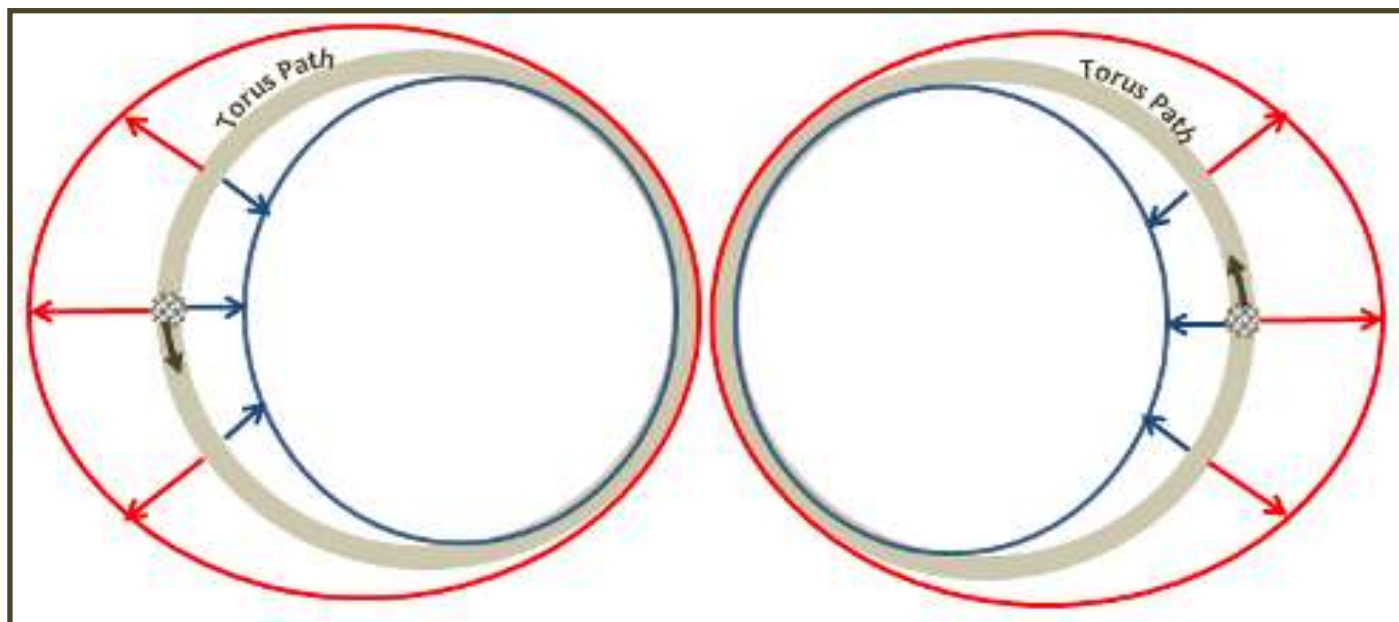


Figure 60: Field Patterns of an Energen Particle Moving in a Circular Path

Assuming that hypothetical energen particles have an affinity for each other, and stick together should their core-energies come into contact with each other, then multiple hypothetical energen particles could travel in unison around a circular path with their core-energy abutting each other. In this scenario, their combined core-energies would be travelling as a torus-shaped structure (shown as the inner torus of figure 61) that could be considered connected to have spin or merged to have viscous flow. Around the inner torus would be an outer torus of less concentrated energy, the field-energy.

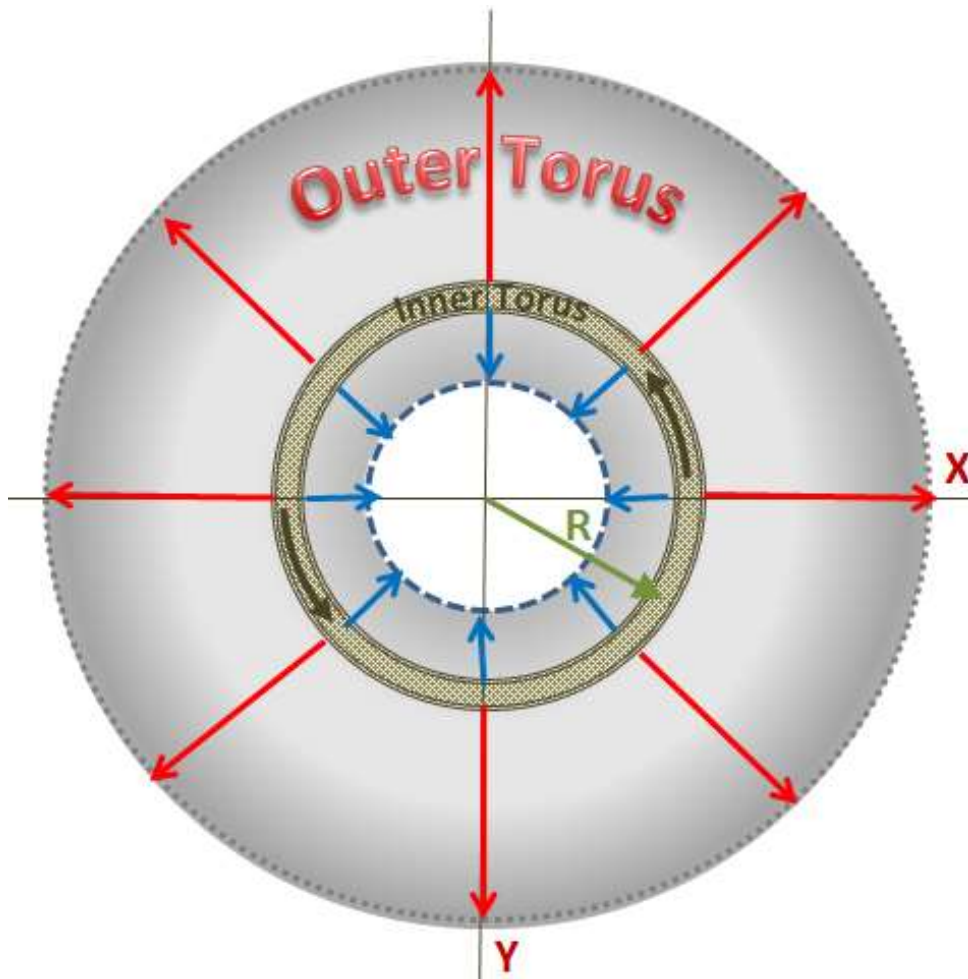


Figure 61: Inner and Outer Torus for multiple Hypothetical Energy Particles

Due to the curvature of the inner core torus, there would be more field energy outside the core torus resulting in the cross-sectional shape of the outer torus being distorted, rather than being circular. This distortion is indicated by the outwardly bulging red ellipsoid in the YZ projection of figure 62.

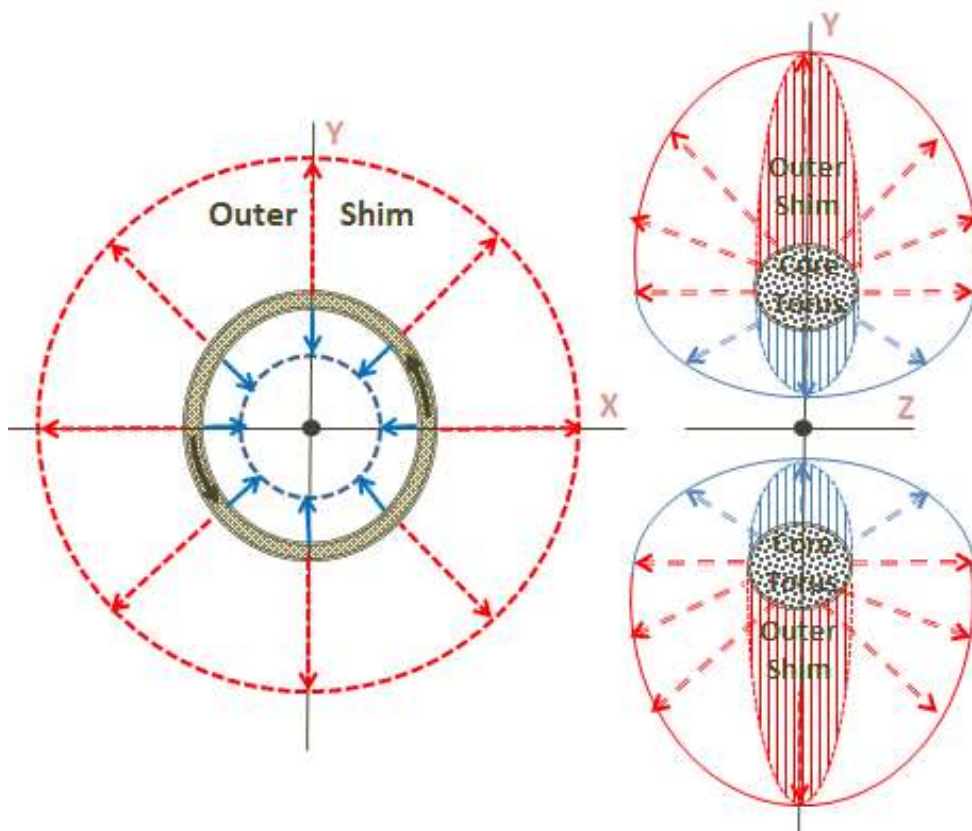


Figure 62: Effective Outer and Inner Energy-Field Shims (Unpolarised)

The field energy has the characteristics of a gas-like viscid fluid that is vulnerable to outside forces, and lateral forces in particular. In order to better demonstrate the effect of lateral forces (force components in the Z-axis direction), the distorted cross-sectional shape of the field energy has been scaled to appear flattened as represented by the striated ellipse labelled **outer shim** in figure 62. The field energy is thus represented in figure 63a by this scaled-down outer shim shape: blue inside the core-energy and red outside of it.

Any sideways force or pressure can readily push the energy field sideways so that it would take on a fan-like conical form such represented in figure 63b in terms of the outer shim. As the energy-field shifts or is pushed sideways, its toroidal spin, which is in synch with the movement of the core-energy, would swing inwards towards the spin axis (the z-axis), reducing its spin radius and causing it to accelerate so as to form an **inflow vortex**.

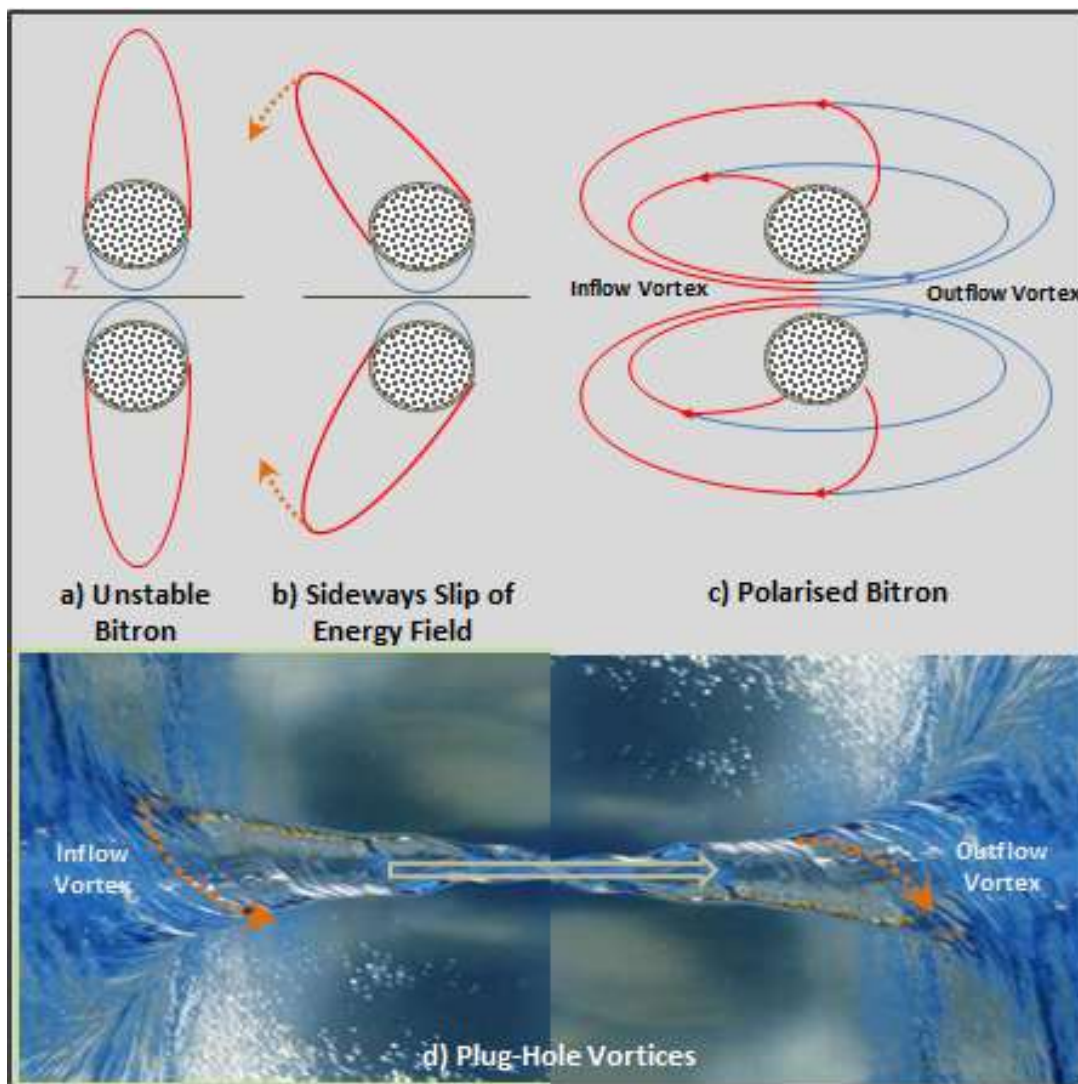


Figure 63: Vortex Formation and Energy-Field Polarisation

The inflow vortex is analogous to a plug-hole vortex in a circular sink full of water (such as shown in the figure 63d graphic); it draws the structure's field-energy towards and through the centre of the torus to form an **outflow vortex** on the other side. The field-energy then flows back to complete the circuit to form a large flattened **outer-torus** around the energy-core torus, as shown in figure 63c. The energy-field flow has thus become **chiral** (or **polarised**).

Whereas the original symmetrical outer field energy was fragile and readily polarised, the polarised (or chiral) form is **stable** under normal conditions. Thus it can be assumed that **only polarised forms** of the structure can exist and be present in Nature.

In summary, STEM proposes that an electron consists of a torus-shaped **semi-solid continuum** of concentrated **core-energy** that can be approximated by multiple small hypothetical energen particles. The torus shaped core-energy is semi-solid and **spins** (or flows as a viscous fluid) at close to the speed of light, surrounded by a swirling **viscid fluid-like** (or gas-like) **atmosphere** outer torus of less concentrated **field-energy** that is **polarised**. The toroidal flow rate of the inner core and outer field-energy is approximately the same, and the structure has a particle-like inner-core surrounded by a gas-like outer torus. And importantly, the polarised field-energy is chiral (i.e. it has **helicity**), and can thus present in one of **two chiral forms**: that of a cetron (left-handed chirality) or an apron (right-handed chirality).

Appendix B: Electron Size and g-Factor

Although Quantum Mechanics (QM) defines the electron as a point particle, as evidenced by the multitude of diagrams representing electrons as spherical particles, the concept of a classical spherical electron would appear to be alive and well. The radial size of the spherical electron remains highly disputed, with various estimates in the range of 10^{-20} to 7×10^{-13} m. [The CODATA radius of the electron](#), which represents "[classical electron radius](#)", is 2.82×10^{-15} m. Earlier estimates by M MacGregor in 1992 [\[16\]](#) placed the radius of an electron in the range of 4×10^{-13} to 7×10^{-13} m. The 2015 Bowen and Mulkern estimate [\[13\]](#) of 3.86×10^{-13} m is at the lower end of MacGregor's range and about 100 times larger than the classical CODATA estimate for an electron radius.

The QM definition of an electron as a point particle makes no logical sense, and results in the electron's momentum and electric charge being considered 'intrinsic' (i.e. of unknown cause), and suggests that the smaller an estimate of electron radius might be, the more acceptable it would be. The point-form definition is a necessary evil required to prevent unwanted singularities within the QM wave equations, and those wave equations model the electron's characteristics quite well mathematically, but do not represent a cohesive or realistic physical model for the electron.

But should an electron have spatial extent, as seems to be the case, does 'the smaller, the better' apply to estimates of electron size? For the classical spherical-electron model, the angular momentum $S = v.m.R$, which means that when the radius (R) gets too small, the rotation speed needed to generate the electron's known angular momentum would have to increase to ridiculous spin speeds. Using the classical CODATA electron radius estimate as an example, the tangential velocity at the electron's outer equatorial plane is:

$$v = S / (m_e \cdot R) = 5.27 \times 10^{-35} / (9.1 \times 10^{-31} \cdot 2.82 \times 10^{-15}) = 2 \cdot 10^{10} \text{ m/s}$$

where $R = 2.82 \times 10^{-15}$ m (CODATA classical spherical-electron radius),

$S = 5.27 \times 10^{-35}$ Js. is the QM estimate of intrinsic spin which is based upon the Bohr electron. It is half the reduced plank constant (**h-bar** or **ħ**) = $\hbar/2 = 0.5 \times 1.054571817 \times 10^{-34} = 5.27 \times 10^{-35}$ Js,

and $m_e =$ the mass of an electron = 9.1×10^{-31} kg.

Thus, for a spherical electron with the CODATA radius of 2.82×10^{-15} m, the outer surface tangential velocity would be $2 \cdot 10^{10}$ m/s, which is about 100 times the speed of light ($c = 3 \times 10^8$ m/sec). For a 10^{-20} m radius (at the lower end of the electron radius range) that tangential speed would be more than a ten million (10^7) times the speed of light!! Because of this spin-related conundrum, conventional Science refrains from using a radial size estimate to calculate the electron's angular momentum (or spin), preferring to assert it to be 'intrinsic', and determining its value via the electron's precessional characteristics.

Experimentally, the **gyromagnetic ratio** for magnetic dipoles, inclusive of particles such as electrons, can be determined from their **precession**, called [Larmor precession](#), which occurs when they are subjected to an externally applied magnetic field (**B** in teslas). When the particle's spin axis is oblique to the direction of the external field, the precession frequency (**f** in hertz) is proportional to the magnetic field strength, or specifically: $f = \gamma/(2\pi) \cdot B$, which allows the gyromagnetic ratio γ to be accurately determined experimentally.

The gyromagnetic ratio (γ) is the ratio magnetic moment to angular momentum, calculated as $\gamma = \mu/S = q/(2m)$, where μ is the electron's magnetic moment and **S** its angular momentum. The [CODATA estimate for \$\mu\$](#) is 9.285×10^{-24} J T⁻¹ rounded, **S** = 5.27×10^{-35} Js (as discussed above), and $q =$ charge of an electron = 1.60218×10^{-19} C (coulomb):

$$\text{Using } \mu \text{ and } S, \quad \gamma_1 = \mu/S = 9.285 \times 10^{-24} / 5.27 \times 10^{-35} = 17.62 \times 10^{10} \text{ (C/kg)}.$$

$$\text{Using } q \text{ and } m_e, \quad \gamma_2 = q/(2 \cdot m_e) = 1.60218 \times 10^{-19} / (2 \times 9.1 \times 10^{-31}) = 8.8 \times 10^{10} \text{ (C/kg)}.$$

Thus, γ as calculated from μ and **S** is approximately double that using q and m , leading to the introduction of the Landé **g**-factor (where **g** is a dimensionless constant) to correct the discrepancy as:

$$\text{Gyromagnetic Ratio } \gamma = \mu / S = g \cdot q / (2 \cdot m_e), \text{ or } g = \gamma_1 / \gamma_2 = 17.62 \times 10^{10} / 8.8 \times 10^{10} = 2.0023 \text{ (or } = 2 \text{ rounded)}$$

The realisation that the spin-related gyromagnetic ratio of an electron is 2, rather than being 1 as expected for the classical spherical-electron using Newtonian Physics, has been problematic, and long considered a quantum-related oddity. Richard Feynman, using **L** for an electron's angular momentum rather than **S**, stated that $\mu = q \cdot \mathbf{L} / (2 \cdot m_e)$ 'is true for orbital motion, but that's not the only magnetism that exists. The electron also has a spin rotation about its own axis (something like the earth rotating on its axis), and as a result of that spin it has both an **angular momentum** and a **magnetic moment**. But for reasons that are **purely quantum-mechanical**—there is no classical explanation—the ratio of μ to **L** for the electron spin is twice as large as it is for orbital motion of the spinning electron' [The Feynman Lectures on Physics](#), vol. 3, chapter 34, p34-6.

Considering the classical spherical electron model, should the maximum speed at its equatorial perimeter be the speed of light ($c = 3 \times 10^8$ m/sec), then its radius $R = S/(v \cdot m_e) = 5.27 \times 10^{-35} / (3 \times 10^8 \times 9.1 \times 10^{-31}) = 1.93 \times 10^{-13}$ m. Although such an electron model would generate the required angular momentum, it would also generate unwanted singularities in the QM wave equations because it cannot validly be represented as a point-particle, and would thus have to be discarded. However, a torus model of the electron is a physical model that has nothing at its centre of mass, and can validly be represented as a point-form particle to satisfy the mathematical requirements of the QM wave equations.

The STEM electron model consists of a torus-shaped energy core that spins or flows, and contains the bulk of the electron's mass. It is a physical model that satisfies the QM wave equations and provides a geometry and size estimates for the electron, which allow the electron's angular momentum to be determined using Newtonian (or classical) Physics.

The energy core's large radius $R = 0.24$ pm = 0.24×10^{-12} m = 2.4×10^{-13} m;
and the small radius $r = 1.6 \times 10^{-13}$ m, as represented in the figure right.

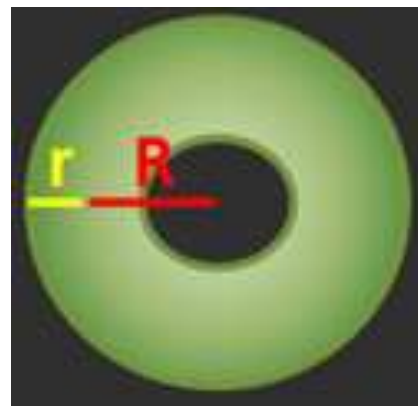
The outer equatorial radius = $R + r = 4 \times 10^{-13}$ m.

Assuming $q =$ charge of an electron = 1.60218×10^{-19} coulomb,

$m_e =$ the mass of an electron = 9.1×10^{-31} kg,

and $v =$ central spin/flow speed of energy core at $R = 1.8 \times 10^8$ m/sec.

(Note: the outer equatorial tangential speed = 3×10^8 m/sec = c approximately)



Then Angular Momentum $S = I \cdot \omega$ where $I =$ moment of inertia = $m_e \cdot (3/4 \cdot r^2 + R^2)$ for a torus,

and $\omega =$ angular velocity = v/R radians/sec

$$= v \cdot m_e \cdot (3/4 \cdot r^2 + R^2) / R$$

$$= 1.8 \times 10^8 \times 9.1 \times 10^{-31} \times (0.75 \times (1.6 \times 10^{-13})^2 + (2.4 \times 10^{-13})^2) / 2.4 \times 10^{-13}$$

$$= 5.24 \times 10^{-35} \text{ Js, which is close to the QM estimate } 5.27 \times 10^{-35} \text{ Js based upon } \hbar/2.$$

Using the CODATA estimate for $\mu = 9.285 \times 10^{-24} \text{ J T}^{-1}$ and $S = 5.24 \times 10^{-35} \text{ Js}$ as calculated above, then:

$$\gamma_1 = \mu/S = 9.285 \times 10^{-2} / 5.24 \times 10^{-35} = 1.771 \times 10^{11}, \text{ and}$$

$$\gamma_2 = q/(2 \cdot m_e) = 8.8 \times 10^{10} \text{ (C/kg) as calculated earlier.}$$

Thus $g = \gamma_1/\gamma_2 = 1.771 \times 10^{11} / 8.8 \times 10^{10} = 2.012$

The angular momentum determined from the geometry and size statistics proposed for the STEM electron model is very close to QM's estimate of 'intrinsic' spin, as is the associated electron g-factor, which is 2.012 compared to QM's estimate of 2.00232 (note that should the speed v at radius R be increased by a mere 0.5% from 1.8×10^8 to 1.81×10^8 , then the estimates for S and g would be identical to the QM estimates).

The STEM toroidal electron model satisfies the QM wave equations and produces a classical (or Newtonian Physics) estimate of angular momentum (and g-factor) that corresponds to QM's 'intrinsic' spin estimate. Richard Feynman can now rest in peace assured that, when an appropriate physical model of the electron is used, there is a 'classical explanation' for why the electron g-factor is 2.

As a final note, an aspect often overlooked when trying to determine the radius of the electron experimentally is that the electron is a very agile and mobile particle. As a continually moving particle, a free electron is a difficult-to-hit target that re-orientates itself and moves instantaneously in response to any electromagnetic field it encounters. The electron is bombarded by just that, electromagnetic field energy in the form of X-rays (i.e. EMR in the X-ray frequency band), with the hit statistics and the deflection patterns being recorded, and then fed into collision simulation software to estimate the radial-size of the electron. It is a complex process fraught with potential error and, although the CODATA radius estimate is quoted to high precision (lots of significant figures), it has very low accuracy (or reliability), as evident in the wide range of estimates that have been made by different techniques and research groups.